PHYSICAL INTERACTION AND FUNCTIONAL STUDIES OF HUMAN SCO1, A MITOCHONDRIAL METALLOCHAPERONE

A Thesis Submitted to the
College of Graduate Studies and Research
in Partial Fulfillment of the Requirements
for the Degree of Master of Science
in the Department of Biochemistry
University of Saskatchewan
Saskatoon

By
AREN BOULET

PERMISSION TO USE

In presenting this thesis in partial fulfilment of the requirements for a Postgraduate degree from the University of Saskatchewan, I agree that the Libraries of this University may make it freely available for inspection. I further agree that permission for copying of this thesis in any manner, in whole or in part, for scholarly purposes may be granted by the professor or professors who supervised my thesis work or, in their absence, by the Head of the Department or the Dean of the College in which my thesis work was done. It is understood that any copying or publication or use of this thesis or parts thereof for financial gain shall not be allowed without my written permission. It is also understood that due recognition shall be given to me and to the University of Saskatchewan in any scholarly use which may be made of any material in my thesis.

Requests for permission to copy or to make other use of material in this thesis in whole or part should be addressed to:

Head of the Department of Biochemistry

University of Saskatchewan

Saskatoon, Saskatchewan, S7N 5E5

ABSTRACT[1]

Cytochrome *c* oxidase (COX) is a multimeric protein complex embedded in the inner mitochondrial membrane that contributes to the electrochemical potential ultimately required for adenosine triphosphate (ATP) synthesis. Synthesis of Cytochrome *c* Oxidase 1 (SCO1) and SCO2 are two of many accessory proteins that facilitate the assembly of individual COX structural subunits into a functional holoenzyme complex. SCO1 and SCO2 also function to regulate cellular copper homeostasis. Both of these functions require that SCO proteins collaborate with several interacting partners. With few exceptions, however, their protein partners have yet to be identified and, as a consequence, we lack mechanistic insight into SCO protein function. To address this gap in our knowledge, I used physical methods to identify interacting partners of SCO1. Physical interactions between potential interacting partners of endogenous SCO1 or overexpressed SCO1-FLAG were stabilized with a chemical crosslinker, and the protein complexes were purified using the appropriate primary antibody. Mass spectrometric analysis of the eluates provided two lists of potential interacting partners that were subsequently filtered by gene ontology function and mitochondrial localization. The final list was comprised of 85 proteins, which were rank ordered based on total peptide counts per protein. Three of these candidate interacting partners were then further characterized; COX20, tricarboxylate transport protein (SLC25A1) and mitochondrial 2-oxoglutarate/malate carrier (SLC25A11). I first confirmed the authenticity of the observed interactions by conducting the reciprocal co-immunoprecipitations in the absence of a chemical crosslinker. I then investigated the effect of transient knockdown of each protein on the abundance of COX II, a direct proxy of total COX content. Knockdown of COX20 and SLC25A1 reduced COX II levels in *SCO1* and *SCO2* patient fibroblasts, but did not affect COX II abundance in control cells. SLC25A11 knockdown lowered COX II abundance in both control and *SCO* patient cells. These data suggest that the ability of SCO1 to interact with each of these proteins somehow facilitates the maturation of the Cu_A site of COX II.

[1] Throughout my thesis, I use capitalized text when referring to a human protein (e.g. SCO1), and italicized, capitalized text when referring to a human gene (e.g. *SCO1*). Yeast proteins and genes are distinguished from their human counterparts by the use of a single capital letter at the beginning of the text in question (e.g. Sco1 or *Sco1*).

ACKNOWLEDGEMENTS

Foremost, I would like to express my gratitude to my supervisor, Dr. Scot Leary. I would like to thank him for providing me with the opportunity to enter the world of science, and the assistance throughout this project. His constant support allowed me to develop my skills and continuously grow as a scientist and as a person. He has always encouraged me to welcome challenges and to constantly push my own limits. His pain-staking efforts in proof-reading my written drafts will always be appreciated. Without his guidance, I would not have been able to finish this project.

I am deeply grateful to the Saskatchewan Health Research Foundation and the Canadian Institutes of Health Research for providing the funding for my project. Without their financial aid my project would have been limited.

I would like to thank my Graduate Advisory Committee, Drs. Jeremy Lee and Dr. Stan Moore, for their encouragement, insightful criticisms, and thought-provoking questions.

I would also like to extend my gratitude to Drs. Myriam Bourens and Antonio Barrientos for supplying the mitochondria from HEK293 cells overexpressing COX20-FLAG, and for allowing me to collaborate with their research. I would also like to extend my gratitude to the Institut de Recherches Cliniques de Montréal for performing the mass spectrometric analysis, and Denis Faubert for his advice and patience when dealing with my questions.

I have greatly benefited from the assistance and support from the members of the Leary lab; including Min Pan, Shelley Stewart, Zakery Baker, Dr. Lianglu Wan, Dr. Lisa Yu, Chris Hlynialuk, and Dr. Erica Ling.

I would also like to thank my parents for financial and emotional support. Finally, I want to express my appreciation for my girlfriend, Carla Thorel. I could not imagine finishing this thesis without her constant love and support. Through long experiments in the lab and the frustrations with confusing results, her positive demeanor and outlook always kept me motivated.

TABLE OF CONTENTS

LIST OF FIGURES

LIST OF TABLES

LIST OF ABBREVIATIONS

AFG3L2	ATPase family member 3-Like 2
APS	Ammonium persulfate
BCS	Bathocuproinedisulfonic acid
bp	Base pair
BSA	Bovine serum albumin
CHCHD3	Coiled-coil-helix-coiled-coil-helix domain-containing protein 3
COX	Cytochrome *c* oxidase
CS	Citrate synthase
DDM	n-Dodecyl-beta-D-Maltoside
DFDNB	1,5-Difluoro-2,4-dinitrobenzene
DMEM	Dulbecco's modified Eagle's media
DMP	Dimethyl pimelimidate
DSG	Disuccinimidyl glutarate
DSS	Disuccinimidyl suberate
DST	Disuccinimidyl tartarate
DTT	Dithiothreitol
EDTA	Ethylenediaminetetraacetic acid
EGTA	Ethylene glycol tetraacetic acid
ERV1	Essential for respiration and vegetative growth protein 1
GST	Glutathione-S-transferase
HEPES	4-(2-hydroxyethyl)-1-piperazine ethanesulfonic acid
HK1	Hexokinase-1
IMM	Inner mitochondrial membrane
IMMT	Inner mitochondrial membrane protein
IMS	Intermembrane space
IPTG	Isopropyl β-D-1-thiogalactopyranoside
LC	Liquid chromatography
LRPPRC	Leucine-Rich Pentatricopeptide Repeat Containing protein
MBA1	multi-copy bypass of AFG3 (ATPase Family Gene)
MIA	Mitochondrial intermembrane space import and assembly

MS	Mass spectrometry
Mss	Mitochondrial splicing suppressor
mt	Mitochondrial
MTERF	Mitochondrial transcription termination factors
mtHSP	Mitochondrial heat shock protein
NADH	Nicotinamide adenine dinucleotide
NDUFS1	NADH-ubiquinone oxidoreductase 75 kDa subunit
NDUFS3	NADH dehydrogenase pubiquinone] iron-sulfur protein 3
OAA	Oxaloacetic acid
OMM	Outer mitochondrial membrane
Oxa1	Oxidase assembly mutant 1
PAGE	Polyacrylamide gel electrophoresis
PAM	Presequence translocase-associated motor
PBS	Phosphate buffered saline
PIC	Protease inhibitor cocktail
RT	Reverse transciptase
SAM	Sorting and assembly machinery
SCO	Synthesis of cytochrome *c* oxidase
SDS	Sodium dodecyl sulfate
siRNA	Small-interfering RNA
SLC25	Solute carrier 25 family
SLC25A1	Tricarboxylate transport protein
SLC25A11	Mitochondrial 2-oxoglutarate/malate carrier
SLC25A3 or PIC2	Phosphate carrier protein
STOML2	Stomatin-like protein 2
TACO1	Translational activator of COX I
t-DOC	Taurodeoxycholic acid
TEMED	Tetramethylethylenediamine
TFAM	Mitochondrial transcription factor A
TFB1M or TFB2M	Mitochondrial transcription factor 1 or 2
TIM	Translocase of the inner mitochondrial membrane

TOM	Translocase of the outer mitochondrial membrane
TUFM	Elongation factor Tu
UQCRC2	Cytochrome b-c1 complex subunit 2
VDAC2	Voltage dependent anion-selective channel protein 2

1 INTRODUCTION

1.1 Mitochondria

Mitochondria are eukaryotic organelles that are generally described as "power plants", because they generate the majority of the adenosine triphosphate (ATP) that is ultimately consumed by various cellular processes (McBride *et al.*, 2006). In addition to their role in energy production, mitochondria are involved in cell signaling, differentiation, apoptosis, and cell cycle control (Horn and Barrientos, 2008; McBride *et al.*, 2006; Pierrel *et al.*, 2007). Mitochondrial dysfunction is thought to play a significant role in aging, and is known to cause early and late onset diseases that affect almost every organ system of the human body (Kazachkova *et al.*, 2013; Zsurka and Kunz, 2013). The ability to maintain a functional population of mitochondria is therefore essential for the health of a eukaryotic cell.

Mitochondria are thought to have originated from a formerly free-living aerobic proteobacterium that was taken up by a larger host cell. Over evolutionary time, the proteobacterium genome has been reduced in size by lateral transfer of the majority of its genes to the host nucleus (Gray *et al.*, 1999). However, the mitochondrion of all eukaryotic cells has retained a multi-copy genome that is small, circular and encodes a number of genes critical to ATP production. Organelle biogenesis therefore requires the coordinate expression of nuclear- and mitochondrially-encoded genes (Anderson *et al.*, 1981; Ott and Herrmann, 2010; Sickmann *et al.*, 2003). The number of mitochondria present in unicellular organisms or in tissues of multicellular organisms varies considerably, with cells having anywhere from one to hundreds of mitochondria (Fernandez-Vizarra *et al.*, 2011).

1.1.1 Mitochondrial structure

Mitochondria are made up of two membranes that separate the organelle into four distinct compartments; the outer mitochondrial membrane (OMM), the intermembrane space (IMS), the inner mitochondrial membrane (IMM) and the matrix. The IMS is located between the OMM and IMM, while the matrix is enclosed within the IMM.

The OMM is semi-permeable, which allows ions and small molecules to move by passive diffusion through transmembrane channel proteins called porins or through the translocase of the outer mitochondrial membrane called the TOM complex (Colombini, 1979; Freitag *et al.*, 1982;

Zalman *et al.*, 1980). The TOM complex, which is a large, multi-protein molecular motor, also functions to import proteins into the organelle, by recognizing the mitochondrial targeting sequences of nuclear-encoded proteins that are translated on cytosolic ribosomes (Neupert and Herrmann, 2007).

Unlike the OMM, the IMM is impermeable and active transport mechanisms are required to move ions, small molecules and proteins across this lipid bilayer (Endo *et al.*, 2011; Neupert and Herrmann, 2007). The translocase of the inner mitochondrial membrane (TIM) complex recognizes the mitochondrial targeting sequence on proteins to facilitate transport across the IMM (Neupert and Herrmann, 2007). While the impermeable nature of the IMM poses a challenge for protein and metabolite transport, it is a feature that is essential for aerobic ATP production. Five multimeric enzyme complexes integral to the IMM function to produce ATP in a process known as oxidative phosphorylation. The first four complexes form the respiratory chain and pump protons across the IMM into the IMS, to generate an electrochemical gradient that is then used by Complex V to synthesize ATP (Figure 1.1). Mitochondria of cells and organisms that rely heavily on oxidative phosphorylation tend to have a highly invaginated IMM, which leads to the formation of structures called cristae. Cristae effectively increase the total surface area of the IMM and allow for higher concentrations of these five complexes to increase energy production (Schultz and Chan, 2001).

The IMS is located between the OMM and IMM. This aqueous environment is more oxidizing and has a lower pH than either the cytosol or the mitochondrial matrix, properties that are attributable at least in part to the proton gradient generated by the respiratory chain (Herrmann and Hell, 2005; Hu *et al.*, 2008). The matrix is completely enclosed by the IMM, and contains the multi-copy mitochondrial genome, along with transcriptional and translational machinery that is required for its expression. This compartment also houses enzymes of the citric acid cycle and those required for fatty acid oxidation. Lastly, the matrix contains labile pools of iron, copper, zinc, and manganese ions required to metallate and mature specific mitochondrial proteins (Pierrel *et al.*, 2007; Rhee *et al.*, 2013).

1.1.2 Protein import into mitochondria

Mitochondria are unique among cellular organelles in that their biogenesis requires the coordinate expression of the nuclear and mitochondrial genomes. Because the overwhelming

majority of mitochondrial proteins are nuclear-encoded, mitochondria have evolved highly sophisticated, multi-protein assemblies to mediate protein import into the organelle, and to facilitate sorting of these proteins to distinct mitochondrial compartments (Becker *et al.*, 2012; Neupert and Herrmann, 2007). All imported proteins are first recognized by subunits of the TOM complex and then transported through the OMM (Endo *et al.*, 2011). Recognition by the TOM complex is contingent upon a mitochondrial targeting sequence (Endo and Kohda, 2002; Mossmann *et al.*, 2012); however, nuclear-encoded mitochondrial proteins exhibit tremendous variability with respect to their targeting sequences and whether or not they are cleaved during protein import or their subsequent maturation (Endo *et al.*, 2011; Neupert and Herrmann, 2007).

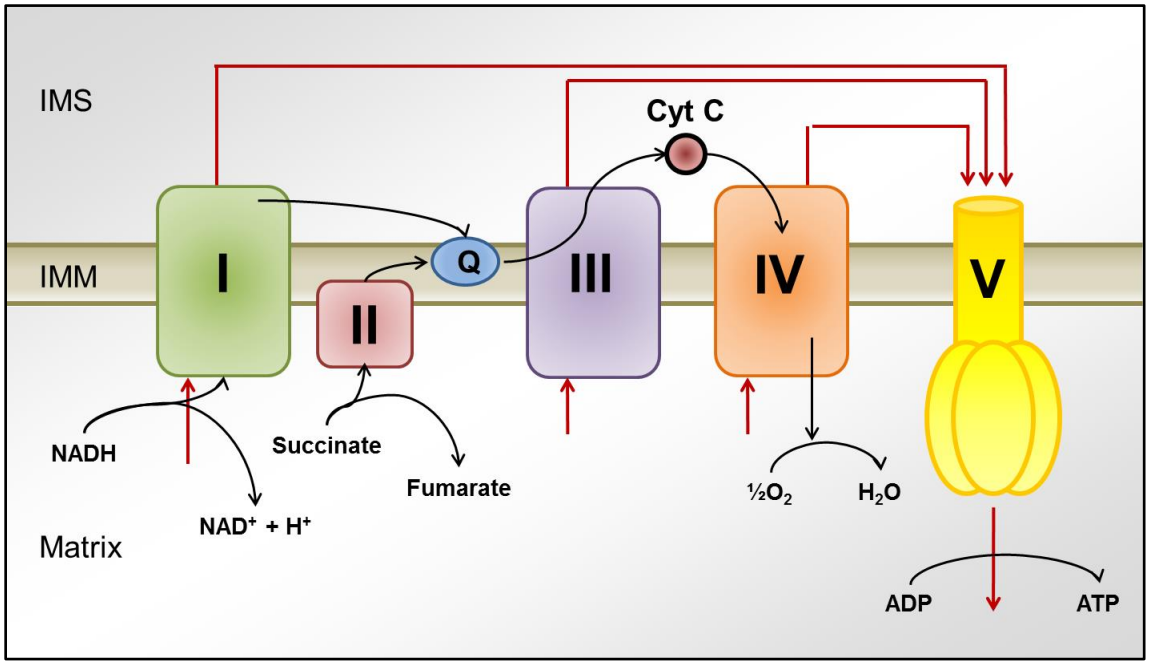

Figure 1.1: Schematic of aerobic respiration. Four multimeric protein complexes (I through IV) form the electron transport chain, which functions to pump protons across the IMM from the matrix to the IMS. The resultant electrochemical gradient is then used by Complex V to produce ATP. The black lines represent the movement of electrons between the protein complexes. The red arrows denote the protons pumped through various protein complexes into the IMS. Complexes I and II shuttle electrons from nicotinamide adenine dinucleotide (NADH) and succinate, respectively, to coenzyme Q (Q). Complex III catalyzes the transfer of electrons from coenzyme Q to cytochrome *c*. The final complex in the electron transport chain, Complex IV, uses electrons from cytochrome *c* to reduce oxygen to water (Redrawn from Schultz and Chan, 2001).

After their translocation through the TOM complex, precursor proteins are recognized by specific sorting pathways and trafficked to distinct mitochondrial compartments (Figure 1.2). Proteins bound by TIM23 (the presequence translocase of the inner mitochondrial membrane) are destined for the matrix or the IMM, if they interact with OXA1 (Oxidase assembly mutant 1) (Hell *et al.*, 1998; Neupert and Herrmann, 2007). The TIM22 (the carrier translocase of the inner mitochondrial membrane) complex also recognizes proteins targeted to the IMM. The SAM (sorting and assembly machinery) complex interacts with proteins that are resident to the OMM, while the MIA (mitochondrial intermembrane space import and assembly) pathway promotes the retention of small soluble proteins within the IMS by inducing conformational changes in their tertiary structure (Becker *et al.*, 2012; Chacinska *et al.*, 2009; Endo *et al.*, 2011; Koehler and Tienson, 2009; Paschen *et al.*, 2005). I will only present the TIM23 and MIA sorting pathways because SCO1, the focus of my M.Sc. thesis research, is integral to the IMM and is known to interact with several soluble, cysteine-rich IMS proteins (Banci *et al.*, 2008; Buchwald *et al.*, 1991; Leary *et al.*, 2004; Leary *et al.*, 2007; Leary *et al.*, 2009; Leary *et al.*, 2013b).

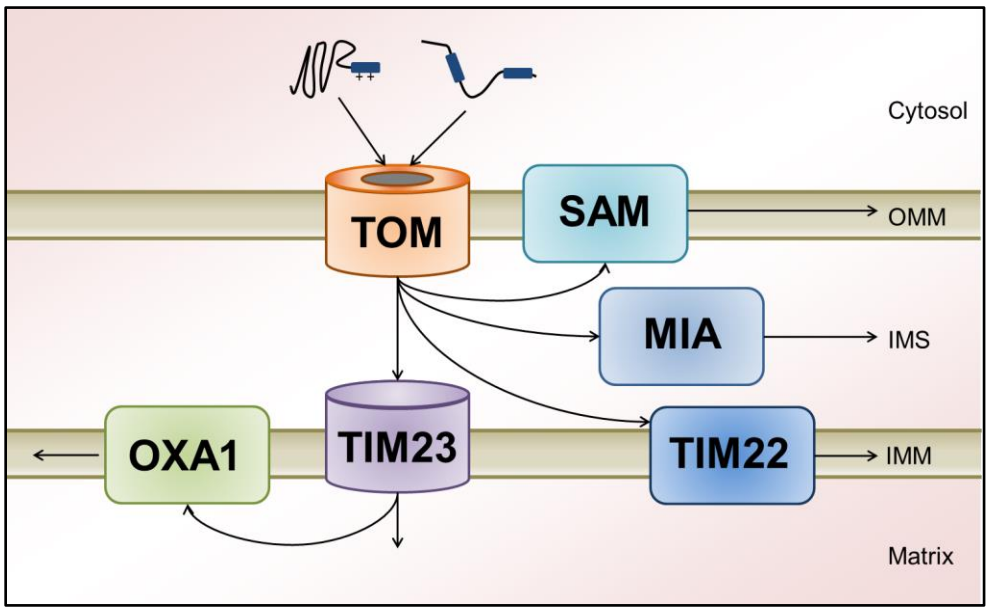

Figure 1.2: Pathways by which nuclear-encoded proteins are imported into and sorted within the mitochondrion. The TOM complex acts as the main entry for proteins into the mitochondrion. The SAM complex interacts with proteins destined for the OMM, while the MIA pathway uses a disulfide relay system to induce conformational changes in target proteins to promote their retention within the IMS. Proteins interacting with the TIM23 complex are targeted to the IMM or matrix, while TIM22 chaperones the insertion of proteins into the IMM (Adapted from Chacinska *et al.*, 2009).

1.1.2.1 The TIM23 pathway

The TIM23 complex and its associated motor, PAM (presequence translocase-associated motor), transport precursor proteins across the IMM (Figure 1.3) (Chacinska *et al.*, 2009; Endo *et al.*, 2011). The TIM23 complex is the most complicated translocase of the mitochondrion, because its energy-dependent activity must be coordinated with that of the TOM complex and the respiratory chain (Herrmann *et al.*, 2012; Neupert and Herrmann, 2007).

The core of TIM23 is formed by three essential subunits; Tim50 which has a receptor domain in the IMS (Geissler *et al.*, 2002; Mokranjac *et al.*, 2009; Tamura *et al.*, 2009; Yamamoto *et al.*, 2002), Tim23 which forms the pore (Alder *et al.*, 2008; Truscott *et al.*, 2001), and Tim17 which recruits the motor proteins required for translocation (Chacinska *et al.*, 2005; Martinez-Caballero *et al.*, 2007). Both Tim50 and Tim23 interact with a fourth non-essential subunit, Tim21, to facilitate transient interactions with proteins of the TOM complex (Chacinska *et al.*, 2005; Meinecke *et al.*, 2006; Mokranjac *et al.*, 2009; Tamura *et al.*, 2009). This provides a route to import proteins directly from the cytosol into the matrix. Tim21 also facilitates interactions between the TIM23 complex and Complexes III and IV of the respiratory chain, and therefore supports protein import that is dependent on a membrane potential (Dienhart and

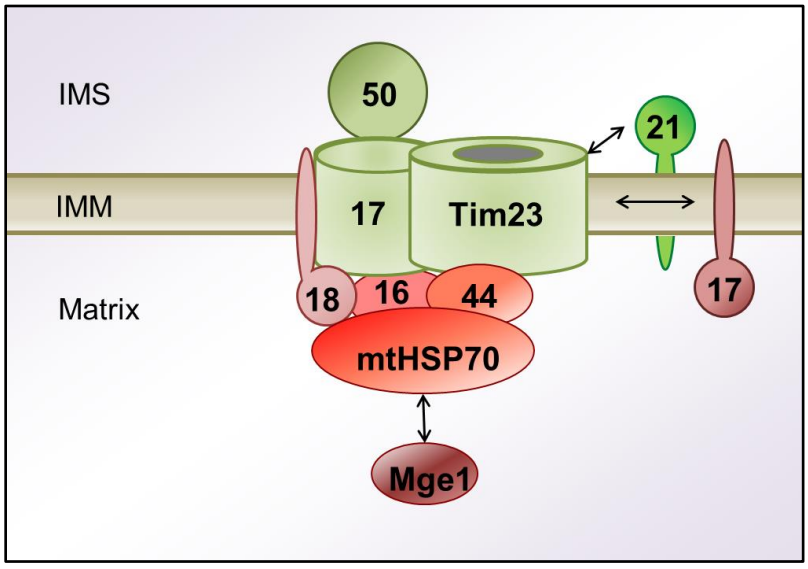

Figure 1.3: The components of the TIM23 and PAM complexes. The TIM23 complex forms the protein-conducting pore (green) while the PAM complex (red) acts as the import motor. TIM23 is made up of three essential subunits (Tim50, Tim17, and Tim23) as well as the non-essential Tim21. The central component of the PAM complex is mtHSP70. Several other regulatory factors are essential to its function (Pam18, Pam16, Pam44, Mge1), while Pam17 function is dispensable (Redrawn from Chacinska *et al.*, 2009).

Stuart, 2008; van der Laan *et al.*, 2006; Wiedemann *et al.*, 2007). The transport and processing of precursor proteins across the IMM also depends on the coordinated and cooperative functions of the TIM23 and PAM complexes. Membrane potential is required to open the Tim23 pore, and supports transport of a positively charged mitochondrial targeting sequence into the negatively charged matrix (Meinecke *et al.*, 2006; Shariff *et al.*, 2004). Once a protein is contained within the TIM23 complex, the matrix localized PAM motor complex is required for active protein transport (Neupert and Herrmann, 2007). The central subunit of the PAM complex is the mitochondrial heat shock protein 70 (mtHsp70) which hydrolyzes ATP to drive the translocation of the polypeptide chain (Chacinska *et al.*, 2009). The PAM complex consists of three more essential subunits; Mge1 which promotes the release of ADP to allow for another round of ATP binding (Schneider *et al.*, 1996), Pam18 which stimulates the ATPase activity (Li *et al.*, 2004), Pam16 which regulates Pam18 (Kozany *et al.*, 2004; Li *et al.*, 2004; Mokranjac *et al.*, 2006), and Tim44 which provides mtHsp70 with a binding site close to the channel (Krayl *et al.*, 2007; Slutsky-Leiderman *et al.*, 2007). Pam17 is not essential but promotes interactions between the TIM23 and PAM complexes, and is released prior to protein translocation (Hutu *et al.*, 2008; Popov-Celeketic *et al.*, 2008). Several proteins are initially translocated into the matrix by the TIM23 complex prior to being exported for their integration into the IMM (Baumann *et al.*, 2002; Herrmann *et al.*, 1997). Although Oxa1 fulfills a critical role in matrix export of these proteins into the IMM, the mechanisms generally remain ill-defined (Hell *et al.*, 1998; Neupert and Herrmann, 2007).

1.1.2.2 The MIA pathway

The MIA pathway recognizes soluble proteins that contain twin CxxxC or Cx_9C motifs and relies on a disulphide relay system to import members of this mitochondrial protein family into the IMS (Chacinska *et al.*, 2009). After being translocated through the TOM complex, the cysteines of these highly conserved motifs are oxidized to form an intramolecular disulfide bond. Their oxidation results in a transition from a linear disordered polypeptide to one that is folded into a helical hairpin, a conformational change that prevents retrotranslocation of the protein into the cytosol (Figure 1.4) (Allen *et al.*, 2003; Becker *et al.*, 2012; Herrmann *et al.*, 2012; Lutz *et al.*, 2003).

The MIA pathway consists of two core proteins; MIA40 and ERV1 (essential for respiration and vegetative growth protein 1) (Chacinska *et al.*, 2004; Chacinska *et al.*, 2009; Mesecke *et al.*, 2005). MIA40, in humans, is a soluble IMS protein that uses a conserved intramolecular disulfide bond to oxidize target proteins (Banci *et al.*, 2009; Chacinska *et al.*,

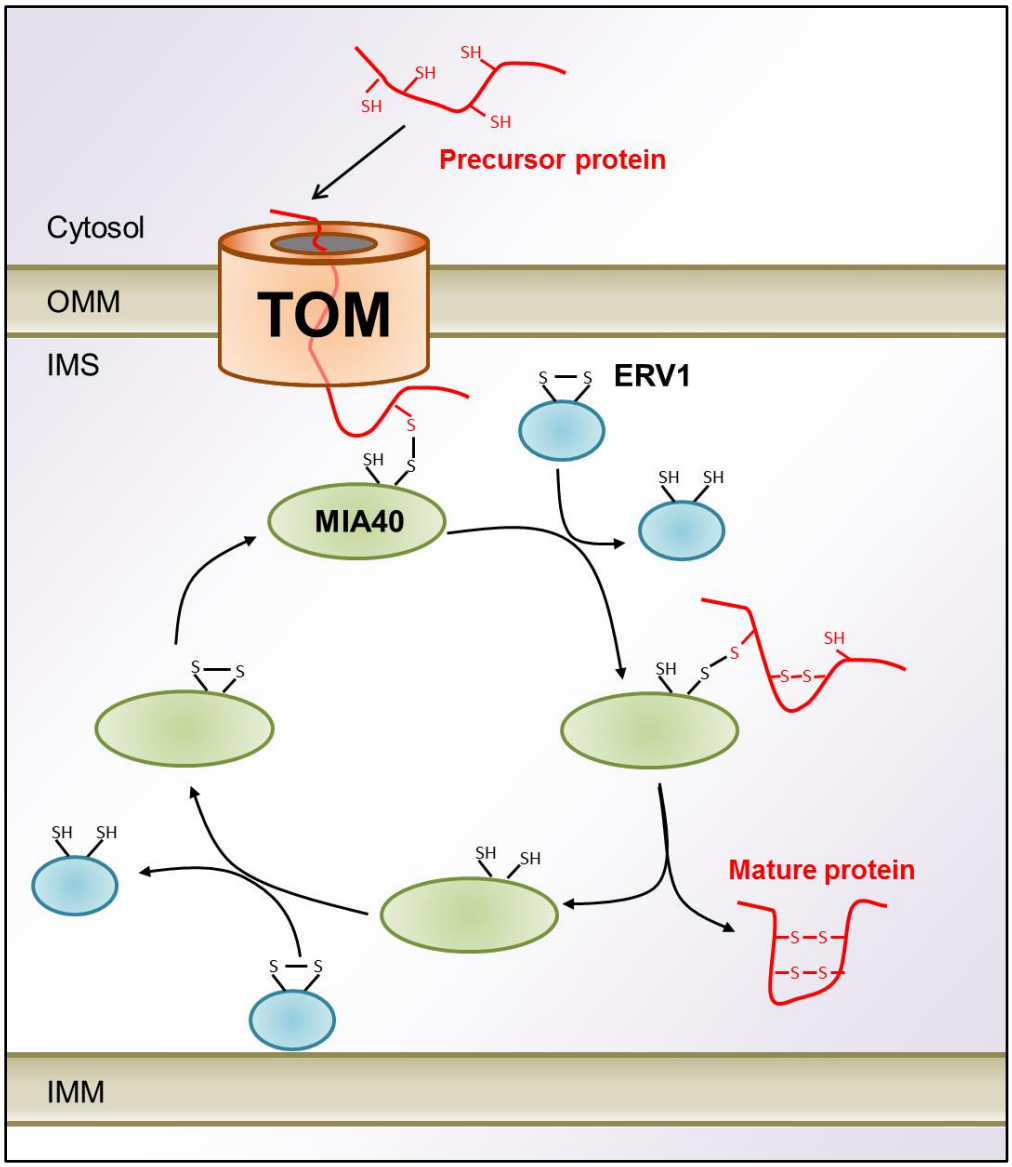

Figure 1.4: Diagram of the MIA pathway. The MIA pathway utilizes a disulfide relay system to oxidize proteins that contain cysteine-rich motifs, thereby forming intramolecular disulfide bonds that prevent their retrotranslocation from the IMS. The MIA pathway consists of two core components; MIA40 and ERV1. MIA40 oxidizes the target twin CxxxC or Cx_9C motifs of newly imported precursor proteins to drive their oxidative folding. ERV1 then oxidizes MIA40, to re-prime it for a subsequent round of protein import. Reduced and oxidized thiol groups are indicated by SH and S-S, respectively. (Adapted from Chacinska *et al.*, 2009)

2009; Milenkovic *et al.*, 2007). This process leaves MIA40 in a reduced and inactive state; however, ERV1 can accept electrons from MIA40, which oxidizes and reactivates the protein (Mesecke *et al.*, 2005; Rissler *et al.*, 2005). ERV1 subsequently delivers the electrons to cytochrome *c* for the production of water, a mechanism that couples the activity of the disulfide relay system to that of the respiratory chain (Bihlmaier *et al.*, 2007; Dabir *et al.*, 2007).

1.1.3 Translation of mitochondrially-encoded proteins

The mammalian mitochondrial genome encodes 13 polypeptides that are part of the catalytic core of various complexes of oxidative phosphorylation; ND1-ND6 and ND4L of Complex I, cytochrome *b* of Complex III, COX I-III of Complex IV, and ATP6 and ATP9 of Complex V (Anderson *et al.*, 1981; Ott and Herrmann, 2010). The transcription of these mRNAs is unique from that of their nuclear counterparts, because the genome is circular and it lacks introns (Clayton, 1982; Graziewicz *et al.*, 2006). The basic human mitochondrial transcriptional machinery is composed of a single RNA polymerase, mitochondrial transcription factor A (TFAM) and either mitochondrial transcription factor B1 (TFB1M) or B2 (TFB2M). The precise contribution of each of these three factors to transcription remains unknown (Falkenberg *et al.*, 2007; Smits *et al.*, 2010). Transcription originates from one of three promoters; HSP1, HSP2, and LSP. Transcripts from the HSP2 and LSP generate polycistronic molecules that contain the majority of messenger RNAs including all those encoding proteins, while the HSP1 transcript contains the 12S and 16S ribosomal RNAs (Falkenberg *et al.*, 2007; Smits *et al.*, 2010). Termination of transcription appears to involve three mitochondrial transcription termination factors (MTERF); MTERF1, MTERF2, and MTERF3. However, the interplay between these 3 factors and the exact mechanism by which transcription is terminated are not yet clear (Smits *et al.*, 2010) Subsequent processing of these polycistronic transcripts results in the release of individual mRNAs and the tRNAs necessary for their translation. The translational apparatus consists of mitochondrial ribosomes (mt-ribosomes), mt-tRNA, translational activators, and other regulatory factors (Herrmann *et al.*, 2013; Smits *et al.*, 2010). The majority of mt-ribosomes are associated with the IMM, to facilitate the co-translational insertion of polypeptides into the lipid bilayer. Membrane insertion is facilitated by a number of protein chaperones, including Oxa1 (Hell *et al.*, 2001; Herrmann *et al.*, 2012). Oxa1 is embedded within the IMM, and is thought to bind mt-ribosomes tightly with its C-terminal tail

(Jia *et al.*, 2003). Oxa1 has also been shown to bind to newly synthesized polypeptides, and mediates their insertion into the IMM by forming a pore in the membrane (Hell *et al.*, 2001; Szyrach *et al.*, 2003). The function of Oxa1 is supported by Mba1 (multi-copy bypass of AFG3 (ATPase Family Gene)), which also associates with mt-ribosomes and plays a role in aligning the ribosome exit tunnel with the site of protein insertion into the membrane (Preuss *et al.*, 2002). However, even in the absence of Mba1 and Oxa1, mt-ribosomes remain partially anchored to IMM suggesting there are more factors involved in co-translational insertion of mitochondrial polypeptides into the membrane (Ott *et al.*, 2006).

1.1.4 Mitochondrial diseases

Mitochondrial diseases are among the most common genetic disorders in humans, with a minimum estimated birth prevalence of 1 in 5,000 (Skladal *et al.*, 2003). More than 150 distinct forms of mitochondrial diseases have been reported to date, and are caused by mutations in either mitochondrial or nuclear DNA (Vafai and Mootha, 2012). Mitochondrial DNA (mt-DNA) disorders are maternally inherited, as mt-DNA is derived from the oocyte (Holt *et al.*, 1988; Vafai and Mootha, 2012; Wallace *et al.*, 1988). The onset of clinical symptoms tends to be later in life, because cells contain multiple copies of mt-DNA and mutated copies of the genome must accumulate to a certain threshold to impair organelle function (Vafai and Mootha, 2012). Pathogenic mutations in nuclear-encoded mitochondrial genes are far more common, and produce a large number of clinically heterogeneous forms of human disease (Schapira, 2012). Not surprisingly, the majority of mitochondrial diseases are caused by defects in oxidative phosphorylation. All of the associated complexes, except Complex II, are composed of both mitochondrially- and nuclear-encoded structural subunits (Vafai and Mootha, 2012). The assembly of individual structural subunits into functional holoenzymes is complicated, and depends on a surprisingly large number of nuclear-encoded accessory proteins termed assembly factors. Mutations in genes encoding these assembly factors therefore affect the assembly and/or stability of one or more complexes of oxidative phosphorylation, which in turn severely impairs ATP synthesis and energy homeostasis (Ghezzi and Zeviani, 2012; Scaglia, 2012). Currently, over 100 pathogenic mutations have been described in nuclear-encoded genes for mitochondrial proteins (Vafai and Mootha, 2012). Little is understood about the underlying clinical phenotypes

of the associated diseases, and the development of effective therapeutic interventions is limited by this gap in our knowledge (Schon and DiMauro, 2003).

1.2 Cytochrome *c* oxidase (COX)

In eukaryotes, COX or Complex IV is a large multimeric protein complex embedded within the IMM. It is the terminal enzyme of the electron transport chain, and it utilizes electrons from cytochrome *c* to catalyze the conversion of oxygen to water, a reaction that also results in the pumping of a proton into the IMS. This proton pumping contributes to the electrochemical gradient required by Complex V for ATP synthesis (Schultz and Chan, 2001).

1.2.1 Structure of COX

Mammalian COX is composed of 13 structural subunits (Tsukihara *et al.*, 1996). Ten of these subunits are nuclear-encoded, while three are encoded by the mitochondrial genome (COX I – III) and form the catalytic core of the enzyme (Fontanesi *et al.*, 2008). COX requires two heme (*a*, a_3) and two copper (Cu_A, Cu_B) prosthetic groups for its catalytic activity along with a magnesium ion and zinc ion (Tsukihara *et al.*, 1995; Tsukihara *et al.*, 1996). Currently, there is no information on the mechanism of delivery for the magnesium and zinc ions found in COX. Similarly, there is no evidence if their presence has an effect on enzyme function (Cobine *et al.*, 2006c; Soto *et al.*, 2012). COX I contains the two heme moieties and a mononuclear copper site, Cu_B. COX II contains a binuclear multi-valent copper site, Cu_A (Fontanesi *et al.*, 2008; Khalimonchuk and Rodel, 2005). Electrons are transferred from cytochrome *c* to the Cu_A site of COX II, and then from heme *a* to the binuclear heme a_3-Cu_B site where O_2 is reduced to water (Yoshikawa *et al.*, 2012). The catalytic core is surrounded by the remaining, nuclear-encoded subunits, which stabilize the holoenzyme and provide allosteric sites for the reversible regulation of its activity (Stiburek and Zeman, 2010).

1.2.2 COX assembly

Biogenesis of COX is an ordered, step-wise process that depends on the coordinate expression of mitochondrially and nuclear-encoded subunits, and the addition of metal co-factors at the appropriate stage of assembly (Cobine *et al.*, 2006c; Stiburek and Zeman, 2010). Maturation of the holoenzyme is preceded by the formation of three distinct assembly

intermediates (S1-S3). Progression through the various stages of assembly is a complex process involving more than 30 nuclear-encoded accessory proteins termed COX assembly factors (Fontanesi *et al.*, 2008). The majority of these COX assembly factors were initially identified in yeast deletion strains that were respiratory-deficient owing to an isolated COX deficiency (Tzagoloff and Dieckmann, 1990). Many of these yeast proteins are highly conserved and have human orthologues, even though there are significant differences between both species with respect to how the holoenzyme is assembled (Barrientos *et al.*, 2002; Scaglia, 2012; Zee and Glerum, 2006).

1.2.2.1 Synthesis and maturation of mitochondrially-encoded COX subunits

COX I-III form the catalytic core of COX, and are relatively large, hydrophobic proteins that are encoded by the mitochondrial genome (Fontanesi *et al.*, 2008; Tsukihara *et al.*, 1996). Their individual mRNAs are all translated by mt-ribosomes that are associated with the IMM, which allows for co-translational insertion of the proteins into the lipid bilayer (Jia *et al.*, 2003; Szyrach *et al.*, 2003). The expression of these core catalytic subunits is tightly regulated (Figure 1.5) (Ott and Herrmann, 2010; Zee and Glerum, 2006). In yeast, several translational activators have been shown to bind the 5' untranslated region of *COX I-III* mRNAs (Costanzo and Fox, 1988; Naithani *et al.*, 2003; Sanchirico *et al.*, 1988). Mss51 (mitochondrial splicing suppressor) and Pet309 are two of these activators that promote the synthesis of Cox1 (Manthey and McEwen, 1995; Perez-Martinez *et al.*, 2003). However, Mss51 has also been shown to form a complex with Cox1 which is thought to provide a negative feedback loop preventing Mss51 from stimulating further translation of *Cox1* mRNA (Perez-Martinez *et al.*, 2003). The Mss51-Cox1 interaction could also serve to stimulate holoenzyme biogenesis by recruiting other COX assembly factors such as Cox14, Cox25, Ssc1, and Mdj1 (Barrientos *et al.*, 2004; Fontanesi *et al.*, 2010; Fontanesi *et al.*, 2011; Mick *et al.*, 2010). Pet111 is integral to the IMM and promotes Cox2 synthesis (Mulero and Fox, 1993). Cox3 translation is activated by a complex composed of Pet54, Pet122, and Pet494 (Brown *et al.*, 1994). Unlike yeast mitochondrial mRNAs, human mitochondrial mRNAs do not contain 5' untranslated regions, and translational activators are therefore thought to recognize motifs 3' of the start codon (Falkenberg *et al.*, 2007; Montoya *et al.*, 1981; Scarpulla, 2008). Mitochondrial mRNAs are polyadenylated which increases stability; however, the potential significance of polyadenylation in regulating translation remains poorly

understood (Tomecki *et al.*, 2004). To date, only two mammalian translational activators of mitochondrially-encoded COX subunits have been identified, and both participate in the translation of *COX I* mRNA; translational activator of COX I (TACO1) (Weraarpachai *et al.*, 2009) and Leucine-Rich Pentatricopeptide Repeat Containing protein (LRPPRC) (Mootha *et al.*, 2002; Sasarman *et al.*, 2010). LRPPRC also appears, however, to play a general role in the stability of mitochondrially-encoded mRNAs (Sasarman *et al.*, 2010), perhaps by facilitating their polyadenylation (Ruzzenente *et al.*, 2012)

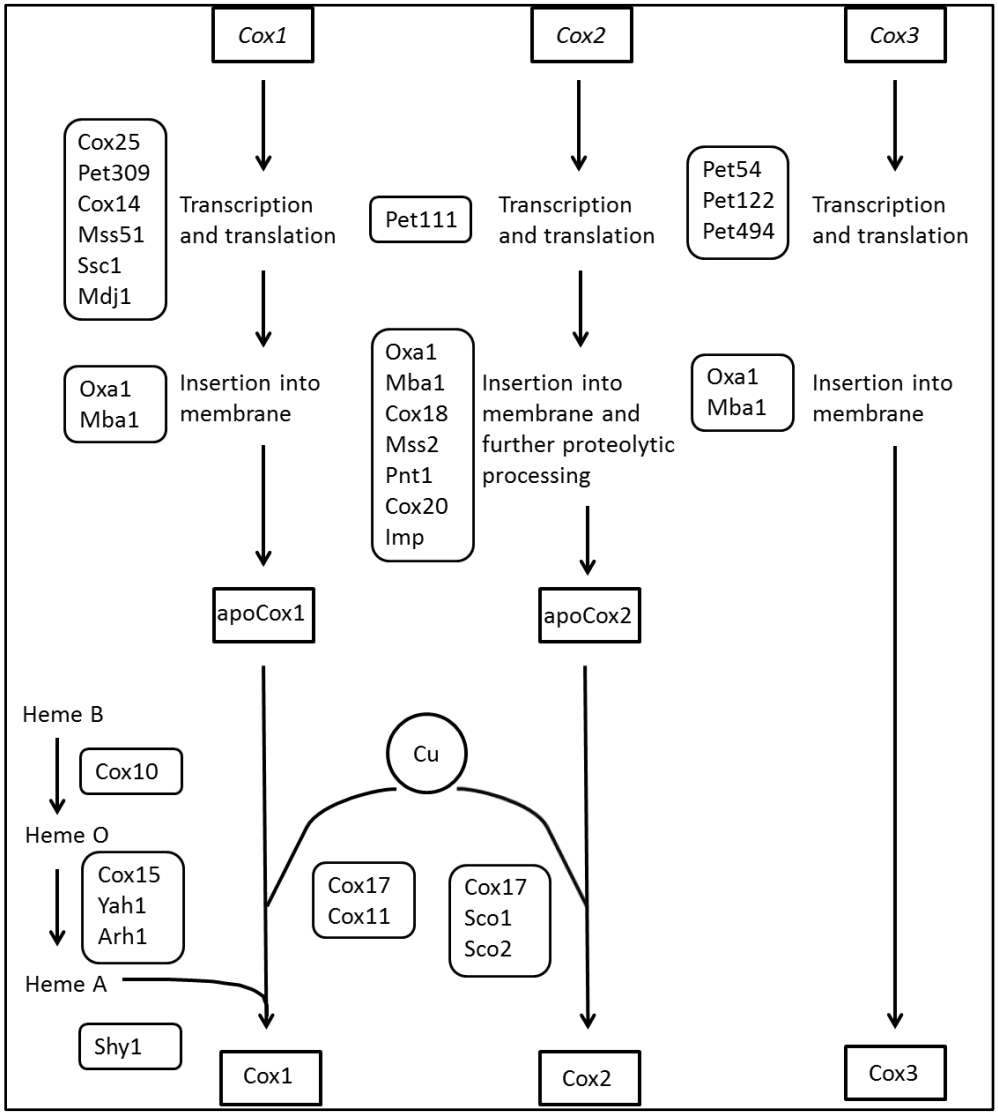

Figure 1.5: The pathway of assembly for mitochondrially-encoded Cox subunits in yeast. COX assembly factors are in rounded rectangles, while COX subunits are in rectangles (Adapted from Zee and Glerum, 2006).

Several additional accessory proteins collaborate with translational activators to facilitate the insertion of newly synthesized Cox1-3 into the IMM and promote subsequent maturation of each polypeptide (Figure 1.5) (Ott and Herrmann, 2010; Zee and Glerum, 2006). The associated molecular mechanisms have been most thoroughly investigated and therefore are best understood for Cox2. Fully matured Cox2 is anchored within the IMM by two transmembrane domains, and its N- and C-termini both protrude into the IMS (Soto *et al.*, 2012). Oxa1 catalyzes the export of the N-terminal tail of newly-synthesized Cox2 across the IMM, a process that anchors its first transmembrane domain within the lipid bilayer (He and Fox, 1997; Hell *et al.*, 1998). In yeast, Cox20 then presents Cox2 to an inner membrane peptidase complex so that its presequence may be cleaved, to yield the mature protein (Hell *et al.*, 2000). The cooperative action of Cox18, Mss2, and Pnt1 (PeNTamidine resistance) then catalyzes the anchoring of the second C-terminal transmembrane domain of Cox2 in the IMM (Broadley *et al.*, 2001; Fiumera *et al.*, 2007; He and Fox, 1999; Saracco and Fox, 2002).

1.2.2.2 Synthesis, delivery and insertion of prosthetic groups during COX assembly

Assembly of a catalytically competent enzyme requires that all prosthetic groups are added to the relevant structural subunits during the assembly process (Cobine *et al.*, 2006a; Cobine *et al.*, 2006c). Much progress has been made with respect to our understanding of how these prosthetic groups are synthesized, delivered and inserted into COX I and COX II (Soto *et al.*, 2012). The heme A required to mature COX I is synthesized within the mitochondrion (Tsukihara *et al.*, 1995). Both COX10 and COX15 are required for the synthesis of heme A (Glerum and Tzagoloff, 1994; Valnot *et al.*, 2000a; Barros *et al.*, 2001; Barros and Tzagoloff, 2002). Yeast Shy1 then catalyzes the insertion of heme A into newly synthesized Cox1 (Mick *et al.*, 2007). Pathogenic mutations in the human orthologue of Shy1, SURF1, cause severe forms of disease associated with an isolated COX deficiency (Smith *et al.*, 2005; Zhu *et al.*, 1998).

While it is now firmly established that a labile copper pool housed in the mitochondrial matrix represents the source of copper used to metallate the Cu_B and Cu_A sites of COX I and COX II, respectively (Cobine *et al.*, 2006a), virtually nothing is known about how that copper is transported to the mitochondrion and within the organelle itself. In fact, the first protein involved in copper transport across the IMM, Pic2, was only identified earlier this year (Vest *et al.*, 2013), and it is clear that many more proteins are involved in the regulating mitochondrial

copper trafficking (Cobine *et al.*, 2006c). Much more is known, however, about the mechanisms that mediate copper delivery to Cox1 and Cox2 within the IMS. Cox17, a small soluble, cysteine-rich metallochaperone within the IMS (Glerum *et al.*, 1996a), binds copper and transfers it to the IMM anchored metallochaperones Cox11 (Carr *et al.*, 2002), SCO1 (Glerum *et al.*, 1996b), and SCO2 (Banci *et al.*, 2007b; Banci *et al.*, 2008; Horng *et al.*, 2004; Papadopoulou *et al.*, 1999). Studies in bacteria (Hiser *et al.*, 1999) and yeast (Carr *et al.*, 2002) provide compelling evidence that Cox11 delivers copper to the Cu_B site of Cox1. Section 1.3 details how SCO1 and SCO2 function to mature the Cu_A site of COX II.

1.2.2.3 Biogenesis of sub-assembly intermediates during COX assembly

COX assembly involves the formation of three distinct assembly intermediates (S1-S3) prior to maturation of the holoenzyme (Figure 1.6) (Fontanesi *et al.*, 2008; Shoubridge, 2001; Soto *et al.*, 2012). In mammals, COX I is inserted and matured within the IMM to form S1. Two nuclear-encoded subunits, COX IV and COX V_a, then associated with mature COX I to form S2. A significant number of subunits, including mature COX II, are then added to the assembling holoenzyme to form S3. The subsequent incorporation of COX VI_a and COX $VII_{a/b}$ into the S3 intermediate yields the mature holoenzyme (Nijtmans *et al.*, 1998; Shoubridge, 2001; Soto *et al.*, 2012)

1.3 SCO1 and SCO2

SCO1 and SCO2 were first identified as high-copy suppressors in a genetic screen of a *Cox17* null yeast strain (Glerum *et al.*, 1996b). Overexpression of either protein suppressed the respiratory deficiency observed in the *Cox17* null stain; however, subsequent deletion of each *SCO* gene demonstrated that only Sco1 was required for growth on a non-fermentable carbon source. Overexpression of Sco2 was unable to rescue the glycerol growth defect of a *Sco1* null strain, but was able to functionally complement a restricted subset of functionally compromised *Sco1* point mutants (Glerum *et al.*, 1996b). Although this led to the suggestion that Sco1 and Sco2 fulfill partially overlapping functions, a defined role for Sco2 in COX assembly has yet to be established (Khalimonchuk and Rodel, 2005). In contrast, both *SCO* genes are essential in humans (Valnot *et al.*, 2000b, Papadopoulou *et al.*, 1999), and each gene product is known to

fulfill independent but cooperative functions in the metallation of the Cu_A site of COX II (Horng *et al.*, 2005; Leary *et al.*, 2004; Leary *et al.*, 2009; Leary, 2010).

1.3.1 SCO1 and SCO2 functions during Cox assembly

Human SCO1 and SCO2 are both essential, and mutations in either gene lead to severe, early onset forms of fatal, tissue-specific disease. To date, three unique mutations have been identified in *SCO1* patients. The first *SCO1* patient died from liver failure and carried a *P174L*

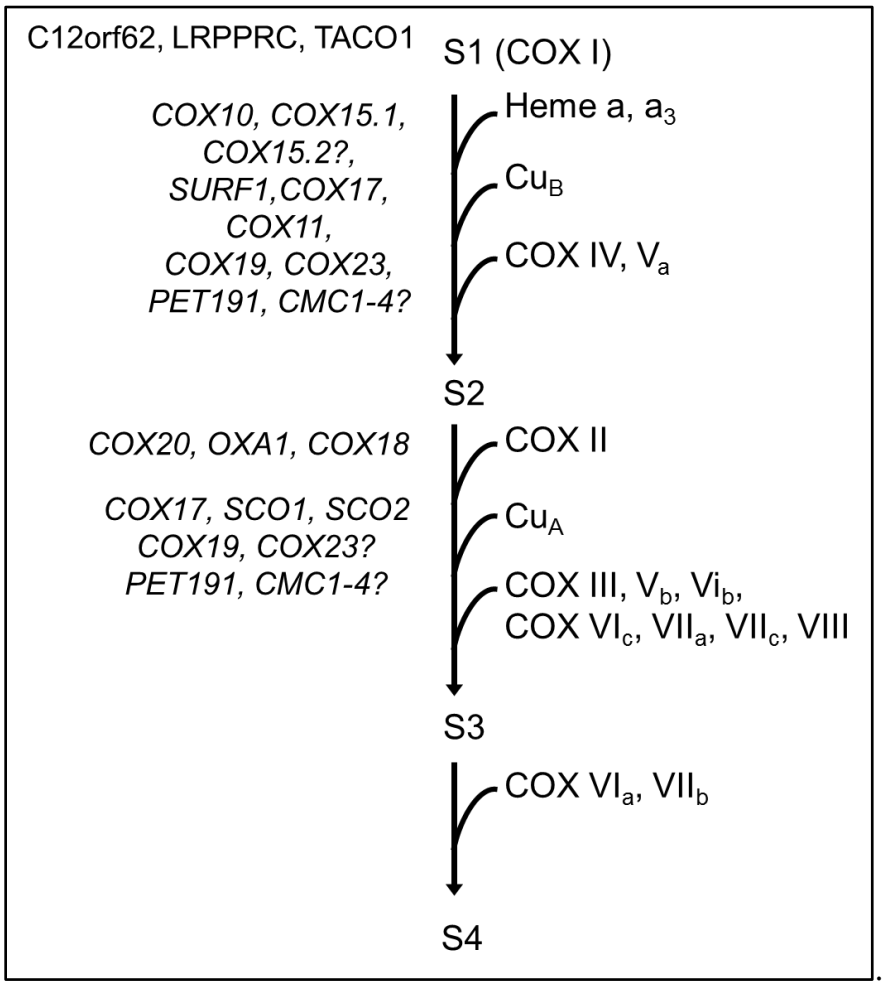

Figure 1.6: Schematic of the step-wise addition of COX subunits to the assembling holoenzyme in humans. Three intermediates (S1 – S3) are produced prior to the formation of the fully assembled holoenzyme (S4). Progression through the various steps of assembly requires the synthesis, delivery and insertion of prosthetic groups, and the ordered incorporation of structural subunits, all of which are shown on the right hand side. All aspects of assembly are facilitated by a large number of nuclear-encoded, accessory proteins termed COX assembly factors, which are shown on the left hand side (Redrawn from Shoubridge, 2001).

missense mutation on one allele, and a nonsense mutation on the second allele (Valnot *et al.*, 2000b). Patients from the second *SCO1* pedigree were homozygous for a *G132S* substitution and died from cardiac failure (Stiburek *et al.*, 2009). The patient from the third *SCO1* pedigree was a compound heterozygote who harboured a *M294V* missense mutation on one allele and a nonsense mutation on the second allele, and who presented with a fatal encephalopathy (Leary *et al.*, 2013a). Mutations in *SCO2* are far more common, and thus far more than 30 pedigrees have been identified. The overwhelming majority of these pedigrees express at least one allele containing an *E140K* missense mutation (Jaksch *et al.*, 2001; Mobley *et al.*, 2009). Although there is some clinical heterogeneity that is observed across *SCO2* pedigrees, all patients eventually succumb from heart failure (Leary *et al.*, 2006). Why mutations in two closely related paralogues that function in the same biochemical pathway produce different, tissue-specific diseases remains an enduring mystery.

Human SCO1 and SCO2 are anchored to the IMM by a single-pass transmembrane domain, and gel filtration data argue that both proteins are homodimers *in vivo* (Leary *et al.*, 2004). The C-terminus of each protein protrudes into the IMS, and has a highly conserved thioredoxin fold that contains a copper-binding site. Cu(I) is coordinated by the two cysteines of a CxxxC motif and highly conserved histidine, while the coordination of Cu(II) requires another, as of yet unidentified ligand (Banci *et al.*, 2006; Banci *et al.*, 2007a). Copper binding is essential to SCO protein function, and both proteins bind Cu(I) or Cu(II) *in vitro* (Leary *et al.*, 2004). Replacing any of the copper-coordinating amino acids with alanines abrogates SCO1 and SCO2 function, which provides further evidence that copper-binding is required for their activity (Horng *et al.*, 2005). Consistent with these observations, the isolated COX deficiency in *SCO1* and *SCO2* patient cells can be rescued when exogenous copper is added to the culture media (Jaksch *et al.*, 2001; Leary *et al.*, 2004; Salviati *et al.*, 2002).

However, the exact relationship between copper-binding and SCO protein function in the context of COX assembly remains unknown, because it is unclear whether one or both SCO proteins transfer copper to COX II during the maturation of its binuclear Cu_A site. How the proposed redox function of SCO1 (Williams *et al.*, 2004) and the demonstrated thiol-disulphide oxidoreductase activity of SCO2 (Leary *et al.*, 2009) affect COX assembly, if at all, remains equally unclear. Further studies are therefore required to better understand the specific roles of each SCO protein during COX assembly.

1.2.3 SCO1 and SCO2 roles in copper homeostasis

Affected *SCO* patient tissues and fibroblasts are both COX and copper deficient, suggesting that SCO1 and SCO2 are bifunctional proteins that fulfill additional roles in the regulation of cellular copper homeostasis (Leary *et al.*, 2007). It was subsequently demonstrated that the cellular copper deficiency phenotype in *SCO* patient fibroblasts is caused by an elevated rate of copper efflux from the cell (Leary *et al.*, 2007), and that this phenotype can be rescued to varying degrees by overexpressing SCO2. Consistent with these observations, redox regulation of the CxxxC motif of SCO1 was recently shown to be critical to the generation of a SCO1-dependent mitochondrial signal that regulates the rate of ATP7A-mediated copper efflux from the cell (Leary *et al.*, 2013b). Transduction of this signal is critically dependent on COX19, which partitions between the IMS and the cytosol in a copper-dependent manner that is perturbed in *SCO* patient cells. These data collectively suggest a model whereby the redox regulation of the CxxxC motif of SCO1 generates a mitochondrial signal that is then transduced to ATP7A by COX19. However, it is clear that other, as yet unidentified proteins are critical to sensing the functional status of SCO1 within the IMS, and transducing a SCO1-dependent redox signal to extra-mitochondrial compartments.

In spite of the profound copper deficiency at the cellular level, mitochondrial copper pools are unaltered in *SCO* patient fibroblasts, suggesting that mechanisms exist to preferentially preserve the organellar metal ion pool (Dodani *et al.*, 2011). Almost nothing, however, is known about how copper is trafficked to, within and from mitochondria. In fact, the first mitochondrial protein involved in organellar copper handling was only identified this year (Vest *et al.*, 2013). Although strong genetic and biochemical evidence was presented that clearly implicate yeast Pic2 in copper transport across the IMM, several genetic and pharmacological stressors had to be applied to observe a copper deficient phenotype in a yeast Pic2 null mutant. This suggests that the mitochondrion contains novel copper trafficking pathways that can functionally complement for the loss of Pic2 function. The identification of these pathways, particularly in the context of copper mobilization from the matrix to the IMS for metallation of the Cu_A and Cu_B sites of COX during holoenzyme assembly, would be invaluable to our understanding of mitochondrial copper handling.

1.4 Rationale, hypothesis and objectives

SCO1 and SCO2 are IMM proteins that must be able to bind copper to function both as COX assembly factors and in a mitochondrial pathway that regulates cellular copper homeostasis. Our understanding of how SCO1 and SCO2 fulfill their various functions is currently limited, because very few of their interacting partners have been identified. I therefore hypothesize that by identifying interacting partners of SCO1 and/or SCO2, and characterizing the functional significance of these physical interaction, I will further our understanding of the mechanisms by which SCO proteins mature the Cu_A site of COX II and regulate cellular copper homeostasis. The objectives of my M.Sc. thesis research then were to;

1. Co-immunoprecipitate SCO1 and SCO2, and identify their interacting partners by mass spectrometry.
2. Validate the observed interactions for a subset of the identified proteins by reciprocal co-immunoprecipitation, and use an RNAi approach to investigate the significance of these interactions to SCO protein function.

2 MATERIALS AND METHODS

2.1 Reagents

Names of reagents and suppliers are listed in Table 2.1. Addresses for each supplier are subsequently listed in Table 2.2.

Table 2.1 List of reagents and suppliers

General Reagents	Supplier
4-(2-hydroxyethyl)-1-piperazineethanesulfonic acid (HEPES)	BioShop
Acetyl Coenzyme A	Roche
Acrylamide	BioShop
Agarose beads	Sigma-Aldrich
Ammonium persulfate (APS)	BioShop
Bathocuproine disulfonic acid (BCS)	Sigma-Aldrich
Bis-acrylamide	BioShop
Bis-tris	Bioshop
Blotto non-fat dry milk	Bio-Rad
Bovine serum albumin (BSA)	BioShop
Bradford protein assay reagent	Bio-Rad
Coomassie Brilliant BlueR-250	Bio-Rad
Cupric chloride	Sigma-Aldrich
Digitonin, high purity	CalbioChem
Ethylenediaminetetraacetic acid (EDTA)	Bioshop
Isopropyl β-D-1-thiogalactopyranoside (IPTG)	Bioshop
2x Laemmli sample loading buffer	Bio-Rad
Monoclonal anti-HA-agarose beads	Sigma-Aldrich
n-Dodecyl-β -D-Maltoside (DDM)	Bioshop
Oxaloacetic acid	Sigma-Aldrich
Phosphate buffered saline (PBS)	Bioshop
Complete protease inhibitor cocktail	Roche
Sodium dodecyl sulfate (SDS)	BioShop

SYBR-Green	Invitrogen
Taurodeoxycholic acid (t-DOC)	Sigma-Aldrich
Tetramethylethylenediamine (TEMED)	Sigma-Aldrich
Triethanolamine	Sigma-Aldrich
Triton X-100	Bioshop
Tween-20	Bioshop
Restriction and modifying enzymes	**Supplier**
*BamH*I	Thermo Scientific
*Not*I	Thermo Scientific
Phusion High-Fidelity DNA polymerase	New England Biolabs
T4 DNA Ligase	New England Biolabs
Cell Culture Reagents	**Supplier**
Antibiotic-antimyotic	Invitrogen
Dulbecco's modified Eagle's media (DMEM)	Invitrogen
Fetal bovine serum	Invitrogen
Hygromycin B	Calbiochem
1,5-dimethyl-1,5-diazaundecamethylene polymethobromide, hexadimethrine bromide (Polybrene)	Sigma-Aldrich
Puromycin	Sigma-Aldrich
Trypsin-EDTA	Invitrogren
Bacteria Culture Reagents	**Supplier**
Ampicillin	Bioshop
Bacto-tryptone	Bioshop
Bacto-yeast	Becton Dickinson
Kanamycin	Bioshop
Chemical crosslinkers	
1,5-Difluoro-2,4-dinitrobenzene (DFDNB),	Thermo Scientific
Dimethyl pimelimidate (DMP)	Thermo Scientific
Disuccinimidyl glutarate (DSG)	Thermo Scientific
Disuccinimidyl suberate (DSS)	Thermo Scientific

Disuccinimidyl tartarate (DST)	Thermo Scientific
Commercial kits	**Supplier**
AminoLink	Thermo Scientific
Antarctic phosphatase	New England Biolabs
E.Z.N.A. Plasmid Mini Kit	Omega Bio-Tek
Gel Extraction Kit	Qiagen
Glutathione-Sepharose beads	GE Life Sciences
jetPRIME™ DNA Transfection Reagent	Polyplus Battery
OneStep RT-PCR kit	Qiagen

Table 2.2 Names and addresses of suppliers

Becton Dickinson	Mississauga, Ontario, Canada
Bioshop	Burlington, Ontario, Canada
Bio-Rad	Mississauga, Ontario, Canada
BectonDickinson	Mississauga, Ontario, Canada
Calbiochem-Millipore	Billerica, MA, USA
GE Life Sciences	Baie d'Urfe, Quebec, Canada
Invitrogen	Burlington, Ontario, Canada
New England Biolabs	Whitby, Ontario, Canada
Omega Bio-Tek	Norcross, GA, USA
Pall	Missausaga, Ontario, Canada
Polyplus Battery	Berkeley, CA, USA
ProteinTech	Chicago, IL, USA
Qiagen	Toronto, Ontario, Canada
Roche	Mississauga, Ontario, Canada
Santa Cruz Biotechnology	Dallas, TX, USA
Sigma-Aldrich	Oakville, Ontario, Canada
Thermo Scientific	Waltham, MA, USA

2.2 Mammalian cells culture

Primary skin fibroblasts were isolated from control subjects and from patients with mutations in *SCO1* (*SCO1-1*, T146X/P174L (Valnot *et al.*, 2000b); *SCO1-2*, V93X/M294V (Leary *et al.*, 2013a) or *SCO2* (*SCO2-9*, R90X/E140K (Leary *et al.*, 2013)). Primary fibroblast cultures were then immortalized by transduction with the *E7* gene of the human papillomavirus and the catalytic subunit of human telomerase (Lochmuller *et al.*, 1999). Fibroblasts, Phoenix amphotropic packaging cells and HEK293 cells were grown in Dulbecco's modified Eagle's media (DMEM) supplemented with 10% fetal bovine serum and 1X antibiotic-antimyotic (Life technologies) at 37°C in an atmosphere of 5% CO_2. Immortalized fibroblasts and HEK293 cells were transduced using the Phoenix amphotropic packaging cell line (kind gift of Dr. G. Nolan, Stanford University) and stable cell lines were selected by supplementing the culture media with 100 mUnits/mL of hygromycin B (Calbiochem) or 2 μg/mL of puromycin (Sigma) (Leary *et al*, 2007).

2.3 Plasmids, bacterial strains and growth media

For co-immunoprecipitations, retroviral expression vectors containing full-length, untagged or epitope-tagged cDNA variants of *SCO1* and *SCO2* were generated prior to my arrival in the lab. *SLC25A1* or *SLC25A11* cDNAs were amplified by reverse-transcriptase PCR (RT-PCR) of RNA isolated from control fibroblasts, and subsequently cloned by homologous recombination into the retroviral overexpression vector pBABE using Gateway® cloning. Plasmids were amplified by transforming chemically competent DH5α or XL1-Blue *E. coli* strains.

Glutathione-S-transferase (GST), GST-SCO1, and GST-SCO2 were expressed from pGEX-6P3 (a kind gift of Dr. Trevor Moraes, University of Toronto; GE Life sciences). Plasmid DNA was then transformed into the chemically competent BL21 Rosetta *E. coli* strain (kind gift of Dr. Stan Moore, University of Saskatchewan), which contains a chromosomal copy of the T7 RNA polymerase under control of the *lac* promoter. Bacteria were therefore grown in media containing isopropyl β-D-1-thiogalactopyranoside (IPTG) to induce the expression of GST alone or GST-fusion proteins.

All bacterial cultures were grown at 37°C in 2YT media (1.6% Bacto-tryptone, 1% Bacto-yeast, 85 mM NaCl, pH 7.4) or 2YT agar plates (0.6% agar) containing 100 μg/mL ampicillin or 50 μg/mL of kanamycin.

2.4 DNA methods

2.4.1 Subcloning

2.4.1.1 Traditional cloning

Crude polyclonal serum had been previously generated against short SCO1 (CASIATHMRPYRKKS) and SCO2 (GRSRSAEQISDSVRRHMAAFRSVLS) peptide sequences (Jaksch *et al.*, 2001; Leary *et al.*, 2004). Full-length *SCO1* and *SCO2* cDNAs were used to amplify these antigenic sequences by PCR. The forward SCO primers contained a *BamH*I restriction site and a two glycine linker 5' of the first codon, while the reverse SCO primers had a *Not*I restriction site 3' of the terminal codon (Table 2.1). PCR amplification of each SCO fragment was carried out in a 20 µL volume containing 1X Phusion HF buffer, 200 µM dNTPs, 0.4 units of Phusion polymerase, 0.5 µM of each primer, and 10 ng of template plasmid. Cycling conditions consisted of an initial denaturation for 3 minutes at 98°C, followed by 30 cycles of 10s denaturation at 98°C, annealing of 30s at 52°C and extension of 15s for 72°C. A final extension of 3 minutes at 72°C was used after the completion of all the cycles. Successful amplification was confirmed by running 10% of the reaction on a 2.5% agarose gel containing nucleic acid stain (1X SYBR-Green). The remainder of the PCR reaction was precipitated by adding 0.3 M sodium acetate, 0.1 M magnesium chloride and 70% ethanol. Samples were incubated at -20°C for 45 minutes and then pelleted at 14,000 *x* g for 15 minutes at 4°C. The pellet was resuspended with 70% ethanol and left at -20°C for 45 minutes again. Following a second spin at 14,000 *x* g for 15 minutes at 4°C, the supernatant was removed and the pellet was allowed to dry at room temperature for 10 minutes. The pellet was then resuspended in triple distilled water and the entire sample was used for subsequent digestions.

Both the parental pGEX-6P3 plasmid (2 µg) and SCO amplicons were digested for 60 minutes at 37°C in a 10 µL volume containing 1X Fermentas fast digest buffer, 5 Units of *BamH*I and 5 Units of *Not*I. Restriction enzymes were then heat inactivated by incubating samples at 65°C for 5 minutes. Following the addition of 1X Antarctic phosphate buffer and 2 Units of Antarctic phosphatase (New England Biolabs), the linearized pGEX-6P3 plasmid was incubated for 20 minutes at 37°C and then heat inactivated at 65°C for 5 minutes. Ligations were subsequently performed in 20 µL volumes that contained 1X T4 DNA Ligase buffer, 1 µL T4 DNA Ligase, 1 µL of linearized, desphosphorylated pGEX-6P3 plasmid and 2.5 µL of the

digested SCO amplicon. Ligation reactions were left overnight at room temperature. The following day, 5 µL of the ligated reaction was transformed into XL-1 Blue *E. coli* cells.

2.4.1.2 Gateway® cloning

Full-length *SLC25A1* and *SCL25A11* cDNAs were amplified and cloned by homologous recombination into the Gateway adapted mammalian retroviral overexpression vector pBABE-puro (Figure 2.1). Total RNA was isolated from control fibroblasts using an RNA purification

Table 2.3: List of primers

Primer name	**Primer sequence**
3' *Not*I pGEX-SCO2	CGTGCGGCCGCCTAGTGATCCAGCAGGTGGAGTC *Not*I
3' *Not*I pGEX-SCO1	CGTGCGGCCGCCTAGCTCTTTTTTCTGTATGGC *Not*I
5' *Bam*H1 pGEX-SCO2	GCAGGATCCGGAGGTGGCGGAGGTGGTCGAACAGAAGCCCTG *Bam*HI
5' *Bam*HI pGEX-SCO1	GCAGGATCCGGAGGTGGCGGAGGTGGTAGGAAGGGACAAATA *Bam*HI
Gateway attB1	GGGGACAAGTTTGTACAAAAAAGCAGGCT
Gateway attB2	GGGGACCACTTTGTACAAGAAAGCTGGGT
Gateway SLC25A11-F	AAAAAGCAGGCTTCACCATGGCGGCGACGGCGAGT
Gateway SLC25A11-R	AGAAGCTGGGTGTTATCAGCCACTGAGGAAGAGAC
Gateway SLC25A1-F	AAAAAAGCAGGCTTCACCATGCCCGCGCCCCGCGCC
Gateway SLC25A1-R	AGAAAGCTGGGTGTTATTCGTCCGTCTTCCACACTTTGTT

kit (Norgen), and then used as a template in a OneStep RT-PCR reaction (Qiagen) with primers designed to amplify each full-length cDNA such that it contained a partial attB1 and attB2 site at its 5' and 3' end, respectively (Table 2.1). PCR amplicons were separated on a 1.5% agarose gel, excised and extracted using a Gel Extraction Kit (Qiagen). Purified amplicons were then used in a subsequent PCR reaction with universal attB1 and attB2 primers to generate complete attB homology arms, and the amplicons were then cloned into the Gateway® entry level donor vector, pDONR, according to manufacturer's instruction. After confirming the authenticity of each construct in pDONR, each *SCO* cDNA was transferred by a second homologous recombination reaction to the destination vector, pBABE-puro.

To ensure the fidelity of all constructs; plasmids were submitted to the NRC Plant Biotechnology Institute (Saskatoon, SK) for Sanger sequencing.

2.4.2 Bacterial transformation

XL-1 Blue or DH5α *E. coli* strains were used for plasmid amplification, and Rosetta BL-21 *E. coli* were used for expression for GST and GST fusion proteins. Chemically competent bacteria were thawed on ice for 10 minutes, and less than 5 µL of plasmid DNA (10 ng) was subsequently added to 30 – 50 µL. Bacteria were then incubated on ice for 30 minutes, heat shocked at 42°C for 45 seconds and cooled on ice for 2 minutes. Bacteria were diluted with 500 µL of pre-warmed SOC media (2% Bacto-tryptone, 0.5% Bacto-yeast, 10 mM MgCl2, 2.5 mM KCl, 8.5 mM NaCl, and 20 mM glucose) and allowed to recover for 1 hour at 37°C while shaking (225 rpm) prior to plating on 2YT media containing either ampicillin (100 µg/mL) or kanamycin (50 µg/mL). Plasmids were isolated and digested using the appropriate restriction enzymes prior to sequencing to ensure their integrity.

2.4.3 Plasmid isolation and DNA quantification

Plasmid DNA was isolated from chemically competent *E. coli* strains using the E.Z.N.A plasmid mini-prep kit according to the manufacturer's instructions. Isolated DNA was diluted

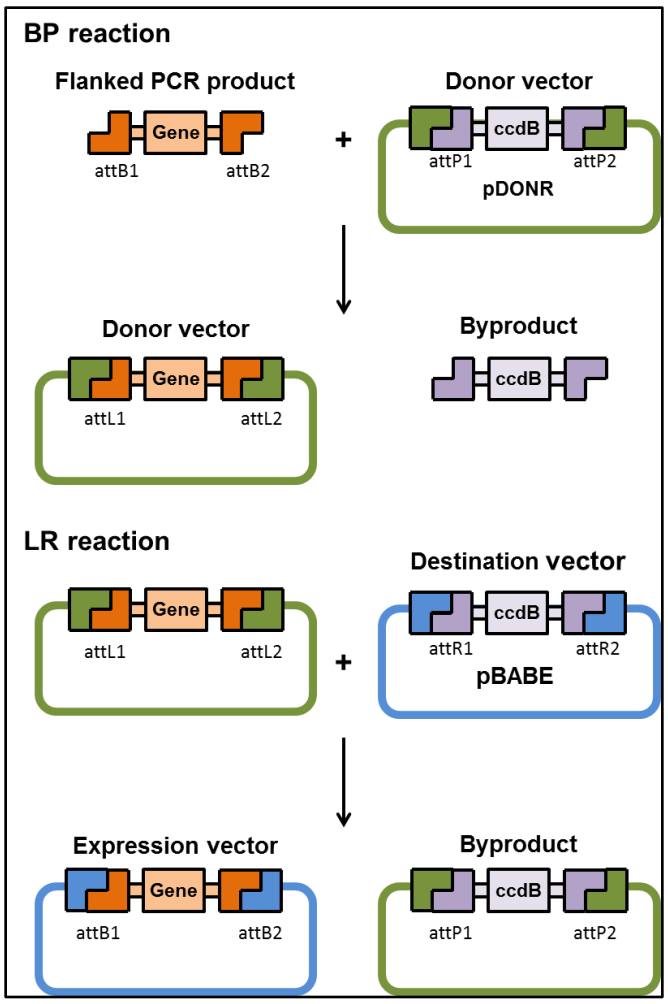

Figure 2.1: Description of Gateway® cloning

1:20 with triple-distilled water, and quantified by measuring the absorbance at 260 nm using a SpectraMAX 190 microplate spectrophotometer (Molecular Devices).

2.5 Retroviral transduction

Human fibroblasts or HEK293 cells were retrovirally transduced with vectors containing cDNAs that allowed for the overexpression of epitope tagged SCO1 or SCO2 variants or the metabolite transporters SLC25A1 or SLC25A11. Retrovirus was packaged using the Phoenix Amphotropic helper-free production system and then used to transduce cell lines as follows;

Day 1; Transfection of Phoenix cells. Phoenix cells were grown to 60-80% confluence and given fresh pre-heated media the day of transfection. JetPRIME™ Transfection Reagent

was used to transfect plasmid DNA according to manufacturer's instructions. Solution was added drop wise to the plate and then the Phoenix cells were placed in the incubator for 24 hours.

Day 2; Detoxification of Phoenix cells. Twenty-four hours post-transfection, media was replaced with fresh media to obtain a higher viral titer.

Day 3; Transduction of human fibroblasts or HEK293 cells. The retroviral-containing media was harvested 48 hours after transfection with plasmid DNA and filtered through a 0.45 µm filter. Polybrene, a cationic polymer that promotes viral infection, was added (5 µg/mL), and sufficient retroviral filtrate was subsequently added to cover the human fibroblasts or HEK293 cells (confluence between 40% and 60%). Cells were placed in the incubator for 2 hours and followed by the addition of fresh media containing polybrene.

Day 4 and 5; Selection for stable overexpressing cell lines. Twenty-four hours post-transduction the media was replaced with fresh media. Forty-eight hours post-transduction the selective agent, either 100 mUnits/mL hygromycin B or 2 ng/mL puromycin, was added. Cells were maintained in media supplemented with the appropriate selection agent.

2.6 Protein isolation

2.6.1 Protein concentration

The Bradford assay was used to quantify the protein concentration of all samples (Bradford, 1976). A standard curve was established using BSA (1 µg – 8 µg or 0.25 µg – 8 µg) in a 96-well plate. Samples (1 – 2 µL) were added to wells, and both the standards and samples were diluted with 250 µL of Bradford protein assay (Biorad). Absorbance was measured at 595 nm, and the protein concentration of samples was calculated using the BSA standard curve.

2.6.2 Whole cell extracts

Cells were harvested by trypsinization or manual scraping, and pelleted at 10,000 *x g* for 1 minute at 4°C. The resultant pellets were resuspended in ice-cold PBS, and centrifuged once again at 10,000 *x g* for 1 min at 4°C. Following protein quantitation, cells were resuspended at 4 mg/mL in PBS containing 1.5% n-Dodecyl-beta-D-Maltoside (DDM; BioShop) and a 1X protease inhibitor cocktail (PIC; Roche), and then lysed at 4^{o}C for 40 min. Lysates were clarified by centrifugation at 10,000 *x g* for 10 min at 4°C, and supernatants were removed and used for subsequent analyses.

2.6.3 Isolation of digitonized mitoplasts

An enriched mitoplast fraction was isolated from fibroblasts that had been transfected with control small-interfering RNA (siRNA) or COX20 siRNA, as previously described (Klement *et al.*, 1995). Briefly, cells were washed with PBS, trypsinized and then neutralized. Cell pellets were washed with ice-cold PBS containing 1X PIC, and pelleted at 10,000 *x g* for 1 minute at 4°C. Following protein quantitation, cells were resuspended at 5 mg/mL in ice-cold PBS. An equal volume of 4 mg/mL of digitonin (Calbiochem) resuspended in PBS was then added, and samples were incubated on ice for 10 minutes. Mitoplasts were isolated at 10,000 *x g* for 10 minutes and lysed for 30 minutes on ice in PBS containing 1.5% DDM and 1X PIC. Samples were vortexed every 5 minutes, and the clarified supernatants were removed after samples had been centrifuged at 16,000 *x g* for 10 minutes at 4°C and used for subsequent immunoblot analysis.

2.7 Co-immunoprecipitations

2.7.1 Purification of SCO1 antibodies from polyclonal serum

SCO1 or SCO2 antibodies were affinity purified by sequential incubation of crude polyclonal serum with a GST column and the appropriate GST-SCO fusion column. BL-21 Rosetta *E. coli* cultures were transformed with pGEX-6P3 plasmids coding for GST alone, GST-SCO1 or GST-SCO2 fusion proteins containing the peptide sequence to which the relevant SCO antibody was raised against. Bacteria were grown overnight in 20 mL of 2-YT media containing 100 µg/mL ampicillin, diluted in 1 L of 2-YT media the next morning and grown until the A_{600} was 0.4. IPTG (0.5 mM) was then added to the shaking culture, and protein expression was induced for 4 hours at 25°C. Bacteria were subsequently pelleted at 4000 *x* g for 5 minutes at 4°C, and washed once with ice cold PBS. Cultures were pelleted again and lysed in a buffer composed of 50 mM Tris (pH 7.0), 150 mM sodium chloride, 1X PIC, 1 mM ethylenediaminetetraacetic acid (EDTA) and 1 mg/mL lysozyme for 45 minutes, follow by sonication on ice three times for 5 second intervals using a Sonifer cell disruptor (Heat systems-ultrasonics) at power level 7. Lysate was incubated with Glutathione-Sepharose beads (GE Life Sciences) and then washed three times with PBS, according to manufacturer's instructions. GST protein was subsequently eluted from the beads using 10 mM reduced glutathione in 50 mM Bis-

Tris at pH 8.0, and purity was verified by staining an sodium dodecyl sulfate (SDS)-PAGE gel with Coomassie Brilliant Blue R-250 (Bio-Rad). Purified GST and GST-fusion proteins were then covalently bound to aldehyde-activated agarose AminoLink columns, as per manufacturer's instructions (Thermo Scientific).

Crude polyclonal SCO1 or SCO2 serum was pre-cleared by incubating it with GST coupled AminoLink columns. The flow through was then incubated with AminoLink columns to which the relevant GST-SCO fusion proteins had been coupled, and washed with two column volumes of PBS. Purified antibody was subsequently eluted with 5% acetic acid, which was immediately neutralized with 2 M Tris. Eluted antibody was concentrated and buffer exchanged in PBS using a 30 kDa centrifugal device (Pall), diluted with an equal volume of glycerol and stored at -20°C.

2.7.2 Mitochondrial isolation by differential centrifugation

Mitochondria used in co-immunoprecipitations were isolated by differential centrifugation. Confluent plates of either HEK293 cells or fibroblasts were washed once with PBS, and manually scraped. Cells were pelleted at 200 *x g* for 5min, and resuspended in STE buffer (10 mM Tris [pH 7.5], 0.25 M sucrose and 1 mM EDTA). Cells were subsequently homogenized on ice with ten strokes in a zero clearance Potter elvehjem homogenizer. Homogenate was centrifuged at 600 *x g* for 10 min at 4°C. The resultant supernatant was removed and spun down again at 600 *x g* for 10 min at 4°C. The second supernatant was then centrifuged at 8000 *x g* for 10 min at 4°C. The pellet was resuspended in STE buffer supplemented with 1X PIC. Homogenate was centrifuged again at 8000 *x g* for 10 min at 4°C and washed once with HIM buffer (220 mM mannitol, 70 mM sucrose, and 1 mM ethylene glycol tetraacetic acid (EGTA) in 10 mM 4-(2-hydroxyethyl)-1-piperazineethanesulfonic acid (HEPES) at pH 7.5). Pellet was resuspended in 1 mL of HIM buffer and the total protein content was quantified by Bradford assay. Mitochondrial isolate was pelleted a final time and aliquots were stored at -80°C.

2.7.3 Incubation with chemical crosslinker

Homobifunctional crosslinkers reactive towards primary amines were used to stabilize protein-protein interactions, based on previously established protocols (Sasarman *et al.*, 2010).

Frozen aliquots of isolated mitochondria were diluted to 0.33 mg/mL in HIM buffer containing 300 µM chemical crosslinker. Three different crosslinkers with increasing spacer arm lengths were used; 1,5-Difluoro-2,4-dinitrobenzene (DFDNB), disuccinimidyl glutarate (DSG) and disuccinimidyl suberate (DSS). Incubation with a given crosslinker was done for 60 minutes on ice, with reactions being quenched by adding 80 mM glycine (pH 8.0) for 10 minutes. Crosslinked mitochondria were subsequently pelleted at 10,000 *x* g for 10 minutes at 4°C, and lysed at 3.5 mg/mL in 50 mM HEPES (pH 7.6), 150 mM NaCl, 1% taurodeoxycholic acid (t-DOC) and 1X PIC. After 40 minutes on ice, lysates were clarified by centrifugation at 16,600 *x g* for 40 minutes at 4°C.

2.7.4 Preparation of magnetic beads

Antibodies were crosslinked to protein A or protein G DynaBeads (Invitrogen) using a combination of the manufacturer's instructions and a previously established protocol (Sasarman *et al.*, 2010). Briefly, dynabeads were washed three times with 0.1 M Na-phosphate (pH 8.0). An antibody solution containing 0.1 M Na-phosphate was then mixed with the Dynabeads at a 1 µL of bead solution:1 µg of antibody ratio, and rotated overnight at 4°C. The next day the antibody solution was removed, washed once with NaP-W1 (0.1 M Na-phosphate [pH 8.0], 0.08% Tween-20) and twice with TEA-W (0.2 M triethanolamine [pH 8.0], 0.08% Tween-20). Antibodies were then chemically coupled to protein A or protein G Dynabeads by incubating for 30 minutes in TEA-W containing 5.4 mg/mL dimethyl pimelimidate (DMP), a reversible homobifunctional crosslinker reactive towards amines. The crosslinking solution was removed and crosslinking was quenched by incubating the beads for 15 minutes in a buffer containing 50 mM Tris (pH 7.5) and 0.08% Tween-20. Beads were then washed three times with NaP-W1 and excess, unbound antibody was eluted with two consecutive 10 minute incubations in 0.1 M glycine (pH 2.5) containing 0.08% Tween-20. Beads were washed three more times with NaP-W1 prior to incubating antibody-crosslinked Dynabeads with mitochondrial extracts. All the wash and incubation volumes were 10 fold the bead volume, except for the 3 NaP-W1 washes prior to antibody incubation, and the first NaP-W1 wash prior to DMP crosslinking which were 5 fold the bead volume. Elution volumes were equivalent to the bead volume. In co-immunoprecipitation experiments where beads-alone controls were used, DynaBeads were taken through this protocol without any antibody.

2.7.5 Co-immunoprecipitations with or without chemical crosslinkers

Lysed mitochondrial extracts that had been chemically crosslinked were incubated with SCO1 or FLAG coupled DynaBeads, or Dynabeads alone. For SCO2-HA co-immunoprecipitations, commercially available agarose beads coated with HA antibodies (Sigma-Aldrich) were used along with agarose beads alone. Samples were incubated with beads overnight at 4°C with rotational mixing. The next morning, beads were washed five times with NaP-W2 (0.1 M Na-phosphate [pH 8.0], 0.08% Tween-20 and 0.05% t-DOC), and the beads were incubated for 10 minutes in 5% acetic acid to elute bound protein. Eluate was immediately neutralized with 2 M unbuffered Tris. Beads were then washed one time with 0.1 M Na-phosphate (pH 8.0) and boiled in 1 X Laemmli sample loading buffer (Bio-Rad) with 100 mM dithiothreitol (DTT).

Co-immunoprecipitations were also performed in the absence of chemical crosslinkers. In these experiments, isolated mitochondria were resuspended at 1.5 mg/mL in a buffer containing 20 mM Tris (pH 7.5), 50 mM potassium chloride, 0.4% DDM and 1X PIC, and lysed for 5 minutes on ice. Extracts were centrifuged at 16,000 *x g* for 30 minutes at 4°C, and the supernatant was incubated overnight at 4°C with rotational mixing with DynaBeads alone or antibody coupled Dynabeads. The next morning, beads were washed three times with a buffer composed of 20mM Tris (pH 7.5) and 50 mM KCl, and the bound protein was eluted by boiling in sample loading buffer supplemented with 100 mM DTT.

2.7.6 Mass spectrometric analysis

For co-immunoprecipitations involving chemical crosslinkers, 20% of the eluate was reserved for Western blot analysis. The remainder of the eluate was precipitated by adding 15% trichloroacetic acid (vol/vol). Samples were vortexed and incubated on ice for 30 minutes prior to being stored overnight at -80°C. The next morning, samples were thawed on ice and pelleted at 20,000 *x g* for 30 minutes at 4°C. Pellets were washed twice with ice cold acetone, and recentrifuged at 20,000 *x g* for 15 minutes at 4°C in between each wash. Pellets were subsequently allowed to dry for 10 minutes at room temperature. Dried pellets were then sent to the Institut de Recherches Cliniques de Montréal, where they were resuspended, trypsinized and

analyzed by LC-MS using an OrbiTrap mass spectrometer. Peptide fragments were assigned to proteins computationally using Scaffold software and the human UniProt protein database.

2.8 Small interfering RNA transfections

Stealth RNAi™ siRNA was designed to target either SLC25A1, or SLC25A11, while constructs against COX20 were kind gifts from Dr. Antonio Barrientos, University of Miami (Invitrogen). BLOCK-iT™ Alexa Fluor Red scrambled siRNA is not homologous to any known gene and was used monitor transfection efficiency (Invitrogen) (Table 2.4). Control and patient fibroblasts were transfected with 12.5 nM siRNA using Lipofectamine RNAiMAX on days 0, 3 and 6 when cells were 40-50% confluent. Cells when then harvested either on day 8 for SLC25A1 and SLC25A11, or day 9 for COX20 knockdowns.

2.9 Protein visualization techniques

2.9.1 SDS-Polyacrylamide gel electrophoresis (PAGE)

Cellular extracts or fractions from co-immunoprecipitations were separated by SDS-PAGE prior to Western blotting or Coomassie blue staining. Samples were mixed with an equal volume of 2X Laemmli sample loading buffer containing 200 mM DTT. Samples were boiled for 5 minutes, or incubated for 10 minutes at 37°C prior to being loading onto SDS-PAGE gels. Pre-cast Criterion (Bio-Rad) or homemade 4-20% gels and manually poured 12% and 15% fixed percentage SDS-PAGE gels were used. The gels were run for 30 minutes at 90 V to allow the

Table 2.4: List of Stealth RNAi™ constructs

Description	**Exon targeted**	**Invitrogen Stealth Oligo ID #**
BLOCK-iT™ Alexa Fluor Red scrambled	N/A	
SLC25A1-1	9	HSS185938
SLC25A1-2	8,9	HSS109962
SLC25A1-3	7,8	HSS109961
SLC25A11-1	6,7	HSS112215
SLC25A11-1	2,3	HSS112214
SLC25A11-1	2,3	HSS112213
COX20 siRNA1	1,2	HSS151056
COX20 siRNA2	2	HSS151057

samples to enter the resolving phase, at which point the voltage was increased to 110V for 30 minutes. The voltage was then increased to 130V until the dye front reached the bottom of the gel, and electrophoresis was discontinued.

2.9.2 Western blotting

For immunoblotting experiments, 10-30 µg of protein was loaded per lane and separated by SDS-PAGE or BN-PAGE. Proteins were transferred to nitrocellulose using semi-dry transfer (Transblot SD from Biorad). Membranes were subsequently blocked overnight with rotational mixing at 4°C with either 5% BSA or 5% Blotto non-fat dry milk (Santa Cruz) dissolved in the appropriate TBST or PBST. Membranes were then incubated overnight at 4°C with rotational mixing in primary antibody solution. Unpurified polyclonal SCO1 (1:200) and SCO2 (1:200), Porin (1:1000) (Millipore), SD70 (1:10000), and COX II (1:1000) (Mitosciences) were diluted in 5% BSA in 20 mM Tris, 135 mM NaCl and 0.1% Tween-20 (Jaksch *et al.*, 2001; Leary *et al.*, 2004). Affinity-purified SCO1 (1:1000) and COX20 (1:1000; kind gift of Dr. Antonio Barrientos, University of Miami) antibodies were diluted in 5% Blotto non-fat dry milk in TBST (25 mM Tris [pH 7.4], 135 mM NaCl, 2.5 mM KCl and 0.1% Tween-20). SLC25A1 (1:1000) and SLC25A11 (1:1000) (ProteinTech) were diluted in 5% Blotto non-fat dry milk in PBS with 0.05% Tween-20. Following incubation in affinity purified primary antibody, membranes were washed six times for five minutes per wash. Membranes incubated with crude antisera were washed six times for 30 minutes per wash. Membranes were then incubated for 60 minutes at room temperature with rotational mixing in the appropriate horseradish peroxidase conjugated secondary antibody (1:5000, BioRad). Washes were subsequently repeated, and the abundance of each protein was detected by regular (Cell Signaling) or enhanced (West-Femto, Thermo-Scientific) chemiluminescence.

2.9.3 Coomassie blue staining

Coomassie Brilliant Blue R-250 was used to stain SDS-PAGE gels to visualize the complexity of the eluate in SCO1-FLAG co-immunoprecipitations or confirm successful purification of GST proteins. Following electrophoresis, SDS-PAGE, gels were washed once and fixed for 30 minutes with destain solution (45% methanol and 10% acetic acid). The gel was then stained for either 60 minutes or overnight in destain solution containing 0.3% Coomassie

Brilliant Blue. Gels were washed with destain solution and rotational mixing until the majority of the background was removed, imaged and stored at 4^{o}C in 10% acetic acid.

3 RESULTS

3.1 Optimization of chemical crosslinking conditions

Co-immunoprecipitations of SCO1 and SCO2 were conducted to identify their potential interacting partners. Because metallochaperones typically associate with their partners through weak and highly transient interactions (Chen *et al.*, 2013), the potential utility of chemical crosslinkers was first evaluated. The goal of these initial experiments was to determine optimal conditions for crosslinker driven formation of higher-order adducts specific to SCO proteins. Isolated mitochondria were incubated with DFDNB, DSG or DSS, three amine reactive, homobifunctional crosslinkers that differ only in their spacer arm length. The effect of adding copper, reductant or respiratory substrates to the buffer on the efficiency of crosslinking was also

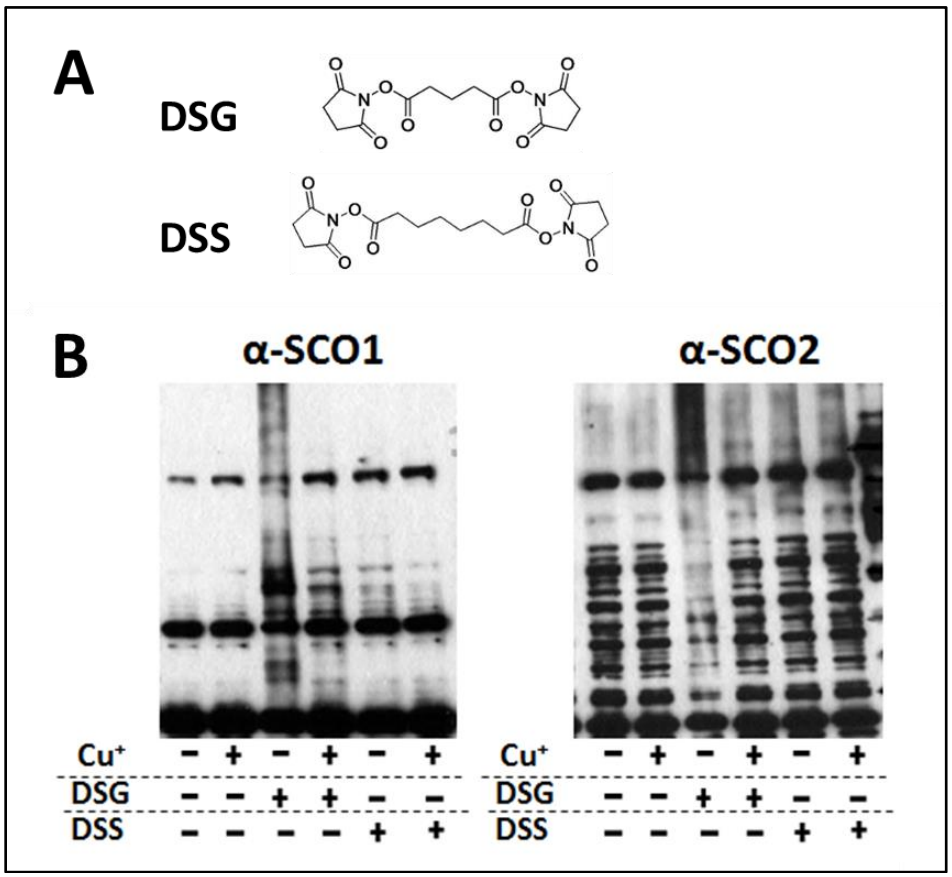

Figure 3.1: Immunoblot analysis of HEK293 mitochondria incubated in the absence or presence of crosslinker. (A) Structures of DSG and DSS, the two homobifunctional compounds used in crosslinking experiments. (B) Isolated mitochondria isolated were incubated in buffer with or without copper, and in the same buffer supplemented with DSG or DSS crosslinkers. Proteins were extracted and separated on a 4-20% SDS-PAGE gel, and membranes were immunoblotted with unpurified SCO1 or SCO2 antibody.

considered. DSG produced the largest increase in the abundance of higher-order, crosslinked SCO protein adducts, an effect that was independent of adding any of the aforementioned elements to the buffer (Figure 3.1 and data not shown). However, Western blotting with our crude SCO1 or SCO2 antiserum showed that these reagents were not suitable for co-immunoprecipitations, because there was a significant amount of non-specific background, even in the absence of crosslinking.

3.2 Co-immunoprecipitation of epitope-tagged SCO1 and SCO2

3.2.1 Characterization of epitope-tagged SCO1 and SCO2

To improve the signal to noise of the experiment, several C-terminal, epitope-tagged variants of SCO1 (SCO1-FLAG, SCO1-Tev/6xHis) and SCO2 (SCO2-HA, SCO2-Tev/6xHis) that had been developed prior to my arrival in the lab were used. Like the wild-type proteins, retroviral overexpression of all epitope-tagged SCO variants rescued the COX deficiency in the relevant *SCO* patient cells, and further reduced residual COX activity in the reciprocal *SCO* patient background (data not shown). To compare the abundance of epitope-tagged SCO variants to that of endogenously expressed SCO proteins, HEK293 cells were transduced with retrovirus packaging each of the *SCO* cDNAs and whole cell extracts were analyzed by Western blotting. The steady-state levels of each epitope-tagged SCO protein were significantly higher than those of either endogenous SCO1 or SCO2 (Figure 3.2). Although forced overexpression systems may promote non-specific interactions between proteins, these epitope tags can be detected with high quality, commercially available monoclonal antibodies. Therefore, epitope-tagged SCO proteins represented attractive targets for the affinity purification of crosslinked SCO protein complexes.

3.2.2 Stabilization of protein-protein interactions by chemical crosslinking

To ensure that the signal to noise was indeed improved and that the epitope tag itself did not promote non-specific crosslinking, crosslinking experiments were repeated in mitochondria isolated from HEK293 cells overexpressing each of the epitope-tagged SCO proteins (Figure 3.3). As expected, the use of antibodies against the epitope tags markedly reduced background immunoreactivity. Western blotting of uncrosslinked and crosslinked protein extracts confirmed the presence of an immunoreactive band of ~60 kDa, consistent with the previous observation

that SCO proteins exist as homodimers *in vivo* (Leary *et al.*, 2004). Because detection of the dimer requires the presence of an epitope tag, the immunoreactive dimers that were observed may consist solely of epitope-tagged SCO proteins or be comprised of an epitope-tagged SCO and a wild-type protein. However, in addition to the monomeric and dimeric form of each SCO protein, a non-specific band was observed for both of the 6x His-tagged SCO proteins, in the presence or absence of crosslinking. For this reason and because of their higher relative expression levels (Fig 3.3), HEK293 cells overexpressing SCO1-FLAG or SCO2-HA were used for subsequent co-immunoprecipitations.

3.2.3 Co-immunoprecipitation of SCO1-FLAG or SCO2-HA

To identify potential interacting partners of SCO1 and SCO2, SCO1-FLAG or SCO2-HA were co-immunoprecipitated from mitochondria isolated from HEK293 cells. Crosslinked mitochondrial extracts were precleared and then incubated with either FLAG or HA antibodies conjugated to beads. Beads were washed, and bound protein was eluted first by incubating in 5% acetic acid and then by boiling in sample loading buffer. Western blot analysis of each fraction confirmed the successful affinity purification and elution of SCO1-FLAG and

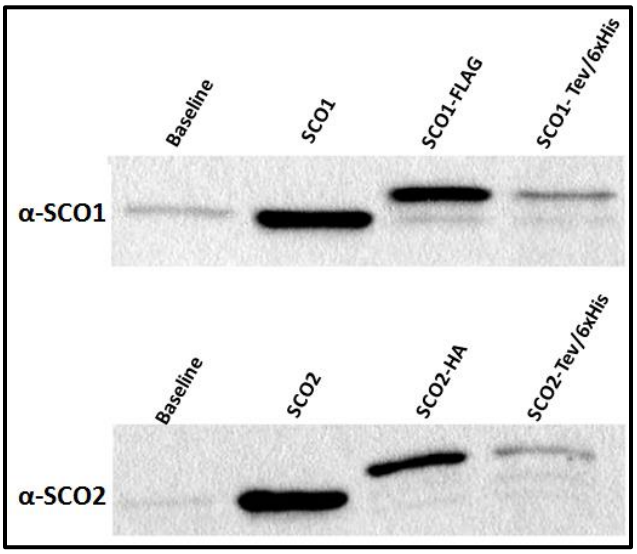

Figure 3.2: Immunoblot analysis of epitope-tagged SCO1 and SCO2 overexpression in HEK293 cells. Whole cell extracts from HEK293 cells stably expressing each SCO variant were lysed and separated on a 12% SDS-PAGE gel. Membranes were blotted with crude antiserum that specifically recognizes SCO1 or SCO2. Baseline denotes untransduced HEK293 cells.

SCO2-HA from the beads (Figure 3.4). For both the anti-FLAG and anti-HA immunoprecipitations, the yield of epitope-tagged SCO protein recovered in the eluate was substantially lower than that which would be predicted based on the observed immunodepletion of the input. However, SCO1-FLAG and SCO2-HA were never detected in the wash fractions and were not recovered by further elution steps (data not shown). Despite the inexplicable loss of some of the immune complex, the eluates contained both endogenous and epitope-tagged SCO proteins, and there was good concordance between the immunoreactivity observed by Western blotting and the major protein species detected by Coomassie staining of the E_2 fraction. Crosslinked SCO1-FLAG and SCO2-HA eluates were therefore analyzed by mass spectrometry, to identify the protein constituents of the E_1 fraction (Figure 3.4).

3.2.4 Mass spectrometric analysis of the eluates

Co-immunoprecipitations were repeated as described above, and extracts from DSG crosslinked mitochondria were incubated with an antibody:bead conjugate or beads alone, to control for

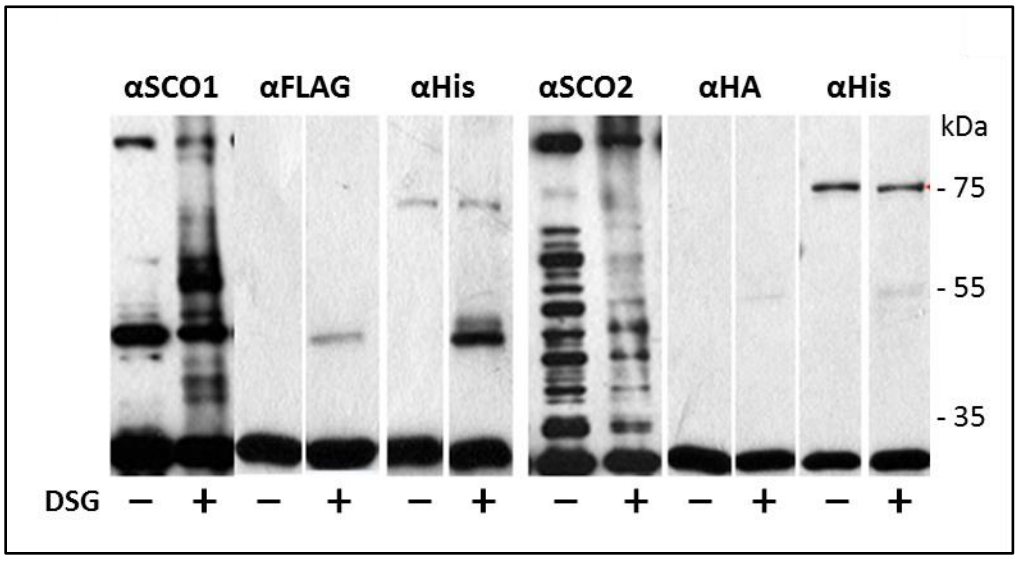

Figure 3.3: Immunoblot analysis of uncrosslinked and crosslinked mitochondrial extracts derived from HEK293 cells. Mitochondria were isolated from untransduced HEK293 cells or from transduced cells overexpressing SCO1-FLAG, SCO1-Tev/6xHis, SCO2-HA, or SCO2-Tev/6xHis. Mitochondria were incubated in the absence or presence of DSG, lysed, and protein extracts were subsequently separated on a 4-20% SDS-PAGE gel. Membranes were then blotted with the appropriate primary antibody; for example, HEK293 cells expressing SCO1-FLAG were blotted with α-FLAG and untransduced cells were blotted using crude antibody specific for SCO1 or SCO2.

non-specific protein binding. One tenth of the protein eluted by acetic acid was analyzed by Western blotting to confirm that each epitope-tagged SCO protein had been successfully immunoprecipitated, and the remainder of this eluate was analyzed by LC-MS to identify its protein constituents. A total of 542 and 436 proteins were identified in the SCO2-HA and SCO1-FLAG eluates, respectively. Although neither SCO protein was identified in the reciprocal co-immunoprecipitation, known COX assembly factors, including COX18 and COX20 (Hell *et al.*, 2000; Tzagoloff and Dieckmann, 1990), and the COX II structural subunit of the COX holoenzyme (Capaldi, 1990) were detected in both pulldowns. However, a large number of unrelated structural proteins, subunits of the other oxidative phosphorylation complexes and mitochondrial proteases were also identified. The disproportionate number of quality control proteins present in the eluates of each co-immunoprecipitation suggested that the overexpression of epitope-tagged SCO proteins may be promoting non-specific interactions, or favouring interactions with proteases. Therefore to determine whether the observed interactions reflected real biology or were an artefact of the overexpression system, co-immunoprecipitations of endogenous SCO proteins were attempted.

3.3 Co-immunoprecipitations of endogenous SCO1 and SCO2

3.3.1 Purification of SCO1 and SCO2 antibodies

Crude polyclonal antisera raised against peptide sequences from SCO1 or SCO2 were affinity purified. However, sequential purification of SCO1 and SCO2 antibodies on a GST column and the appropriate GST-SCO fusion protein column, only yielded a useful analytical reagent for SCO1 (Figure 3.5, data not shown). Because of the inability to generate an affinity-purified SCO2 antibody, the focus of the remainder of my M.Sc. project shifted towards identifying potential interacting partners of SCO1.

3.3.2 Validation of affinity-purified SCO1 antibody for co-immunoprecipitation experiments

The ability to co-immunoprecipitate endogenous SCO1 opened up the possibility of identifying interacting partners in control cells, and investigating whether these interactions were perturbed in patient cells that harbour alleles with pathogenic mutations in *SCO1* or *SCO2*.

Fibroblasts from the *SCO1-2* patient were included in these experiments, even though the steady-state levels of the SCO1 M294V variant are less than 5% of those of the wild-type protein in control and *SCO2* patient cells (Figure 3.6).

To ensure that our affinity-purified SCO1 antibody is able to detect crosslinked SCO1 protein adducts, isolated mitochondria from control and *SCO1-2* patient fibroblasts were incubated in the presence or absence of DSG and analyzed by Western blotting. A significant accumulation of higher order, crosslinked adducts was observed in control cells, but not in

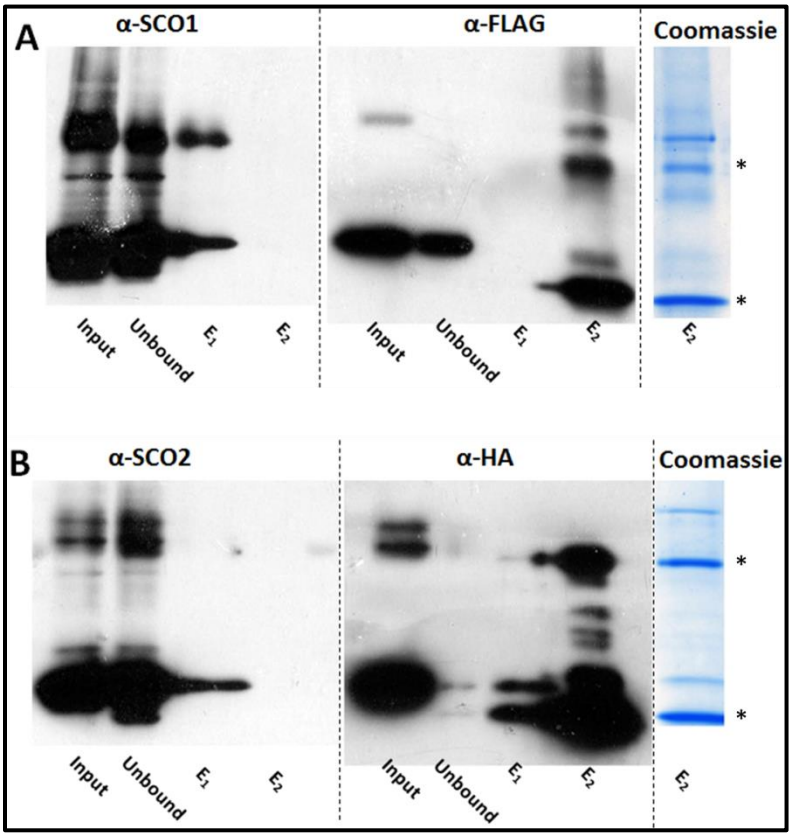

Figure 3.4: Immunoblot and Coomassie stain analyses of SCO1-FLAG (A) and SCO2-HA (B) co-immunoprecipitations. Crosslinked mitochondrial extracts were precleared with beads devoid of antibody, and then incubated overnight with antibodies specific for the appropriate epitope. After five washes, beads were first eluted with acetic acid (E_1), and residual protein was removed by boiling in sample loading buffer with reductant (E_2). Equal fractions (10%) of each sample were separated by SDS-PAGE and membranes were blotted with the indicated primary antibodies. The remainder of the E_2 fraction (90% of total) was loaded on a separate SDS-PAGE gel, and post-stained with Coomassie blue to visualize the total protein profile. Bands corresponding to the light and heavy chains are labelled with an asterisk.

in *SCO1-2* patient fibroblasts (Figure 3.7), arguing that the affinity-purified antibody is capable of specifically pulling down crosslinked adducts containing endogenously expressed SCO1.

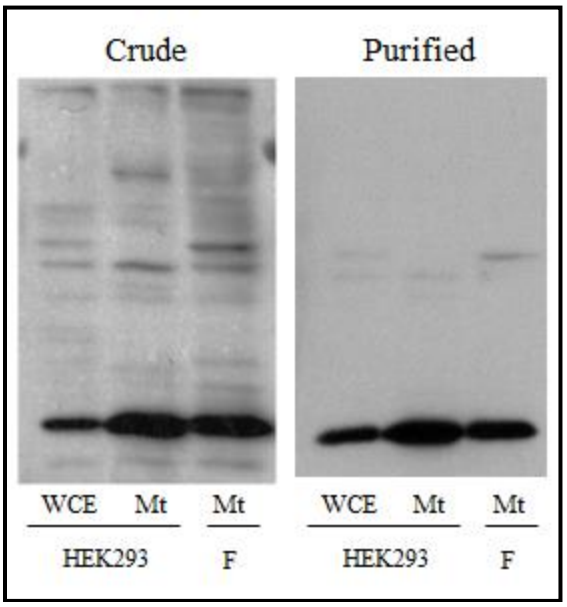

Figure 3.5: Comparative analysis of membranes blotted with either crude or affinity-purified SCO1 antiserum. Whole cell extracts (WCE) from HEK293 cells and mitochondrial (Mt) extracts from HEK293 cells and fibroblasts (F) were separated by SDS-PAGE. Membranes were subsequently blotted with crude or purified SCO1 antibodies.

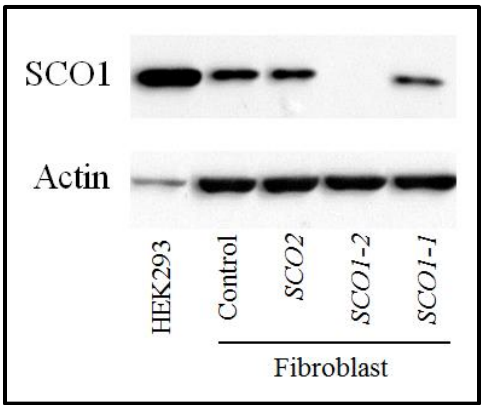

Figure 3.6: Immunoblot analysis of SCO1 abundance in fibroblasts and HEK293 cells. Whole cell extracts were generated by lysing cells in PBS containing 1.5% DDM and a complete protease inhibitor cocktail. Lysates from HEK293 cells and fibroblasts from control and *SCO* patient backgrounds were separated on a 12% SDS-PAGE gel. The resultant membrane was subsequently blotted with anti-SCO1. Blotting with anti-actin served as a loading control.

3.3.3 Co-immunoprecipitation of endogenous SCO1 from control and *SCO* patient mitochondria.

To optimize quantitative pulldown of endogenous SCO1, co-immunoprecipitations were performed in the absence of crosslinker. Purified SCO1 antibody was incubated with mitochondrial extracts at an antibody to protein ratio that was effective for co-immunoprecipitation of SCO1-FLAG (1:7.5), and at an antibody to total protein ratio that was 4 fold higher (4:7.5). Protein bound to the antibody-bead complex was first eluted in 5% acetic acid, and then by boiling in sample loading buffer (Figure 3.8A). This analysis showed that incubation with 5% acetic acid (E1) was sufficient to elute all of the bound SCO1, and that the 1:7.5 ratio of antibody to protein was unable to quantitatively deplete SCO1 from the input fraction. To determine the minimal amount of antibody required for quantitative SCO1 pulldown, co- immunoprecipitations were repeated with varying antibody to protein ratios. These analyses demonstrated that the majority of SCO1 was depleted from the input fraction using a ratio of 3:7.5 (Figure 3.8B), a result that was not affected by crosslinking (data not shown). This ratio was therefore used for all future co-immunoprecipitation experiments.

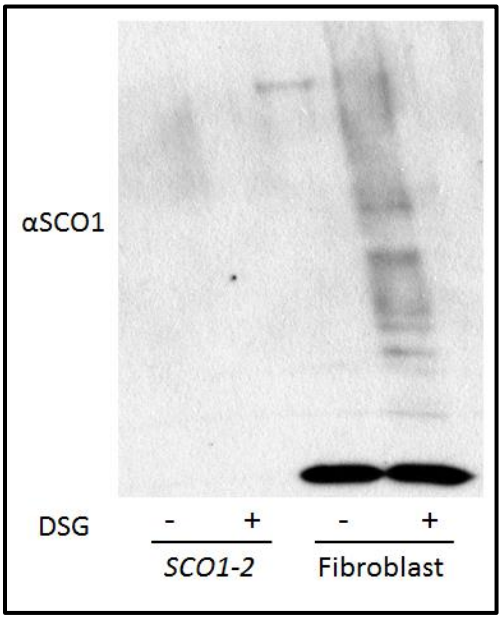

Figure 3.7: Immunoblot analysis of crosslinked mitochondrial extracts. Mitochondria isolated from control and *SCO1-2* patient fibroblasts were incubated with or without DSG. Protein extracts were separated on a 4-20% SDS-PAGE gel, and the membrane was immunoblotted with affinity-purified SCO1 antibody.

To ensure that sufficient protein was present in the eluate to identify interacting partners, large-scale co-immunoprecipitations were conducted with crosslinked mitochondrial extracts isolated from control, *SCO1-1, SCO1-2* and *SCO2* patient fibroblasts. Crosslinked mitochondrial extracts from control fibroblasts were also incubated with DynaBeads alone, which served as an internal, negative control. Following elution with 5% acetic acid, a fraction of the eluate was analyzed by Western blotting to confirm the co-immunoprecipitation was successful, and that it contained higher order, crosslinked SCO1 adducts (Figure 3.9). The remainder of the eluate (80%) was TCA precipitated, and sent for LC-MS analysis.

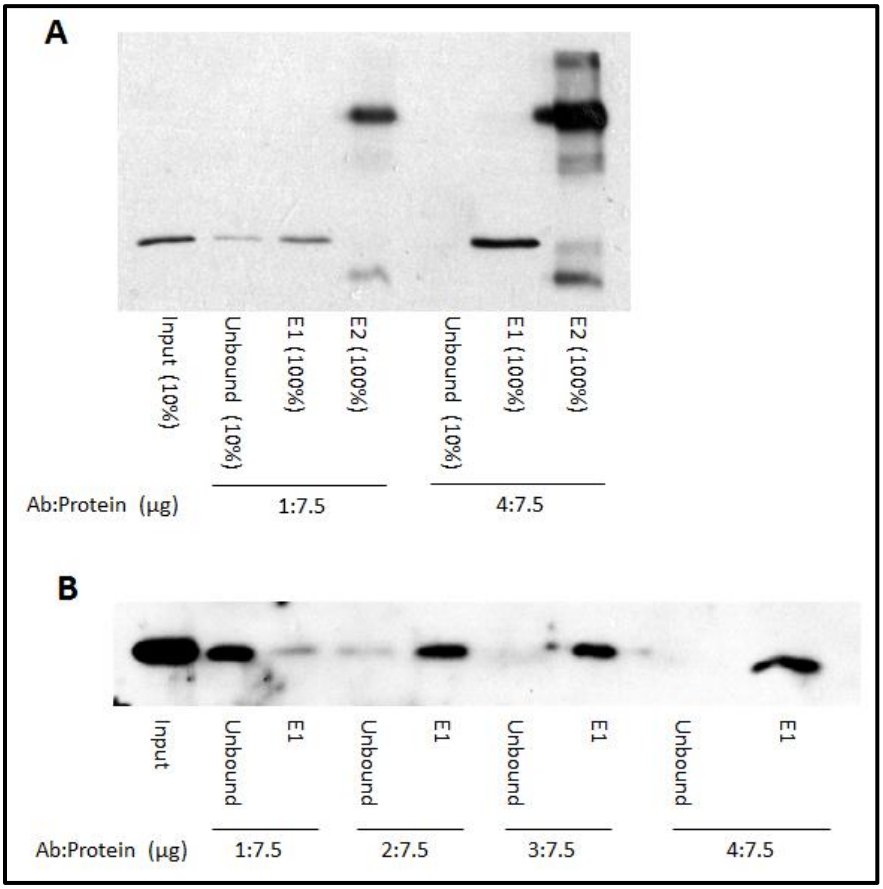

Figure 3.8: Optimization of co-immunoprecipitation of endogenous SCO1. (A) Endogenous SCO1 was co-immunoprecipated using either a ratio of antibody-bead complex to total mitochondrial protein of 1:7.5 or 4:7.5. Beads were washed, and incubated sequentially in acetic acid (E1) and boiling sample loading buffer with reductant (E2). Acetic acid elutions were TCA precipitated, the indicated percentage of each fraction was separated a 4-20% SDS-PAGE gel, and the membrane was then blotted with crude SCO1 antibody. (B) Co-immunoprecipitations were performed as described in panel A, with the antibody-bead to protein ratio being increased as indicated. Equal percentages (50%) of all samples were separated on a 4-20% SDS-PAGE and blotted with affinity-purified SCO1 antibody.

3.3.4 Mass spectrometric analysis of the eluates

Mass spectrometric analysis of SCO1 eluates isolated from control and *SCO* patient cells identified 653 different proteins that were common to all samples.

3.4 Prioritization of candidate interacting partners

Mass spectrometric analysis of eluates from both the epitope-tagged and endogenous co-immunoprecipitations of SCO1 produced large lists of potential interacting partners. Specifically, 436 and 653 unique proteins were identified in the FLAG-tagged and endogenous SCO1 co-immunoprecipitations. There was therefore a pressing need to collate and refine these two datasets, to generate a prioritized list of candidate interactions worthy of further investigation. Because of the potential confounding effects of using an overexpression system, candidate interacting partners identified by co-immunoprecipitating endogenous SCO1 were first considered. To begin, proteins with a significant peptide count (>5) in the beads alone control

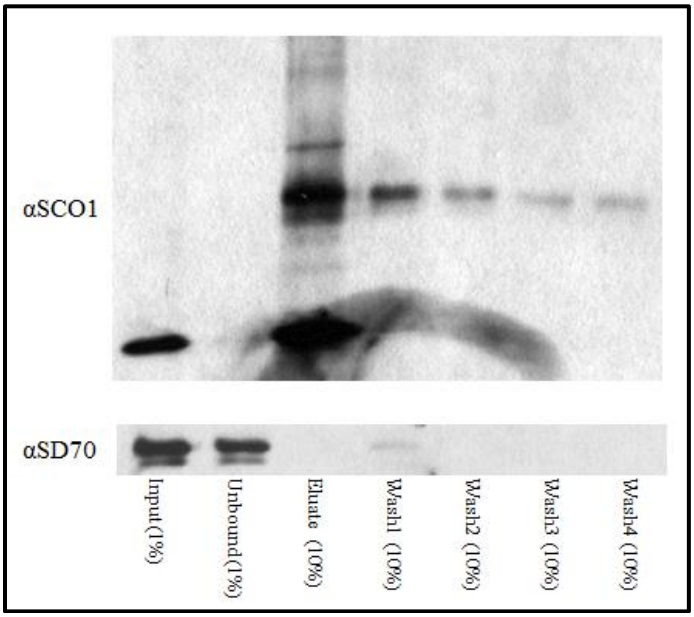

Figure 3.9: Validation of SCO1 co-immunoprecipitation by Western blot analysis. Crosslinked mitochondrial extracts from control fibroblasts were immunoprecipitated with affinity-purified SCO1 antibody. The eluate was TCA precipitated, and a percentage of each fraction was separated on a 12% SDS-PAGE gel. The resultant membrane was blotted with purified SCO1 antibody, followed by an antibody which recognizes SD70, another mitochondrial protein that is associated with the inner membrane.

were removed from the list. Proteins with annotated gene ontology functions related to immunity or the cytoskeleton were then discarded, as were those that are not contained within MitoCarta, a gold standard compendium of all known human mitochondrial proteins (Pagliarini *et al.*, 2008). This strategy collectively reduced the list of candidate interacting partners to a total of 157 proteins, which were then rank ordered based on the total number of peptide fragments identified for each protein. Because there was still a significant number of potential interacting partners, the candidate interactions identified in the SCO1-FLAG co-immunoprecipitation were prioritized using the identical strategy. This reduced the final list of potential interacting partners of SCO1-FLAG to 141, 85 of which were also identified by co-immunoprecipitation of the endogenous protein.

After collating the two datasets, SCO1 was the third ranked hit based on total number of peptides identified per protein (Table 3.1). However, none of the top ranked proteins was an attractive candidate, given the curated literature describing their function (see Discussion, for more details). Other proteins that were identified had fewer peptide fragments. Many of these were known COX structural subunits or COX assembly factors, while others were metabolite transporters (Table 3.2). Therefore, the focus of the remainder of my M.Sc. studies was to validate the observed physical interaction between SCO1 and COX20, a known COX assembly factor with an ill-defined role in holoenzyme biogenesis; and between SCO1 and SLC25A1 and SLC25A11, two metabolite transporters that may also be involved in trafficking copper across the inner mitochondrial membrane.

3.5 Characterization of COX20, a COX assembly factor

If SCO1 and COX20 function together during COX assembly, pathogenic mutations in *SCO1* or *SCO2* that interfere with COX assembly may affect the steady-state levels of COX20. Indeed, Western blot analysis showed a modest increase in the abundance of COX20 in *SCO1-1* and *SCO2-9* patient cells (Figure 3.10).

Table 3.1: Proteins with highest peptide numbers identified in eluates of co-immunoprecipitations of SCO1-FLAG (-FLAG) from HEK293 cells and SCO1 from control (Ctrl) fibroblasts.

Peptides identified (#)		Protein name
-FLAG	**Ctrl**	
16	66	Mitochondrial inner membrane protein (IMMT)
14	40	Stomatin-like protein 2 (STOML2)
42	31	SCO1
1	30	Hexokinase-1 (HK1)
6	29	NADH-ubiquinone oxidoreductase 75 kDa subunit (NDUFS1)
10	29	Cytochrome b-c1 complex subunit 2 (UQCRC2)
3	28	NADH dehydrogenase [ubiquinone] iron-sulfur protein 3, (NDUFS3)
15	27	Elongation factor Tu (TUFM)
12	26	Coiled-coil-helix-coiled-coil-helix domain-containing protein 3, (CHCHD3)
16	25	Voltage-dependent anion-selective channel protein 2 (VDAC2)

.

Table 3.2: Rank ordered proteins in eluates of co-immunoprecipitations of SCO1-FLAG (-FLAG) from HEK293 cells and SCO1 from control (Ctrl) fibroblasts that are known (A) and potential (B) interacting partners of SCO1.

A

Peptides identified (#)		Protein name
-FLAG	**Ctrl**	
1	4	Cytochrome c oxidase subunit 4 (COX4)
0	4	Cytochrome c oxidase subunit 5B (COX5B)
2	2	Cytochrome c oxidase subunit 2 (COX II)

B

Peptides identified (#)		Protein name
-FLAG	**Ctrl**	
7	20	Phosphate carrier protein (SLC25A3 or PIC2)
7	15	Tricarboxylate transport protein (SLC25A1)
2	9	Mitochondrial 2-oxoglutarate/malate carrier (SLC25A11)
2	2	Cytochrome c oxidase protein 20 (COX20)

3.5.1 Validation of physical interaction between SCO1 and COX20

To validate the observed interaction between SCO1 and COX20, I took advantage of a cell line generated by a collaborator (Dr. Antonio Barrientos, University of Miami). More specifically, TALENs technology was used to knockout the *COX20* gene in HEK293 cells, and FLAG-tagged COX20 was then stably overexpressed in one of the resultant knockout clones, to create a line hereafter named KO-*COX20* + COX20-FLAG (Bourens *et al.*, 2014). Consistent with the mass spectrometry data, SCO1 was co-purified by immunoprecipitation of COX20-FLAG from uncrosslinked mitochondria (Bourens *et al.*, 2014). The reciprocal immunoprecipitation with our SCO1 antibody also resulted in the specific pulldown of a small amount of FLAG-tagged COX20 (Figure 3.11).

3.5.2 Effect of siRNA knockdown of COX20 on COX II abundance

To better understand the functional significance of the physical interaction between COX20 and SCO1, COX20 was transiently knocked down in control and *SCO* patient fibroblasts. Transfection of cells with BLOCK-iT Alexa scrambled siRNA served as an internal, negative, control. Untreated and siRNA treated cells were harvested and a digitonized fraction was subsequently analyzed by Western blotting (Figure 3.12). Treatment with either *COX20* siRNA1 or siRNA2 significantly reduced the abundance of COX20 in control and patient fibroblast lines, and modestly, but reproducibly, reduced the levels of COX II in *SCO* patient

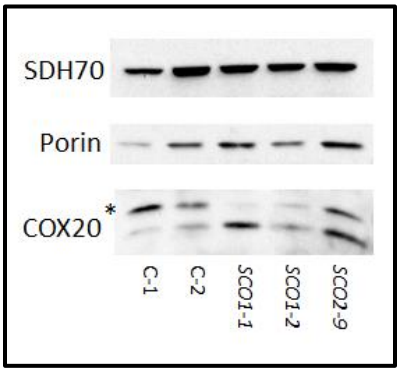

Figure 3.10: Steady-state protein levels of COX20. Control (C-1 and C-2) and *SCO* patient fibroblasts were permeabilized using digitonin to enrich the lysate for mitochondria. Samples were separated using a 15% SDS-PAGE gel and blotted with the appropriate antibodies. SDH70 and Porin were used as mitochondrial loading controls. The asterisk (*) indicates a background band observed with the COX20 antibody.

cells. Because the abundance of COX II is a marker of holoenzyme content, this result provides genetic evidence that further supports an important role for an interaction between COX20 and SCO1 in COX assembly.

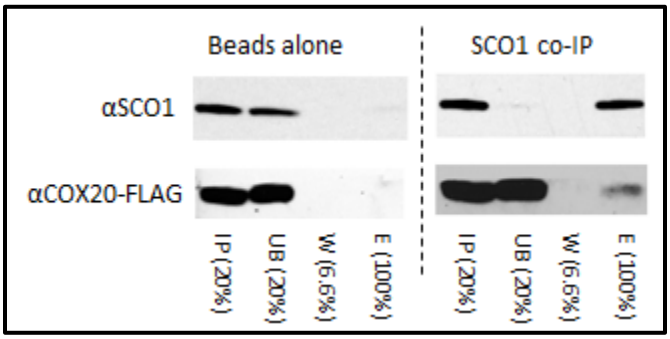

Figure 3.11: SCO1 interacts with epitope-tagged COX20. Mitochondria isolated from the KO-*COX20* + COX20-FLAG cell line were lysed (IP) and incubated overnight with a SCO1 antibody-bead conjugate. Unbound extract (UB) was removed, and beads were washed three times (W) prior to boiling in sample loading buffer with reductant (E). The washes were pooled, and a percentage of each fraction was separated on a 15% SDS-PAGE gel. The blot was then probed with purified SCO1 and FLAG antibodies.

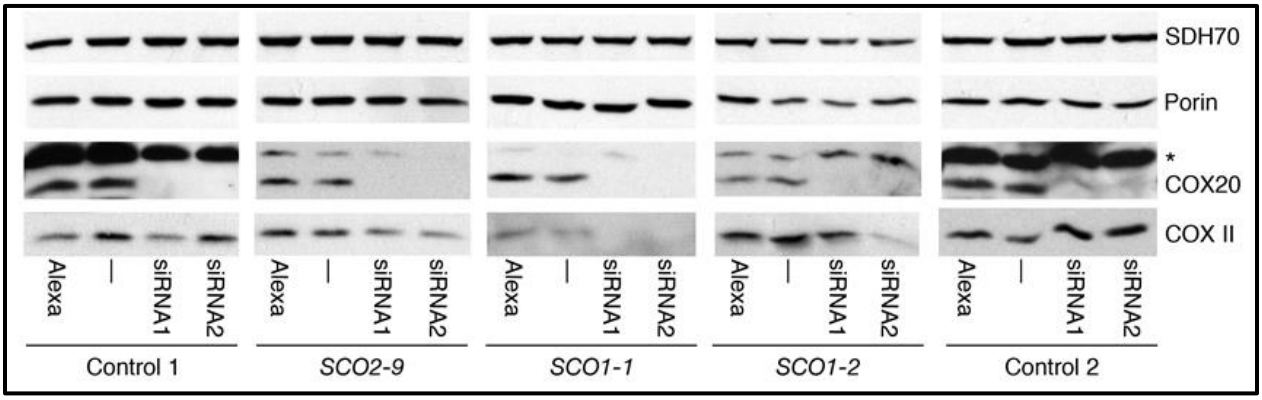

Figure 3.12: Knockdown of COX20 reduces COX II levels in SCO patient fibroblasts. Control and patient fibroblasts were transfected with two separate siRNA constructs targeted to COX20 for 9 days. On day 9, cells were harvested and permeabilized using digitonin to enrich the lysate for mitochondria. Samples were separated using SDS-PAGE and blotted with the appropriate antibodies. SDH70 and Porin were used as loading controls. The asterisk (*) indicates a background band observed with the COX20 antibody.

3.6 Characterization of metabolite transporters SLC25A1 and SLC25A11

If SLC25A1 or SLC25A11 physically interact with SCO1, their abundance may be affected in *SCO* patient cells that present with copper deficiencies. However, Western blot analysis showed no change in SLC25A1 or SLC25A11 protein levels in patient fibroblasts (Figure 3.13).

3.6.1 Validation of physical interactions

In yeast, Pic2 was recently identified as the first copper transporter of the inner mitochondrial membrane (Vest *et al.*, 2013). It is unknown whether its human homologue, SCL25A3, fulfills a similar role in copper transport. SLC25A3 was identified as potential interacting partner of SCO1, however no high-quality antibodies were available for further analysis. Two other SLC family members, SLC25A1 and SLC25A11, were also identified as potential interacting partners of SCO1, and good quality antibodies raised against each of these proteins are commercially available. Therefore, SCO1, SLC25A1, or SLC25A11 were purified with the appropriate primary antibody from uncrosslinked mitochondria derived from control fibroblasts. Western blot analysis demonstrated that SLC25A1 and SLC25A11 were co-immunoprecipitated with SCO1 (Figure 3.14A). Consistent with this observation, SCO1 was also found in the eluate

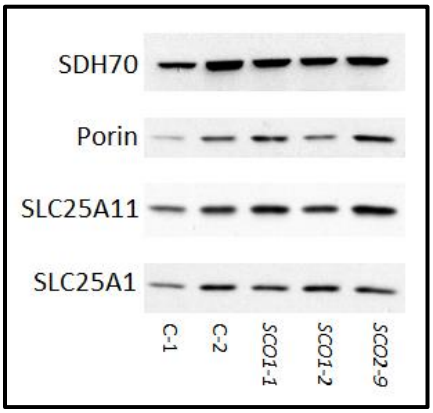

Figure 3.13: Steady-state protein levels of SLC25A1 and SLC25A11. Control and *SCO* patient fibroblasts were permeabilized using digitonin to enrich the lysate for mitochondria. Samples were separated using SDS-PAGE and blotted with the appropriate antibodies. SDH70 and Porin were used as mitochondrial loading controls.

upon co-immunoprecipitation with either the SLC25A11 or SLC25A1 antibody (Figures 3.14B and 3.14C). Membranes were blotted with antibodies against CORE1, a subunit of Complex III, as a control.

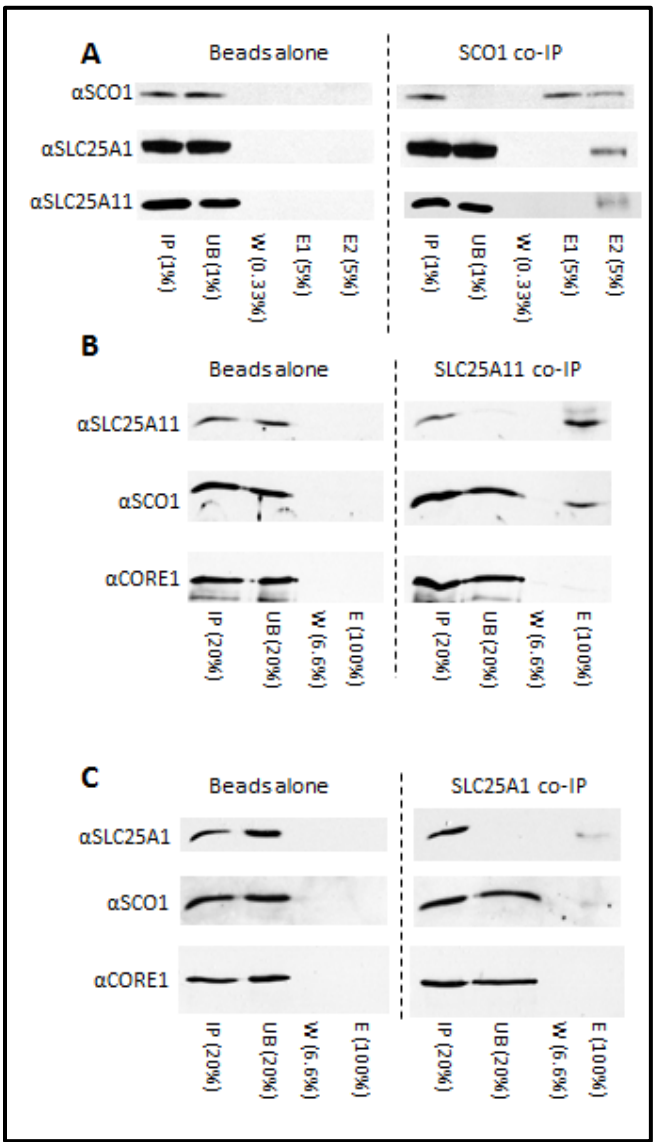

Figure 3.14: SCO1 interacts with SLC25A11 and SLC25A1 without the addition of chemical crosslinkers. Mitochondria were isolated from control fibroblasts and subsequently lysed (IP). Lysate was then incubated with SCO1 (A), SLC25A11 (B), or SLC25A1 (C) antibodies conjugated to beads overnight. Unbound extract (UB) was removed, and beads were washed three times (W) followed by elution in acetic acid (E1) and/or boiling in sample loading buffer with reductant (E2 or E). Samples were separated by SDS-PAGE followed by blotting with the appropriate antibodies.

3.6.2 Effect of siRNA knockdown of SLC25A1 or SLC25A11 on COX II abundance

Copper is required for the maturation of the Cu_A site of COX II and subsequent insertion of the protein into the assembling holoenzyme. Therefore, if interactions between SCO1 and SLC25A1 or SLC25A11 are involved in copper transport across the inner mitochondrial membrane and delivery of the metal ion to COX II, we reasoned that manipulating the expression of either metabolite transporter may affect COX II abundance. HEK293 cells were stably transduced with cDNAs to overexpress SLC25A1 or SL25A11, and whole cell extracts were separated by SDS-PAGE. While stable drug resistant cell lines were isolated, there was no discernible overexpression of either SLC25A1 or SLC25A11, even though there was a significant and reproducible decrease in COX II steady-state-levels (Figure 3.15A and 3.15B). To determine whether the reduced levels of COX II were simply a consequence of overexpressing an inner mitochondrial membrane protein, extracts were also prepared from HEK293 cells overexpressing SCO1 or SCO2. The abundance of COX II was only affected in HEK293 cells overexpressing the metabolite transporters (Figure 3.15C).

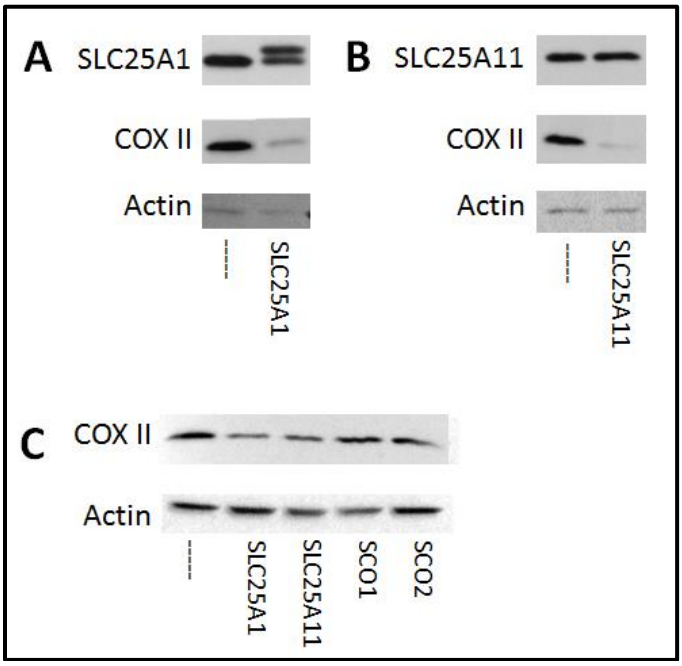

Figure 3.15: Overexpression of SLC25A1 or SLC25A11 affects COX II levels. Retroviral vectors containing SLC25A1 (A) or SLC25A11 (B) were transduced into HEK293 cells. Whole cell extracts were separated using SDS-PAGE and blotted with appropriate antibodies. (C) Retroviral vectors containing SLC25A1, SLC25A11, SCO1 or SCO2 were transduced into HEK293 cells. Actin was used as a loading control.

To further investigate a role for SLC25A1 or SLC25A11 in COX assembly, their abundance was transiently knocked down in control and *SCO* patient fibroblasts using specific siRNAs. After 8 days, untreated or siRNA treated fibroblasts were harvested and whole cell extracts were analyzed by Western blotting. Significant knockdown of SLC25A11 was observed in all fibroblast lines transiently transfected with any of 3 different siRNA constructs, with siRNA1 having the most modest effect on SLC25A11 abundance (Figure 3.16A). COX II abundance was reduced in control (C-1 and C-2) and *SCO1-2* patient fibroblasts in which the steady-state levels of SLC25A11 were not immunologically detectable. In contrast, the steady-state levels of COX II in *SCO2* patient fibroblasts were independent of SLC25A11 abundance. Successful knockdown of SLC25A1 was also observed in all fibroblast lines; however, siRNA1 was the least effective of the three siRNAs (3.16B). Although SLC25A1 knockdown did not affect COX II abundance in control (C-1 and C-2) and *SCO1-1* fibroblasts, the steady-state levels of COX II were increased in *SCO1-1* and *SCO2-9* fibroblasts in which SLC25A1 abundance was significantly reduced but remained immunologically detectable. However, the potential relationship between SLC25A1 and COX II in these genetic backgrounds appears to be complicated, because more efficient knockdown of SLC25A1 led to a complete loss of immunologically detectable COX II. To further evaluate whether the effect of knocking down SLC25A1 or SLC25A11 was specific to COX or also affected the abundance of other complexes of oxidative phosphorylation, extracts from C-1 and *SCO1-2* fibroblasts transfected with siRNA were blotted with antibodies against subunits from the other three complexes of the electron transport chain (Figure 3.16C). These analyses demonstrated that the abundance of Complexes I, II and III is unaffected when either SLC25A1 or SLC25A11 are knocked down.

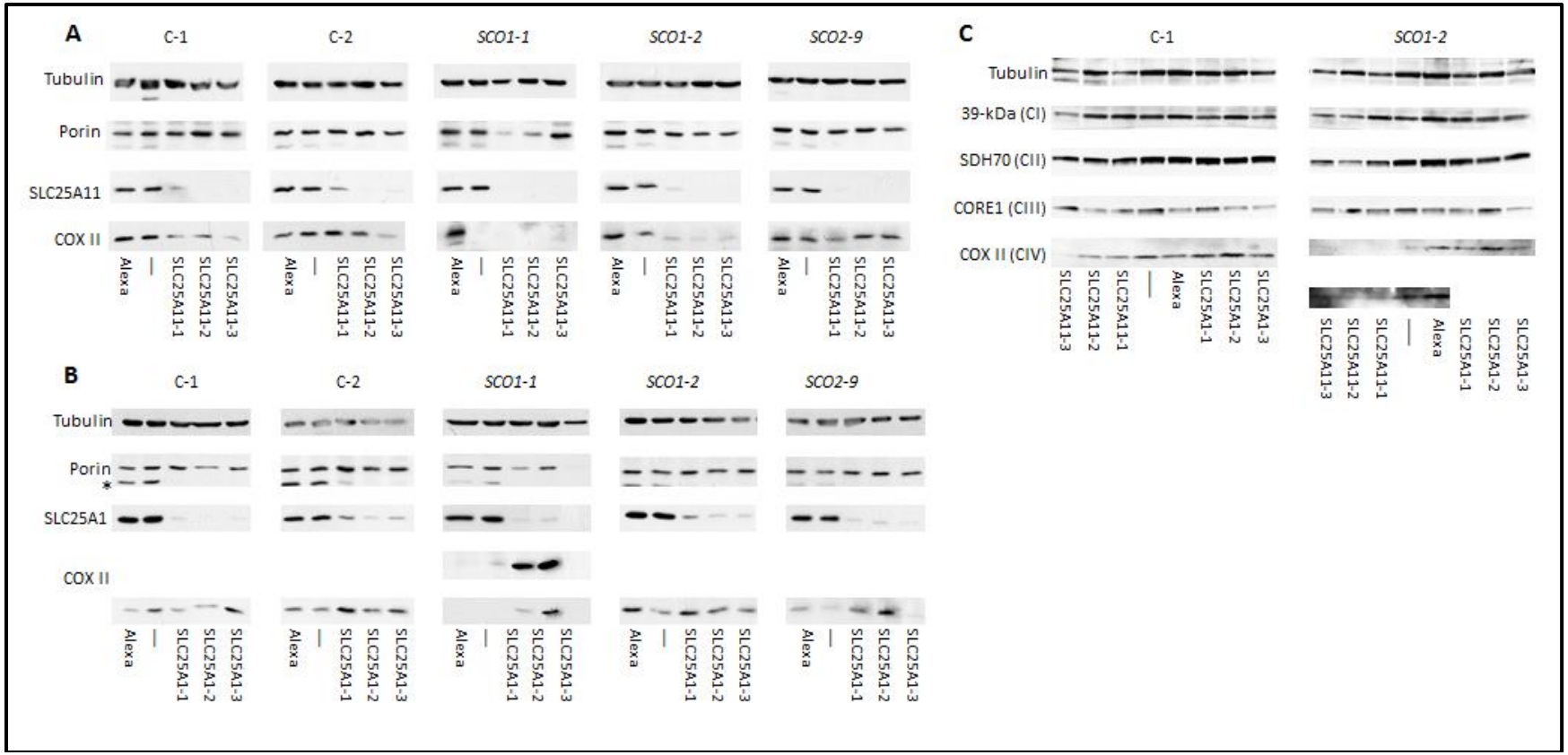

Figure 3.16: Knockdown of SLC25A11 and SLC25A1 in control and SCO patient fibroblasts. Control (C-1 and C-2) and *SCO* patient fibroblasts were transfected with three siRNA constructs targeted to SLC25A11 or SLC25A1. On day 8, cells were harvested and lysate was separated on SDS-PAGE gels. Membranes were subsequently blotted to verify knockdown of SLC25A11 (A) or SLC25A1 (B) with the indicated primary antibodies. Tubulin and Porin were used as cytoplasmic and mitochondrial loading controls, respectively. The asterisk denotes residual chemiluminescence from the SLC25A1 antibody. Separate membranes were blotted with antibodies against structural subunits from other OXPHOS complexes (C).

4 DISCUSSION

4.1 Interpretation of hit list of potential interacting partners of SCO1.

A greater understanding of how SCO1 metallates COX II or contributes to the mitochondrial regulation of cellular copper homeostasis requires the identification of its interacting partners. Physical interaction studies with metallochaperones are challenged by the highly transient nature of their interactions, and the fact that these interactions are typically stabilized by weak, non-covalent bonds (Chen *et al.*, 2013). To address these challenges, I used a chemical crosslinking approach to stabilize interactions between SCO1 and its protein partners. Overexpressed SCO1-FLAG or endogenous SCO1 were subsequently immunoprecipitated from mitochondria, and co-eluted proteins were identified by mass spectrometry. As expected, the list of potential interacting partners was large, and the number of non-specific hits was significant. Structural proteins and subunits from other oxidative phosphorylation complexes were enriched. However, this was not surprising because the COX holoenzyme forms large super-structures termed respirasomes that are comprised of many of the enzyme complexes of oxidative phosphorylation (Shoubridge, 2012). Therefore, the close proximity of these enzyme complexes to the machinery that promotes their assembly could potentiate their crosslinking to SCO1, even though evidence ascribing any functional significance to these interactions is currently lacking. Several mitochondrial proteases were also identified in the eluate fractions of both SCO1 and SCO1-FLAG immunoprecipitations. This argues that enrichment for proteases is not simply due to the overexpression of an epitope-tagged variant, something that has been observed in previous studies that have employed co-immunoprecipitation as an experimental strategy (Stiburek *et al.*, 2012). Several structural subunits of the COX holoenzyme were also identified in my co-immunoprecipitations, including the catalytic core subunit COX II and two of the protein constituents of the S2 assembly intermediate, COX IV and COX Va (Fontanesi *et al.*, 2008; Tsukihara *et al.*, 1995; Tsukihara *et al.*, 1996). The co-purification of these structural subunits with SCO1 further supports the idea that SCO1 is essential for the maturation of COX II at the S2 stage of holoenzyme assembly (Leary *et al.*, 2004; Nijtmans *et al.*, 1998; Shoubridge, 2001).

COX I and SCO2 are two proteins that I expected to co-elute with SCO1 that were not detected in the mass spectrometric analyses. COX I is the core catalytic subunit of COX that seeds holoenzyme assembly and, along with COX IV and COX Va, forms the S2 assembly intermediate (Fontanesi *et al.*, 2008). COX I is a very hydrophobic protein, and its hydrophobic

nature is believed to have prevented lateral gene transfer to the nucleus (Gray *et al.*, 1999). Perhaps the physico-chemical properties of COX I promoted its aggregation and therefore precipitation, either during purification of the immune complex or subsequent processing of the sample (Gray *et al.*, 1999; Tsukihara *et al.*, 1996). SCO2 was also not identified as a potential interacting partner of SCO1, even though significant molecular genetic evidence argues that each protein fulfills an essential, complementary function at the S2 stage of COX assembly (Leary *et al.*, 2004; Leary *et al.*, 2009). SCO1 and SCO2 are present as homodimers in fibroblasts, and COX assembly is only affected by overexpressing a given SCO protein in the reciprocal *SCO* patient background (e.g. SCO1 overexpression in *SCO2* patient cells) (Leary *et al.*, 2004). The inability of overexpressed SCO1 or SCO2 to reduce COX activity in control cells argues that only a small percentage of the SCO1 protein pool interacts with the SCO2 protein pool. Thus, capturing a physical interaction between SCO proteins that is detectable by mass spectrometry may require that immunoprecipitations be conducted following experimental manipulations that promote COX assembly (e.g. pulse-chase labeling) (Leary *et al.*, 2009). It is important to note, however, that there is no evidence of a direct physical interaction between human SCO1 and SCO2 in the literature. This raises the possibility that SCO proteins act sequentially to mature COX II by interacting with the polypeptide directly or with one or more of the COX assembly factors that chaperones COX II during its maturation.

My co-immunoprecipitation experiments also did not reveal any obvious candidates that may be involved in the generation or transduction of a SCO1-dependent mitochondrial redox signal that regulates cellular copper homeostasis. Recently, functional genetic experiments identified COX19 as a critical component of this signal transduction pathway (Leary *et al.*, 2013b). The fact that COX19 was not present in the eluate suggests that it may not interact with SCO1 directly, or that it does but the physical interaction was not detected due to technical limitations of the experiment. I favour the latter possibility, because the resultant hit list from the mass spectrometric analysis did not contain any soluble, IMS localized proteins, even though it is well established that COX17 transfers copper to SCO1 via ligand exchange (Banci *et al.*, 2007b; Banci *et al.*, 2008; Cobine *et al.*, 2006b). My inability to detect interactions between SCO1 and IMS proteins like COX17 and COX19 may be explained by the rapid on/off kinetics of their interactions, which would make them more difficult to crosslink chemically. Efficient crosslinking of membrane proteins and IMS factors may also have been challenged by the fact

that this latter group of proteins moves in three dimensions. Alternatively, the OMM may have been damaged during mitochondrial isolation, which would have significantly reduced the abundance of IMS proteins available for subsequent crosslinking reactions.

Mass spectrometric analysis of eluates from FLAG-tagged and endogenous SCO1 co-immunoprecipitations provided lists of candidate interacting partners that were too large and therefore made an unbiased validation approach impractical. As such, a set of rationalized criteria was used to generate a prioritized list of candidate interacting partners from the two datasets. Proteins with annotated gene ontology functions related to the cytoskeleton or immune-related processes were discarded, because SCO1 has no role in either of these broad biological processes. The MitoCarta database was then used to remove any remaining proteins that are not localized to the mitochondrion, because SCO1 is tethered to the IMM and therefore can only physically interact with other mitochondrial proteins. The resultant list contained 85 proteins that were then rank ordered based on the total number of identified peptide fragments. SCO1 was the third highest ranked protein on the final list, with two other proteins having higher peptide counts; IMMT and STOML2. IMMT is involved in mitochondrial cristae remodeling, while STOML2 interacts with Complexes I and II is thought to be involved in mitochondrial biogenesis (Christie *et al.*, 2011; John *et al.*, 2005). Other identified proteins with high peptide counts included structural subunits of oxidative phosphorylation complexes (NDUFS1, NDUFS3, UQCRC2), a protein involved in maintaining mitochondrial cristae integrity (CHCHD3), an OMM pore protein (VDAC2) (Yu *et al.*, 1995; Darshi *et al.*, 2011; Iwata *et al.*, 1998; Brandt, 2006), and a mitochondrial translation factor (TUFM) (Valente *et al.*, 2007). However, none of these proteins represented strong candidates worthy of further investigation, because a clear connection between their function and that of SCO1 is currently lacking. Therefore, in the interest of time and money, I chose to validate and characterize interactions between SCO1 and three candidates with lower peptide counts; COX20, a known COX assembly factor with an ill-defined role in holoenzyme biogenesis; and, SLC25A1 and/or SLC25A11, two transporters that may be involved in translocating copper across the IMM.

4.2 Significance of the interaction between SCO1 and COX20 to COX assembly

My M.Sc. project was part of a larger collaborative effort that investigated the significance of the physical interaction between SCO1 and COX20 to COX assembly (Bourens

et al, submitted). My contribution to this research was to establish that SCO1 co-immunoprecipitated COX20, and to evaluate the effect of COX20 knockdown on COX assembly in control, *SCO1* and *SCO2* patient fibroblasts. I was able to show that both in the absence and presence of crosslinkers, a small amount of COX20 co-eluted with SCO1. I further demonstrated that siRNA knockdown of COX20 reduced the steady-state levels of COX II, a direct proxy of COX content, in *SCO1* and *SCO2* patient fibroblasts, but not in control fibroblast lines. Taken together, these data are consistent with a model whereby SCO1 physically interacts with COX20, and that this interaction is critical to COX assembly likely at the S2 stage of holoenzyme biogenesis, because this assembly intermediate accumulates in *SCO* patient fibroblasts and in COX20 knockdown or knockout cells (Bourens et al, submitted).

While these findings advance our mechanistic understanding of COX assembly, the specific function of human COX20 remains poorly understood. In contrast, the yeast homologue has been studied extensively. Cox20 interacts with Cox2 following Oxa1-mediated translocation of its N-terminal domain across the IMM, and presents Cox2 to the IMP peptidase complex to facilitate the proteolytic removal of its N-terminal presequence (He and Fox, 1997; Hell *et al.*, 1998; Hell *et al.*, 2000). Cox20 then collaborates with Cox18 to promote the subsequent export of the C-terminal domain of Cox2 (Funes *et al.*, 2004; Saracco and Fox, 2002). Existing data suggest that Oxa1 does not physically interact with Cox20, and that Cox2 is required to stabilize the interaction between Cox18 and Cox20 (Elliott *et al.*, 2012). The mechanisms that govern the insertion of newly synthesized COX II into the IMM and facilitate subsequent maturation of the polypeptide in humans are not well understood. Although human cells express homologues of yeast Cox18, Cox20 and Oxa1 (Haque *et al.*, 2010; Sacconi *et al.*, 2005; Szklarczyk *et al.*, 2013), their respective roles in COX assembly remain poorly defined. Interestingly, OXA1L was identified by mass spectrometric analysis of chemically crosslinked eluates from SCO1 co-immunoprecipitations. However, it is unlikely that the observed interaction directly relates to COX assembly, as SCO1 interact with COX II after the protein has been translocated into the IMM by OXA1L. Because OXA1L also has a role in targeting newly imported mitochondrial proteins to the IMM (Hell *et al.*, 2001), it is possible that co-elution of OXA1L with SCO1 reflects an interaction between the two proteins that is critical to insertion of SCO1 into the lipid bilayer.

Yeast Cox20 is also thought to act as a chaperone to stabilize Cox2 during its maturation (Elliott *et al.*, 2012). Consistent with the idea that this chaperone function is conserved in higher eukaryotes and relates to the maturation of the Cu_A site of COX II, my Western blot analysis showed that the abundance of COX20 is modestly increased in *SCO1* and *SCO2* patient fibroblasts. This suggests that cells attempt to address the loss of SCO1 or SCO2 function by increasing the steady-state levels of COX20. While highly speculative, one could test this hypothesis by determining whether overexpression of COX20 rescues the COX deficiency in *SCO* patient cells. I would also analyze the COX20 abundance in patient cells with isolated COX deficiencies caused by pathogenic mutations in other COX assembly factors such as *COX10* or *SURF1* (Antonicka *et al.*, 2003; Lee *et al.*, 2012; Stiburek *et al.*, 2005; Valnot *et al.*, 2000a). If COX20 abundance is unchanged, this would further support the idea that SCO patient cells increase the steady-state levels of COX20 in an attempt to rescue the COX assembly defect.

Unlike other COX assembly factors, human COX20 does not appear to be essential for holoenzyme biogenesis. HEK293T cells in which COX20 is knocked out still have roughly 25% of the COX content of the parental line (Bourens et al, submitted). Moreover, a pathogenic T52P mutation in COX20 severely impairs COX assembly, particularly in striated muscle, but is not associated with early onset fatal clinical outcomes (Doss *et al.*, 2013; Szklarczyk *et al.*, 2013). However, Western blot analysis demonstrated that *COX20* patient fibroblasts express low, but detectable levels of the T52P mutant (Szklarczyk *et al.*, 2013). This suggests that the T52P substitution does not abolish COX20 function, and that sufficient residual function remains to support COX assembly. Future studies of other *COX20* pedigrees will be required to determine the importance of COX20 function to COX assembly in different cell types (Szklarczyk *et al.*, 2013), and a full understanding of COX20 function awaits the identification of all factors that are required to stabilize COX II and metallate its Cu_A site.

4.3 Characterizing the potential roles of SCL25A1 and/or SLC25A11 in mitochondrial copper transport

The mitochondrial matrix contains a labile pool of copper that can be accessed for metallation of Cox1 and Cox2 during COX assembly (Cobine *et al.*, 2006a). In humans, the components involved in the regulated trafficking of copper ions to, within and from mitochondria remain unknown. My project provided evidence that two IMM transporters,

SLC25A1 and SLC25A11, interact with SCO1, and that these interactions are directly relevant to COX assembly. Knockdown of either transporter reduced COX II levels in *SCO1* and *SCO2* patient fibroblasts, while knockdown of SLC25A11 also lowered COX II abundance in control fibroblasts. Why control cell lines transduced with a *SLC25A1* or *SLC25A11* cDNA also exhibit a reduction in COX II abundance, even though by Western blot analysis neither transporter appeared to be overexpressed, remains unclear. However, the fact that the steady-state levels of COX II were reduced in control fibroblasts upon knockdown of SLC25A11 suggests that it plays a more prominent role than SLC25A1 in COX assembly. COX assembly defects in cells with attenuated expression of either transporter may reflect a compromised ability to traffic copper across the IMM for its eventual loading by SCO1 into COX II. It will be important to directly address this possibility by quantifying the effect of knocking down each protein in isolation and together on total cellular and mitochondrial copper content.

The majority of mitochondrial copper is bound by a soluble, anionic complex defined as the copper ligand (CuL) (Cobine *et al.*, 2004). Data from previous studies suggest that the CuL complex may resemble a metabolite or nucleotide (Yang *et al.*, 2005). Therefore, copper transport across the IMM may rely on one or more mitochondrial metabolite transporters. The solute carrier 25 (SLC25) family of proteins consists of nuclear-encoded transporters embedded in the IMM, and in unique cases other organellar membranes. These carriers are highly conserved, and are responsible for the transport of metabolites, nucleotides, and co-factors across membranes. SLC25 transporters typically have primary substrates, but are also able to transport other related compounds, albeit with lower affinity (Palmieri, 2004; Palmieri *et al.*, 2011; Palmieri, 2013; Picault *et al.*, 2004). This provides overlapping substrate specificity among family members and redundant pathways for transport of a given molecule. Consistent with these observations, a phosphate carrier of the IMM, Pic2, was recently identified as the first mitochondrial copper transporter in yeast (Vest *et al.*, 2013). A role for the human homologue of Pic2, SLC25A3, in copper transport has not yet been identified, and although human SLC25A3 co-immunoprecipitated with SCO1 in chemically crosslinked eluates, we could not find any commercial antibodies of suitable quality to further investigate the potential significance of this interaction. In contrast, robust reagents were available for SLC25A1 and SLC25A11 and the importance of these proteins to SCO1 function was therefore further characterized. SLC25A1 predominantly catalyzes the import of malate while simultaneously exporting citrate from the

matrix (Capobianco *et al.*, 1995; Palmieri *et al.*, 1972b; Palmieri, 2013). Patients with pathogenic mutations in *SLC25A1* present with severe neonatal epileptic encephalopathy. This condition often results in early death, and is associated with increased levels of several Krebs cycle intermediates and elevated serum levels of 2-hydroxyglutarate (Nota *et al.*, 2013). SLC25A11 has been shown to transport 2-oxoglutarate into the matrix, in exchange for malate or other dicarboxylic acids (Monne *et al.*, 2013; Palmieri *et al.*, 1972a; Robinson and Chappell, 1967).

Functional redundancy may explain the difficulty the scientific community has had with respect to the identification of IMM copper transporters. In fact, mitochondrial iron transport is known to rely on multiple SLC family members who, although they exhibit varying degrees of specificity for iron transport, are nonetheless able to functionally complement for the loss of each other's function (Gordon *et al.*, 2006; Muhlenhoff *et al.*, 2003; Yoon *et al.*, 2011). The potential roles of SLC25A1 and SLC25A11 in mitochondrial copper trafficking require further experimentation. Both SLC25A1 and SLC25A11 are bi-directional antiport transporters, suggesting they could traffic copper to or from the matrix (Palmieri, 2013). However, because SCO1 does not have a known role in the regulated trafficking of copper to the matrix, I favour the idea that one or both of these transporters exports copper to the IMS. Multiple lines of evidence support a model whereby SCO1 receives copper from COX17 (Banci *et al.*, 2007b; Banci *et al.*, 2008; Cobine *et al.*, 2006b). Given that free copper is essentially undetectable in the cell (Rae *et al.*, 1999), and that free copper within the IMS would be predicted to potentiate Fenton chemistry, one possibility is that SLC25A1 and/or SLC25A11 supply copper to IMS metallochaperones like COX17 for its subsequent delivery to SCO1. The fact that I observed a physical interaction between SCO1 and both transporters, however, suggests that this may involve the formation of a ternary complex containing SLC25A1 or SLC25A11, COX17 and SCO1. A second, mutually exclusive possibility is that SCO1 interacts with SLC25A1 and/or SLC25A11 to inhibit their copper transport activity, although this seems less likely because *SCO1* patient fibroblasts maintain wild-type levels of mitochondrial copper even in the face of a severe copper deficiency at the cellular level (Dodani *et al.*, 2011). Further mechanistic insight into the trafficking of copper across the IMM will require the identification and functional characterization of most, if not all, relevant transporters.

4.4 Future directions

In addition to identifying and confirming the physical interaction between SCO1 and COX20, SLC25A1 and SLC25A11, my M.Sc. thesis work identified a substantial number of additional proteins that may also interact with SCO1 and be worthy of further investigation. The fact that the stability of newly synthesized COX II is significantly affected by mutations in *SCO1* and *SCO2* (Leary *et al.*, 2009) suggests that both SCO proteins may affect COX II stability by interacting with one or more mitochondrial proteases. Interestingly, immunoprecipitation of SCO1-FLAG and endogenous SCO1 identified two proteases as potential interacting partners of SCO1; ATPase family member 3-Like 2 (AFG3L2) and YME1L. Both proteases are structurally similar and anchored to the IMM by either one or two transmembrane domains (Gerdes *et al.*, 2012; Rugarli and Langer, 2012). The catalytic region of YME1L resides in the IMS and reductions in its abundance leads to accumulation of non-assembled respiratory chain subunits (Leonhard *et al.*, 1996; Stiburek *et al.*, 2012). The catalytic domains of AFG3L2 face the matrix side of the IMM (Gerdes *et al.*, 2012; Lee *et al.*, 2011), and patients with loss of function mutations in *AFG3L2* present with neurodegenerative disorders associated with defective mitochondrial quality control (Maltecca *et al.*, 2008). Therefore, while perturbed function of YME1L or AFG3L2 would exert pleiotropic effects on the expression of structural subunits of the complexes of oxidative phosphorylation, their interaction with SCO1 is worth further pursuing because they may act to degrade COX II that is not fully matured and inserted into the assembling holoenzyme. Another potential interacting partner of SCO1 of interest was LRPPRC, a post-transcriptional regulatory factor that stabilizes mt-mRNA transcripts, including *COX I, COX II* and *COX III* (Cooper *et al.*, 2006; Mootha *et al.*, 2002; Sasarman *et al.*, 2010). Mouse embryotic fibroblasts lacking *LRPPRC* exhibit a severe COX deficiency and slight decreases in the abundance of other oxidative phosphorylation complexes that contain mtDNA-encoded subunits (Xu *et al.*, 2012). Because LRPPRC is localized to the matrix, it would interact with the soluble N-terminal tail of SCO1 that is also localized to that mitochondrial compartment. I believe that such an interaction would serve to efficiently couple COX II translation with the subsequent maturation of the polypeptide.

5 REFERENCES

Alder, N.N., Jensen, R.E., and Johnson, A.E. (2008). Fluorescence mapping of mitochondrial TIM23 complex reveals a water-facing, substrate interacting helix surface. Cell. *134*, 439-450.

Allen, S., Lu, H., Thornton, D., and Tokatlidis, K. (2003). Juxtaposition of the two distal CX3C motifs via intrachain disulfide bonding is essential for the folding of Tim10. J. Biol. Chem. *278*, 38505-38513.

Anderson, S., Bankier, A.T., Barrell, B.G., de Brujin, M.H., Coulson, A.R., Drouin, J., Eperon, I.C., Nierlich, D.P., Roe, B.A., and Sanger, F. (1981). Sequence and organization of the human mitochondrial genome. Nature *290*, 457-465.

Antonicka, H., Leary, S.C., Guercin, G., Agar, J.N., Horvath, R., Kennaway, N.G., Harding, C.O., Jaksch, M., and Shoubridge, E.A. (2003). Mutations in COX10 result in a defect in mitochondrial heme A biosynthesis and account for multiple, early-onset clinical phenotypes associated with isolated COX deficiency. Hum. Mol. Genet. *12*, 2693-2702.

Banci, L., Bertini, I., Calderone, V., Ciofi-Baffoni, S., Mangani, S., Martinelli, M., Palumaa, P., and Wang, S. (2006). A hint for the function of human Sco1 from different structures. Proc. Natl. Acad. Sci. U. S. A. *103*, 8595-8600.

Banci, L., Bertini, I., Cefaro, C., Ciofi-Baffoni, S., Gallo, A., Martinelli, M., Sideris, D.P., Katrakili, N., and Tokatlidis, K. (2009). MIA40 is an oxidoreductase that catalyzes oxidative protein folding in mitochondria. Nat. Struct. Mol. Biol. *16*, 198-206.

Banci, L., Bertini, I., Ciofi-Baffoni, S., Gerothanassis, I., Leontari, I., Martinelli, M., and Wang, S. (2007a). A structural characterization of human SCO2. Structure *15*, 1132-1140.

Banci, L., Bertini, I., Ciofi-Baffoni, S., Hadjiloi, T., Martinelli, M., and Palumaa, P. (2008). Mitochondrial copper(I) transfer from Cox17 to Sco1 is coupled to electron transfer. Proc. Natl. Acad. Sci. U. S. A. *105*, 6803-6808.

Banci, L., Bertini, I., Ciofi-Baffoni, S., Leontari, I., Martinelli, M., Palumaa, P., Sillard, R., and Wang, S. (2007b). Human Sco1 functional studies and pathological implications of the P174L mutant. Proc. Natl. Acad. Sci. U. S. A. *104*, 15-20.

Barrientos, A., Barros, M.H., Valnot, I., Rotig, A., Rustin, P., and Tzagoloff, A. (2002). Cytochrome oxidase in health and disease. Gene *286*, 53-63.

Barrientos, A., Zambrano, A., and Tzagoloff, A. (2004). Mss51p and Cox14p jointly regulate mitochondrial Cox1p expression in *Saccharomyces cerevisiae*. EMBO J. *23*, 3472-3482.

Barros, M.H., Carlson, C.G., Glerum, D.M., and Tzagoloff, A. (2001). Involvement of mitochondrial ferredoxin and Cox15p in hydroxylation of heme O. FEBS Lett. *4921*, 133-138.

Barros, M.H., Nobrega, F.G., and Tzagoloff, A. (2002). Mitochondrial ferredoxin is required for heme A synthesis in *Saccharomyces cerevisiae*. J. Biol. Chem. *277,* 9997-10002.

Barros, M.H., and Tzagoloff, A. (2002). Regulation of the heme A biosynthetic pathway in *Saccharomyces cerevisiae*. FEBS Lett. *516,* 119-123.

Baumann, F., Neupert, W., and Herrmann, J.M. (2002). Insertion of bitopic membrane proteins into the inner membrane of mitochonrdia involves an export step from the matrix. J. Biol. Chem. *277,* 21405-21413.

Becker, T., Bottinger, L., and Pfanner, N. (2012). Mitochondrial protein import: from transport pathways to an integrated network. Trends Biochem. Sci. *37,* 85-91.

Bihlmaier, K., Meseck, N., Terziyska, N., Bien, M., Hell, K., and Herrmann, J.M. (2007). The disulfide relay system of mitochondria is connected to the respiratory chain. J. Cell Biol. *179,* 389-395.

Bourens, M.; Boulet, A.; Leary, S.C.; Barrientos, A. (2014) Human COX20 cooperates with SCO1 and SCO2 to mature COX2 and promote the assembly of cytochrome c oxidase. Hum. Mol. Genet. [Epub ahead of print].

Bradford, M.M. (1976) Rapid and sensitive method for the quantitation of microgram quantities of protein utilizing the principle of protein-dye binding. Anal. Biochem. 72, 248-254

Brandt, U. (2006). Energy converting NADH: quinone oxidoreductase (complex I). Annu. Rev. Biochem. *75,* 69-92.

Broadley, S.A., Demlow, C.M., and Fox, T.D. (2001). Peripheral mitochondrial inner membrane protein, Mss2p, required for export of the mitochondrially coded Cox2p C tail in *Saccharomyces cerevisiae*. Mol. Cell Biol. *21,* 7663-7672.

Brown, K.R., Allan, B.M., and Hegg, E.L. (2002). Identification of novel hemes generated by heme A synthase: evidence for two successive monooxygenase reactions. Biochemistry *41,* 10906-10913.

Brown, N.G., Costanzo, M.C., and Fox, T.D. (1994). Interactions among three proteins that specifically activate translation of the mitochondrial COX3 mRNA in *Saccharomyces cerevisiae*. Mol. Cell Biol. *14,* 1045-1053.

Buchwald, P., Krummeck, G., and Rodel, G. (1991). Immunological identification of yeast Sco1 protein as a component of the inner mitochondrial membrane. Molecular & General Genetic *229,* 413-420.

Capaldi, R. (1990). Structure and Function of Cytochrome *c* Oxidase. Annu. Rev. Biochem. *59,* 569-596.

Capobianco, L., Bisaccia, F., Michel, A., Sluse, F.E., and Palmieri, F. (1995). The N- and C-termini of the tricarboxylate carrier are exposed to the cytoplasmic side of the inner mitochondrial membrane. FEBS Lett. *357,* 297-300.

Carr, H.S., George, G.N., and Winge, D.R. (2002). Yeast Cox11, a protein essential for cytochrome *c* oxidase assembly, is a Cu(I)-binding protein. J. Biol. Chem. *277*, 31237-31242.

Chacinska, A., Koehler, C.M., Milenkovic, D., Lithgow, T., and Pfanner, N. (2009). Importing mitochondrial proteins: machineries and mechanisms. Cell *138,* 628-644.

Chacinska, A., Lind, M., Frazier, A.E., Dudek, J., Meisinger, C., Geissler, A., Sickmann, A., Meyer, H.E., Truscott, K.N., Guiard, B., Pfanner, N., and Rehling, P. (2005). Mitochondrial presequence translocase: switching between TOM tethering and motor recruitment involves Tim21 and Tim17. Cell *120,* 817-829.

Chacinska, A., Pfannschmidt, S., Wiedemann, N., Kozjak, V., Sanjuan Szklarz, L.K., Schulze-Specking, A., Truscott, K.N., Guiard, B., Meisinger, C., and Pfanner, N. (2004). Essential role of Mia40 in import and assembly of mitochondrial intermembrane space proteins. EMBO J. *23,* 3734-3746.

Chen, P., Keller, A.M., Joshi, C.P., Martell, D.J., Andoy, N.M., Benitez, J.J., Chen, T., Santiago, A.C., and Yang, F. (2013). Single-molecule dynamics and mechanisms of metalloregulators and metallochaperones. Biochemistry *52,* 7170-7183.

Christie, D., Lemke, C., Elias, I., Chau, L., Kirchhof, M., Li, B., Ball, E., Dunn, S., Hatch, G., and Madrenas, J. (2011). Stomatin-like protein 2 binds cardiolipin and regulates mitochondrial biogenesis and function. Mol. Cell Biol. *18*, 3845-3856.

Clayton, D.A. (1982). Replictaion of animal mitochondrial DNA. Cell *28*, 693-705.

Cobine, P.A., Ojala, D., Rigby, K.M., and Winge, D.R. (2004). Yeast contain a non-proteinaceous pool of copper in the mitochondrial matrix. J. Biol. Chem. *279*, 14447-14455.

Cobine, P.A., Pierrel, F., Bestwick, M.L., and Winge, D.R. (2006a). Mitochondrial matrix copper complex used in metallation of cytochrome oxidase and superoxide dismutase. J. Biol. Chem. *48*, 36552-36559.

Cobine, P.A., Pierrel, F., Leary, S.C., Sasarman, F., Horng, Y., Shoubridge, E., and Winge, D. (2006b). The P174L mutation in human Sco1 severely compromises Cox17-dependent metallation but does not impair copper binding. J. Biol. Chem. *281*, 12270-12276.

Cobine, P.A., Pierrel, F., and Winge, D.R. (2006c). Copper trafficking to the mitochondrion and assembly of copper metalloenzymes. Biochim. Biophys. Acta. *1763*, 759-772.

Colombini, M. (1979). A candidate for the permeability pathway of the outer mitochondrial membrane. Nature *279*, 643-645.

Cooper, M.P., Qu, L., Rohas, L.M., Lin, J., Yang, W., Erdjument-Bromage, H., Tempst, P., and Spiegelman, B.M. (2006). Defects in energy homeostasis in Leigh syndrome French Canadian variant through PGC-1α/LRP130 complex. Genes Dev. *20,* 2996-3009.

Costanzo, M.C., and Fox, T.D. (1988). Specific translational activation by nuclear gene products occurs in the 5' untranslated leader of a yeast mitochondrial mRNA. Proc. Natl. Acad. Sci. U. S. A. *85,* 2677-2681.

Dabir, D.V., Leverich, E.P., Lim, S.K., Tsai, F.D., Hirasawa, M., Knaff, D.B., and Koehler, C.M. (2007). A role for cytochrome *c* and cytochrome *c* peroxidase in electron shuttling from Erv1. EMBO J. *26,* 4801-4811.

Darshi, M., Mendiola, V., Mackey, M., Murphy, A., Koller, A., Perkins, G., Ellisman, M., and Taylor, S. (2011). CHCHD3, an inner mitochondrial membrane protein, is essential for maintaining crista integrity and mitochondrial function. J. Biol. Chem. *286,* 2918-2932.

Dienhart, M.K., and Stuart, R.A. (2008). The yeast Aac2 protein exists in physical association with the cytochrome bc_1-COX supercomplex and TIM23 machinery. Mol. Biol. Cell. *19,* 3934-3943.

Dodani, S., Leary, S.C., Cobine, P., Winge, D., and Chang, C. (2011). A Targetable Fluorescent Sensor Reveals that Copper-Deficient *SCO1* and *SCO2* Patient Cells Prioritize Mitochondrial Copper Homeostasis. J. Am. Chem. Soc. *133,* 8606-8016.

Doss, S., Lohmann, K., Seibler, P., Arns, B., Klopstock, T., Zuhlke, C., Freimann, K., Winkler, S., Lohnau, T., Drungowski, M., *et al.* (2013). Recessive dystonia-ataxia syndrome in a Turkish family caused by a COX20 (FAM36A) mutation. J. Neurol. 207-212.

Elliott, L.E., Saracco, S., and Fox, T.D. (2012). Multiple roles of the Cox20 chaperone in assembly of Saccharomyces cerevisiae cytochrome *c* oxidase. Genetics *190,* 559-567.

Endo, T., and Kohda, D. (2002). Functions of outer membrane receptors in mitochondrial protein import. Biochim. Biophys. Acta. *1592,* 3-14.

Endo, T., Yamano, K., and Kawano, S. (2011). Sructural insight into the mitochondrial protein import system. Biochim. Biophys. Acta. *1808,* 955-970.

Falkenberg, M., Larsson, N.G., and Gustafsson, C.M. (2007). DNA replication and transcription in mammalian mitochondria. Annu. Rev. Biochem. *76,* 679-699.

Fernandez-Vizarra, E., Enriquez, J.A., Perez-Martos, A., Montoya, J., and Fernandez-Silva, P. (2011). Tissue-specific differences in mitocohndrial activity and biogenesis. Mitochondrion *1,* 207-213.

Fiumera, H.L., Broadley, S.A., and Fox, T.D. (2007). Translocation of mitochondrially synthesized Cox2 domains from the matrix to the intermembrane space. Mol. Cell Biol. *27,* 4664-4673.

Fontanesi, F., Clemente, P., and Barrientos, A. (2011). Cox25 teams up wtih Mss51, Ssc1, and Cox14 to regulate mitochondrial cytochrome *c* oxidase subunit expression and assembly in *Saccharomyces cerevisiae*. J. Biol. Chem. *286,* 555-566.

Fontanesi, F., Soto, I.C., and Barrientos, A. (2008). Cytochrome *c* oxidase biogenesis: new levels of regulation. IUBMB Life *286,* 555-566.

Fontanesi, F., Soto, I.C., Horn, D., and Barrientos, A. (2010). Mss51 and Ssc1 facilitate translational regulation of cytochrome *c* oxidase biogenesis. Mol. Cell Biol. *30,* 245-259.

Freitag, H., Neupert, W., and Benz, R. (1982). Purification and characterization of a pore protein of the outer mitochondrial membrane from *Neurospora crassa*. European Journal of Biochemistry / FEBS *123,* 629-636.

Funes, S., Nargang, F.E., Neupert, W., and Herrmann, J.M. (2004). The Oxa2 protein of *Neurospora crassa* plays a critical role in the biogenesis of cytochrome oxidase and defines a ubiquitous subbranch of the Oxa1/YidC/Alb3 protein family. Mol. Biol. Cell. *15,* 1853-1861.

Geissler, A., Chacinska, A., Truscott, K.N., Wiedemann, N., Brandner, K., Sickmann, A., Meyer, H.E., Meisinger, C., Pfanner, N., and Rehling, P. (2002). The mitochondrial presequence translocase: an essential role of Tim50 in directing preproteins to the import channel. Cell *111,* 507-518.

Gerdes, F., Tatsuta, T., and Langer, T. (2012). Mitochondrial AAA proteases - Towards a molecular understanding of membrane-bound proteolytic machines. Biochim. Biophys. Acta. *1823,* 49-55.

Ghezzi, D., and Zeviani, M. (2012). Assembly factors of human mitochondrial respiratory chain complexes: physiology and pathophysiology. Adv. Exp. Med. Biol. *748,* 65-106.

Glerum, D.M., Shtanko, A., and Tzagoloff, A. (1996a). Characterization of COX17, a yeast gene involved in copper metabolism and assembly of cytochrome oxidase. J. Biol. Chem. *271,* 14504-14509.

Glerum, D.M., Shtanko, A., and Tzagoloff, A. (1996b). SCO1 and SCO2 act as high copy suppressors of a mitochondrial copper recruitment defect in *Saccharomyces cerevisiae*. J. Biol. Chem. 20531-20535.

Glerum, D.M., and Tzagoloff, A. (1994). Isolation of a human cDNA for heme A:farnesyltransferase by functional complementation of yeast cox10 mutant. Proc. Natl. Acad. Sci. U. S. A. *91,* 8452-8456.

Gordon, D.M., Lyver, E.R., Lesuisse, E., Dancis, A., and Pain, D. (2006). GTP in the mitochondrial matrix plays a crucial role in organellar iron homeostasis. Biochem. J. *400,* 163-168.

Gray, M.W., Burger, G., and Lang, B.F. (1999). Mitochondrial evolution. Science *283,* 1476-1481.

Graziewicz, M.A., Longley, M.J., and Copeland, W.C. (2006). DNA polymerase in γ in mitochondrial DNA replication and repair. Chemical Reviews *106,* 383-405.

Haque, M.E., Elmore, K.B., Tripathy, A., Koc, H., Koc, E.C., and Spremulli, L.L. (2010). Properties of the C-terminal tail of human mitochondrial inner membrane protein Oxa1L and its interactions with mammalian mitochondrial ribosomes. J. Biol. Chem. *36,* 28353-28362.

He, S., and Fox, T.D. (1999). Mutations affecting a yeast mitochondrial inner membrane protein, pnt1p, block export of a mitochondrially synthesized fusion protein from the matrix. Mol. Cell Biol. *19,* 6598-6607.

He, S., and Fox, T.D. (1997). Membrane translocation of mitochondrially coded Cox2p: distinct requirements for export of N- and C-termini and dependence on the conserved protein Oxa1p. Mol. Biol. Cell *8,* 1449-1460.

Hell, K., Herrmann, J.M., Pratje, E., Neupert, W., and Stuart, R.A. (1998). Oxa1p, an essential component of the N-tail protein export machinery in mitochondria. Proc. Natl. Acad. Sci. U. S. A. *95,* 2250-2255.

Hell, K., Neupert, W., and Stuart, R.A. (2001). Oxa1p acts as a general membrane insertion machinery for proteins encoded by mitochondrial DNA. EMBO J. *20,* 1281-1288.

Hell, K., Tzagoloff, A., Neupert, W., and Stuart, R. (2000). Identification of Cox20p, a novel protein involved in the maturation and assembly of cytochrome oxidase subunit 2. J. Biol. Chem *275,* 4571-4578.

Herrmann, J.M., and Hell, K. (2005). Chopped, trapped, or tacked-protein translocation into the IMS of mitochondria. Trends Biochem. Sci. *30,* 205-211.

Herrmann, J.M., Longen, S., Weckbecker, D., and Depuydt, M. (2012). Biogenesis of mitochondrial proteins. Adv. Exp. Med. Biol. *748,* 41-64.

Herrmann, J.M., Neupert, W., and Stuart, R.A. (1997). Insertion into the mitochondrial inner membrane of a polytopic protein, the nuclear-encoded Oxa1p. EMBO J. *16,* 2217-2226.

Herrmann, J.M., Woellhaf, M.W., and Bonnefoy, N. (2013). Control of protein synthesis in yeast mitochondria: the concept of translational activators. Biochim. Biophys. Acta. *1833,* 286-294.

Hiser, L., Di Valentin, M., Hamer, M., and Hosler, J. (1999). Cox11p is required for stable formation of the Cu_B and magnesium centers of cytochrome *c* oxidase. J. Biol. Chem *275*, 619-623.

Holt, I.J., Harding, A.E., and Morgan-Hughes, J.A. (1988). Deletions of muscle mitochondrial DNA in patients with mitochondrial myopathies. Nature *313*, 717-719.

Horn, D., and Barrientos, A. (2008). Mitochondrial copper metabolism and delivery to cytochrome *c* oxidase. IUBMB Life *60*, 421-429.

Horng, Y., Cobine, P., Maxfield, A., Carr, H., and Winge, D. (2004). Specific copper transfer from the Cox17 metallochaperone to both Sco1 and Cox11 in the assembly of yeast cytochrome *c* oxidase. J. Biol. Chem. *279*, 35334-35340.

Horng, Y., Leary, S., Cobine, P., Young, F., George, G., Shoubridge, E., and Winge, D. (2005). Human Sco1 and Sco2 function as copper-binding proteins. J. Biol. Chem. *280*, 24114-24122.

Hu, J., Dong, L., and Outten, C.E. (2008). The redox environment in the mitochondrial intermembrane space is maintained separately from the cytosol and matrix. J. Biol. Chem. *283*, 29126-29134.

Hutu, D.P., Guiard, B., Chacinska, A., Becker, D., Pfanner, N., Rehling, P., and van der Laan, M. (2008). Mitochondrial protein import motor: differential role of Tim44 in the recruitment of Pam17 and J-complex to the presequence translocase. Mol. Biol. Cell. *19*, 2641-2649.

Iwata, S., Lee, J., Okada, K., Lee, J., Iwata, M., Rasmussen, B., Link, T., Ramaswamy, S., and Jap, B. (1998). Complex structure of the 11-subunit bovine mitochondrial cytochrome bc1 complex. Science *281*, 64-71.

Jaksch, M., Paret, C., Stucka, R., Horn, N., Müller-Höcker, J., Horvath, R., Trepesch, N., Stecker, G., Freisinger, P., Thirion, C., *et al.* (2001). Cytochrome *c* oxidase deficiency due to mutations in SCO2, encoding a mitochondrial copper-binding protein, is rescued by copper in human myoblasts. Hum. Mol. Genet. *10*, 3025-3035.

Jia, L., Dienhart, M., Schramp, M., McCauley, M., Hell, K., and Stuart, R.A. (2003). Yeast Oxa1 interacts with mitochondrial ribosomes: the importance of the C-terminal hydrophilic region of Oxa1. EMBO J. *22*, 6438-6447.

John, G., Shang, Y., Li, L., Renken, C., Manella, C., Selker, J., Rangell, L., Bennett, M., and Zha, J. (2005). The mitochondrial inner membrane protein mitofilin controls cristae morphology. Mol. Biol. Cell *16*, 1543-1554.

Kazachkova, N., Ramos, A., Santos, C., and Lima, M. (2013). Mitochondrial DNA damage patterns and aging: revising the evidences for humans and mice. Aging and Disease *4*, 337-350.

Khalimonchuk, O., and Rodel, G. (2005). Biogenesis of cytochrome *c* oxidase. Mitochondrion. *5*, 363-388.

Klement, P., Nijtmans, L., Van den Bogert, C., and Houstek, J. (1995). Analysis of oxidative phosphorylation complexes in cultured human fibroblasts and amnioacytes by blue-native-electrophoresis using mitoplasts isolated with the help of digitonin. Anal. Biochem. *231*, 218-224.

Koehler, C.M., and Tienson, H.L. (2009). Redox regulation of protein folding in the mitochondrial intermembrane space. Biochim. Biophys. Acta. *1793*, 139-145.

Kozany, C., Mokranjac, D., Sichting, M., Neupert, W., and Hell, K. (2004). The J domain-related cochaperone Tim16 is a constituent of the mitochondrial TIM23 preprotein translocase. Nat. Struct. Mol. Biol. *11*, 234-241.

Krayl, M., Lim, J.H., Martin, B., Guiard, B., and Voos, W. (2007). A cooperative action of the ATP-dependent import motor complex and the inner membrane potential drives mitochondrial preprotein import. Mol. Cell Biol. *27*, 411-425.

Leary, S.C. (2010). Redox Regulation of SCO Protein Function: Controlling Copper at a Mitochondrial Crossroad. . Antioxid. Redox Signal. *13*, 1403-1416.

Leary, S.C., Antonicka, H., Sasarman, F., Weraarpachai, W., Cobine, P.A., Pan, M., Brown, G.K., Brown, R., Majewski, J., Ha, K.C., Rahman, S., and Shoubridge, E.A. (2013a). Novel mutations in SCO1 as a cause of fatal infantile encephalopathy and lactic acidosis. Human Mutation 1366-1370.

Leary, S.C., Cobine, P.A., Kaufman, B.A., Guercin, G.H., Mattman, A., Palaty, J., Lockitch, G., Winge, D.R., Rustin, P., Horvath, R., and Shoubridge, E.A. (2007). The human cytochrome *c* oxidase assembly factors SCO1 and SCO2 have regulatory roles in the maintenance of cellular copper homeostasis. Cell Metabolism *5*, 9-20.

Leary, S.C., Cobine, P.A., Nishimura, T., Verdijk, R.M., de Krijger, R., de Coo, R., Tarnopolsky, M.A., Winge, D.R., and Shoubridge, E.A. (2013b). COX19 mediates the transduction of a mitochondrial redox signal from SCO1 that regulates ATP7A-mediated cellular copper efflux. Mol. Biol. Cell. *24*, 683-691.

Leary, S.C., Kaufman, B., Pellchia, G., Gguercin, G., Mattman, A., Jaksch, M., and Shoubridge, E. (2004). Human SCO1 and SCO2 have independent, cooperative functions in copper delivery to cytochrome *c* oxidase. Hum. Mol. Genet. *13*, 1839-1848.

Leary, S.C., Mattman, A., Wait, T., Koehn, d.C., Clarke, L.A., Chan, S., Lomax, B., Eydooux, P., Vallance, H.D., and Shoubridge, E.A. (2006). A hemizygous SCO2 mutation in an early onset rapidly progressive, fatal cardiomyopathy. Mol. Genet. Metab. *89*, 129-133.

Leary, S.C., Sasarman, F., Nishimura, T., and Shoubridge, E. (2009). Human SCO2 is required for the synthesis of CO II and as a thiol-disulphide oxidoreductase for SCO1. Hum. Mol. Genet. *18,* 2230-2240.

Leary, S.C., Sasarman, F., Nishimurar, T., and Shoubridge, E.A. (2009). Human SCO2 is required for the synthesis of COX II and as a thiol-disulphide oxidoreductase for SCO1. Human. Mol . Genet. *18,* 2230-2240.

Lee, I.C., El-Hattab, A.W., Wang, J., Li, F.Y., Weng, S.W., Craigen, W.J., and Wong, L.J. (2012). SURF1-associated leigh syndrome: a case series and novel mutations. Human Mutation *33,* 1192-1200.

Lee, S., Augustin, S., Tatsuta, T., Gerdes, F., Langer, T., and Tsai, F.T. (2011). Electron cyromicroscopy structure of a membrane-anchored mitochondrial AAA protease. J. Biol. Chem. *286,* 4404-4411.

Leonhard, K., Herrmann, J.M., Stuart, R.A., Mannhaupt, G., Neupert, W., and Langer, T. (1996). AAA proteases with catalytic sites on opposite membrane surfaces comprise a proteolytic system for the ATP-dependent degradation of inner membrane proteins in mitochondria. EMBO J. *15,* 4128-4229.

Li, Y., Dudek, J., Guiard, B., Pfanner, N., Rehling, P., and Voos, W. (2004). The presequence translocase-associated protein import motor of mitochondria: Pam16 functions in an antagonistic manner to Pam18. J. Biol. Chem. *279,* 38047-38054.

Lochmuller, H., Johns, T., and Shoubridge, E.A. (1999). Expression of the E6 and E7 genes of human papillomavirus (HPV16) extends the life span of human myoblasts. Experimental Cell Research. *186,* 186-193.

Lutz, T., Neupert, W., and Herrmann, J.M. (2003). Import of small Tim proteins into the mitochondrial intermembrane space. EMBO J. *22,* 4400-4408.

Maltecca, F., Aghaie, A., Schroeder, D.G., Cassina, L., Taylor, B.A., Phillips, S.J., Malaguti, M., Previtali, S., Guenet, J.L., Quattrini, A., Cox, G.A., and Casari, G. (2008). The mitochondrial protease AFG3L2 is essential for axonal development. J. Neurosci. *28,* 2827-2836.

Manthey, G.M., and McEwen, J.E. (1995). The product of the nuclear gene PET309 is required for translation of mature mRNA and stability or production of intron-containing RNAs derived from the mitochondrial COX1 locus of *Saccharomyces cerevisiae*. EMBO J. *14,* 4031-4043.

Martinez-Caballero, S., Grigoriev, S.M., Herrmann, J.M., Campo, M.L., and Kinally, K.W. (2007). Tim17p regulates the twin pore structure and voltage gating of the mitochondrial protein import complex TIM23. J. Biol. Chem. *282,* 3584-3593.

McBride, H.M., Neuspiel, M., and Wasiak, S. (2006). Mitochondria: more than just a powerhouse. Curr. Biol. *16,* 551-560.

Meinecke, M., Wagner, R., Kovermann, P., Guiard, B., Mick, D.U., Hutu, D.P., Voos, W., Truscott, K.N., Chacinska, A., Pfanner, N., and Rehling, P. (2006). Tim50 maintains the permeability barrier of the mitochondrial inner membrane. Science *312,* 1523-1526.

Mesecke, N., Terziyska, N., Kozany, C., Baumann, F., Neupert, W., Hell, K., and Herrmann, J.M. (2005). A disulfide relay system in the intermembrane space of mitochondria that mediates protein import. Cell *121,* 1059-1069.

Mick, D.U., Vukotic, M., Piechura, H., Meyer, H.E., Warscheid, B., Deckers, M., and Rehling, P. (2010). Coa3 and Cox14 are essential for negative feedback regulation of COX1 translation in mitochondria. J. Cell Biol. *191,* 141-154.

Mick, D.U., Wagner, K., van der Laan, M., Frazier, A.E., Perschil, I., Pawlas, M., Meyer, H.E., Warscheid, B., and Rehling, P. (2007). Shy1 couples Cox1 translation regulation to cytochrome c oxidase assembly. EMBO J. *26,* 4347-4358.

Milenkovic, D., Gabriel, K., Guiard, B., Schulze-Specking, A., Pfanner, N., and Chacinska, A. (2007). Biogenesis of the essential Tim9-Tim10 chaperone complex of mitochondria: site-specific recognition of cysteine residues by the intermembrane space receptor Mia40. J. Biol. Chem. *282,* 22472-22480.

Mobley, B., Enns, G., Wong, L., and Vogel, H. (2009). A novel homozygous SCO2 mutation, p.G193S, causing fatal infantile cardioencephalomyopathy. Clinical Neuropathology. *28,* 143-149.

Mokranjac, D., Bourenkov, G., Hell, K., Neupert, W., and Groll, M. (2006). Structure and function of Tim14 and Tim16, the J and J-like components of the mitochondrial protein import motor. EMBO J. *25,* 4675-4685.

Mokranjac, D., Sichting, M., Popov-Celeketic, D., Mapa, K., Gevorkyan-Airapetov, L., Zohary, K., Hell, K., Azem, A., and Neupert, W. (2009). Role of Tim50 in the transfer of precursor proteins from the outer to inner membrane of the mitochondria. Mol. Biol. Cell. *20,* 1400-1407.

Monne, M., Miniero, D.V., Iacobazzi, V., Bisaccia, F., and Fiermonte, G. (2013). The mitochondrial oxoglutarate carrier: from identification to mechanism. Journal of Bioenergetics and Biomembranes. *45,* 1-13.

Montoya, J., Ojala, D., and Attardi, G. (1981). Distinctive features of the 5'-terminal sequences of the human mitochondrial mRNAs. Nature *290,* 465-470.

Mootha, V.K., Lepage, P., Miller, K., Bunkenborg, J., Reich, M., Hjerrild, M., Delmonte, T., Villeneuve, A., Sladek, R., Xu, F., *et al.* (2002). Identification of a gene causing human cytochrome *c* oxidase deficienccy by integrative genomics. Proc. Natl. Acad. Sci. U. S. A. *100,* 605-610.

Mossmann, D., Meisinger, C., and Vogtle, F.N. (2012). Processing of mitochondrial presequences. Biochim. Biophys. Acta. *1819*, 9-10.

Muhlenhoff, U., Stadler, J.A., Richhardt, N., Seubert, A., Eickhorst, T., Schweyen, R.J., Lill, R., and Wiesenberger, G. (2003). A specific role of the yeast mitochondrial carriers MRS3/4p in mitochondrial iron acquisition under iron-limiting conditions. J. Biol. Chem. *278*, 40612-40620.

Mulero, J.J., and Fox, T.D. (1993). PET111 acts in the 5'-leader of the Saccharomyces cerevisiae mitochondrial COX2 mRNA to promote its translation. Genetics *133*, 509-516.

Naithani, S., Saracco, S.A., Butler, C.A., and Fox, T.D. (2003). Interactions among COX1, COX2, and COX3 mRNA specific translational activator proteins on the inner surface of the mitochondrial inner membrane of Saccharomyces cerevisiae. Mol. Biol. Cell. *14*, 324-333.

Neupert, W., and Herrmann, J.M. (2007). Translocation of proteins into mitochondria. Annu. Rev. Biochem. *76*, 723-749.

Nijtmans, L., Taanman, J., Muijsers, A.O., Speiker, D., and van den Bogert, C. (1998). Assembly of cytochrome-c oxidase in cultured human cells. Eur. J. Biochem. *254*, 389-394.

Nota, B., Struys, E.A., Pop, A., Jansen, E.E., Fernandez Ojeda, M.R., Kanhai, W.A., Kranendijk, M., van Dooren, S.J., Bevova, M.R., Sistermans, E.A., *et al.* (2013). Deficiency in SLC25A1, encoding the mitochondrial citrate carrier, causes combined D-2- and L-2-hydroxyglutaric aciduria. Am. J. Hum. Genet. *4*, 627-631.

Ott, M., and Herrmann, M. (2010). Co-translational membrane insertion of mitochondrially encoded proteins. Biochim. Biophys. Acta. *767*, 767-775.

Ott, M., Prestele, M., Bauerschmitt, H., Funes, S., Bonnefoy, N., and Herrmann, J.M. (2006). Mba1, a membrane-associated ribosome receptor in mitochondria. EMBO J. *25*, 1603-1610.

Pagliarini, D., Calvo, S., Chang, B., Sheth, S., Vafai, S., Ong, S., Walford, G., Sugiana, C., Boneh, A., Chen, W., *et al.* (2008). A mitochondrial protein compendium elucidates complex I disease biology. Cell. *1*, 112-123.

Palmieri, F. (2013). The mitochondrial transporter family SLC25: Identification, properties and physiopathology. Molecular Aspects of Medicine *34*, 464-484.

Palmieri, F. (2004). The mitochondrial transporter family (SLC25): physiological and pathological implications. Pflügers Archiv: European Journal of Physiology *447*, 689-709.

Palmieri, F., Pierri, C.L., De Grassi, A., Nunes-Nesi, A., and Fernie, A.R. (2011). Evolution, structure and function of mitochondrial carriers: a review with new insights. Plant Journal: For Cell and Molecular Biology. *66*, 161-181.

Palmieri, F., Quagliarielle, E., and Klingenberger, M. (1972a). Kinectics of the oxoglutarate carrier in rat-liver mitochondria. Eur. J. Biochem. *29,* 408-416.

Palmieri, F., Stipani, I., Quagliariello, E., and Klingenberg, M. (1972b). Kinetic study of the tricarboxylate carrier in rat liver mitochondria. Eur. J. Biochem. *26,* 587-594.

Papadopoulou, L., Sue, C., Davidson, M., Tanji, K., Nishion, I., Sadlock, J., Selby, J., Glerum, D., Van Coster, R., Lyon, G., *et al.* (1999). Fatal infantile cardioencephalomyopathy with COX deficiency and mutations in SCO2, a COX assembly gene. Nat. Genet. *23,* 333-337.

Paschen, S.A., Neupert, W., and Rapaport, D. (2005). Biogenesis of beta-barrel membrane proteins of mitochondria. Trends Biochem. Sci. *30,* 575-582.

Perez-Martinez, X., Broadley, S.A., and Fox, T.D. (2003). Mss51p promotes mitochondrial Cox1p synthesis and interacts with newly synthesized Cox1p. EMBO J. *22,* 5951-5961.

Picault, N., Hodges, M., Palmieri, L., and Palmieri, F. (2004). The growing family of mitochondrial carriers in Arabidopsis. Trends in Plant Science *9,* 138-146.

Pierrel, F., Cobine, P.A., and Winge, D.R. (2007). Metal ion availability in mitochondria. Biometals *20,* 675-682.

Popov-Celeketic, D., Mapa, K., Neupert, W., and Mokranjac, D. (2008). Active remodeling of the TIM23 complex during translocation of preproteins into the mitochondria. EMBO J. *27,* 1469-1480.

Preuss, M., Leonhard, K., Hell, K., Stuart, R.A., Neupert, W., and Herrmann, J.M. (2002). Mba1, a novel component of the mitochondrial protein export machinery of the yeast *Saccharomyces cerevisiae*. J. Biol. Chem. *277,* 12846-12853.

Rae, T.D., Schmidt, P.J., Pufahl, R.A., Culotta, V.C., and O'Halloran, T.V. (1999). Undetectable intracellular free copper: the requirement of a copper chaperone for superoxide dismutase. Science *348,* 805-808.

Rhee, H.W., Zou, P., Udeshi, N.D., Martell, J.D., Mootha, V.K., Carr, S.A., and Ting, A.Y. (2013). Proteomic mapping of mitochondria in living cells via spatially restricted enzymatic tagging. Science *339,* 1328-1332.

Rissler, M., Wiedemann, N., Pfannschmidt, S., Gabriel, K., Guiard, B., Pfanner, N., and Chacinska, A. (2005). The essential mitochondrial protein Erv1 cooperates with Mia40 in biogenesis of intermembrane space proteins. J. Mol. Biol. *353,* 485-492.

Robinson, B.H., and Chappell, J.B. (1967). The inhibition of malate, tricarboxylate and oxoglutarate entry into mitochondria by 2-n-butylmalonate. Biochem. and Biophys. Comm. *28,* 249-255.

Rugarli, E.I., and Langer, T. (2012). Mitochonrdial quality control: a matter of life and death for neurons. EMBO J. *31,* 1336-1349.

Ruzzenente, B., Metodiev, M.D., Wredenberg, A., Bratic, A., Park, C.B., Camara, Y., Milenkovic, D., Zickermann, V., Wibom, R., Hultenby, K., *et al.* (2012). LRPPRC is necessary for polyadenylation and coordination of translation of mitochondrial mRNAs. EMBO J. *31,* 443-456.

Sacconi, S., Trevisson, E., Pistollato, F., Baldoin, M., Rezzonico, R., Bouget, I., Desnuelle, C., Tenconi, R., Basso, G., DiMauro, S., and Salviati, L. (2005). hCOX18 and hCOX19: Two human genes involved in cytochrome *c* oxidase assembly. Biochem. and Biophys. Comm. *337,* 832-839.

Salviati, L., Hernandez-Rosa, E., Walker, W.F., Sacconi, S., DiMauro, S., Schon, E.A., and Davidson, M. (2002). Copper supplementation restores cytochrome c oxidase activity in cultured cells from patients with SCO2 mutations. Biochem. J. *363,* 321-327.

Sanchirico, M.E., Fox, T.D., and Mason, T.L. (1988). Accumulation of mitochondrially synthesized Saccharomyces cerevisiae Cox2p and Cox3p depends on targeting information in untranslated portions of their mRNAs. EMBO J. *17,* 5796-5804.

Saracco, S.A., and Fox, T.D. (2002). Cox18p is required for export of the mitochondrially encoded *Saccharomyces cerevisiae* Cox2p C-tail and interacts with Pnt1p and Mss2p in the inner membrane. Mol. Biol. Cell. *13,* 1122-1131.

Sasarman, F., Brunel-Guitton, C., Antonicka, H., Wai, T., Shoubridge, E., and LSFC Consortium. (2010). LRPPRC and SLIRP Interact in a ribonucleoprotein complex that regulates posttranscriptional gene expression in mitochondria. Mol. Biol. Cell *21,* 1315-1323.

Scaglia, F. (2012). Nuclear gene defects in mitochondrial disorders. Methods Mol. Biol. *837,* 17-34.

Scarpulla, R.C. (2008). Transcriptional paradigms in mammalian mitochondrial biogenesis and function. Physiological Reviews *88,* 611-638.

Schapira, A.H. (2012). Mitochondrial diseases. Lancet *379,* 1825-1834.

Schneider, H.C., Westermann, B., Neupert, W., and Brunner, M. (1996). The nucleotide exchange factor MGE exerts a key function in the ATP-depedent cycle of mt-Hsp70-Tim44 interaction driving mitochondrial protein import. EMBO J. *15,* 5796-5803.

Schon, E.A., and DiMauro, S. (2003). Medicinal and genetic approaches to the treatment of mitochondrial disease. Curr. Med. Chem. *10,* 2523-2533.

Schultz, B., and Chan, S. (2001). Structures and proton-pumping strategies of mitochondrial respiratory enzymes. Ann. Rev. Biophys. and Biomol. Struct. *30,* 23-65.

Shariff, K., Ghosal, S., and Matouschek, A. (2004). The force exerted by the membrane potential during protein import into the mitochondrial matrix. Biophys. J. *86*, 3648-3652.

Shoubridge, E.A. (2012). Supersizing the mitochondrial respiratory chain. Cell Metab. *15*, 271-272.

Shoubridge, E.A. (2001). Cytochrome c oxidase deficiency. Am. J. Med. Genet. *106*, 46-52.

Sickmann, A., Reinders, J., Wagner, Y., Joppich, C., Zahedi, R., Meyer, H.E., Schonfisch, B., Perschil, I., Chacinska, A., and Guiard, B. (2003). The proteome of Saccharomyces cerevisiae mitochondria. Proc. Natl. Acad. Sci. U. S. A. *100*, 13207-13212.

Skladal, D., Halliday, J., and Thorburn, D.R. (2003). Minimum birth prevalence of mitochondrial respiratory chain disorders in children. Brain. *126*, 1905-1912.

Slutsky-Leiderman, O., Marom, M., Iosefson, O., Levy, R., Maoz, S., and Azem, A. (2007). The interplay between components of the mitochondrial protein translocation motor studied using purified components. J. Biol. Chem. *282*, 33935-33942.

Smith, D., Gray, J., Mitchell, L., Antholine, W.E., and Hosler, J. (2005). Assembly of cytochrome-c oxidase in the absence of assembly protein Surf1 leads to loss of the active site heme. J. Biol. Chem. *280*, 17652-17656.

Smits, P., Smeitink, J., and van den Heuvel, L.P. (2010). Mitochondrial translation and beyond: processes implicated in combined oxidative phosphorylation deficiencies. Journal of Biomedicine & Biotechnology *2010*, 1-24.

Soto, I.C., Fontanesi, F., Liu, J., and Barrientos, A. (2012). Biogenesis and assembly of eukaryotic cytochrome *c* oxidase catalytic core. Biochim. Biophys. Acta. *1817*, 883-897.

Stiburek, L., Cesnekova, J., Kostkova, O., Fornuskova, D., Vinsova, K., Wenchich, L., Houstek, J., and Zeman, J. (2012). YME1L controls the accumulation of respiratory chain subunits and is required for apoptotic resistance, cristae morphogenesis, and cell proliferation. Mol. Biol. Cell. *23*, 1010-1023.

Stiburek, L., Vesela, K., Hansikova, H., Hulkova, H., and Zeman, J. (2009). Loss of function of Sco1 and its interaction with cytochrome *c* oxidase. . Am. J. Physiol. Cell Physiol. *296*, 1218-1226.

Stiburek, L., Vesela, K., Hansikova, H., Pecina, P., Tesarova, M., Cerna, L., Houstek, J., and Zeman, J. (2005). Tissue-specific cytochrome c oxidase assembly defects due to mutations in SCO2 and SURF1. Biochem. J. *392*, 625-632.

Stiburek, L., and Zeman, J. (2010). Assembly factors and ATP-depedent proteases in cytochrome *c* oxidase biogenesis. Biochim. Biophys. Acta. *1197*, 1149-1158.

Szklarczyk, R., Wanschers, B., Nitmans, L., Rodenburg, R., Zschocke, J., Dikow, N., van den Brand, M., Hendriks-Franssen, M., Glissen, C., Veltman, J., *et al.* (2013). A mutation in the FAM36A gene, the human ortholog of COX20, impairs cytochrome c oxidase assembly and is associated with ataxia and muscle hypotonia. Hum. Mutat. Genet. *22*, 656-667.

Szyrach, G., Ott, M., Bonnefoy, N., Neupert, W., and Herrmann, J.M. (2003). Ribosome binding to the Oxa1 complex facilitates cotranslational protein insertion in mitochondria. EMBO J. *22*, 6448-6457.

Tamura, Y., Harada, Y., Shiota, T., Yamano, K., Watanabe, K., Yokota, M., Yamamoto, H., Sesaki, H., and Endo, T. (2009). Tim23-Tim50 pair coordinates functions of translocators and motor proteins in mitochondrial protein import. J. Cell. Biol. *184*, 129-141.

Tomecki, R., Dmochowska, A., Gewartowski, K., Dziembowski, A., and Stepien, P.P. (2004). Identification of a novel human-encoded mitochondrial poly(A) polymerase. Nucleic Acids Research *34*, 6001-6014.

Truscott, K.N., Kovermann, P., Geissler, A., Merlin, A., Meijer, M., Driessen, A.J., Rassow, J., Pfanner, N., and Wagner, R. (2001). A presequence and voltage-sensitive channel of the mitochondrial preprotein translocase formed by Tim23. Nat. Struct. Biol. *8*, 1074-1082.

Tsukihara, T., Aoyama, H., Yamashita, E., Tomizaki, T., Yamaguchi, H., Shinzawa-Itoh, K., Nakashima, R., Yaono, R., and Yoshikawa, S. (1996). The Whole Structure of the 13-Subunit Oxidized Cytochrome *c* oxidase at 2.8 A. Science *269*, 1069-1074.

Tsukihara, T., Aoyama, H., Yamashita, E., Tomizaki, T., Yamaguchi, H., Shinzawa-Itoh, K., Nakashima, R., Yaono, R., and Yoshikawa, S. (1995). Structures of metal sites of oxidized bovine heart cytochrome c oxidase at 2.8 A. Science *269*, 1069-1074.

Tzagoloff, A., and Dieckmann, C. (1990). PET genes of Sacchraomyces cerevisiae. Microbiol. Mol. Biol. Rev. *54*, 211-225.

Vafai, S., and Mootha, V.K. (2012). Mitochondrial disorders as windows into an ancient organelle. Nature *491*, 374-383.

Valente, L., Tiranti, V., Marsano, R., Malfatti, E., Fernandez-Vizarra, E., Donnini, C., Mereghetti, P., De Gioia, L., Burlina, A., Castellan, C., *et al.* (2007). Infantile encephalopathy and defective mitochondrial DNA translation in patients with mutations of mitochondrial elongation factors EFG1 and EFTu. Am. J. Hum. Genet. *80*, 44-58.

Valnot, I., Kreist-Retzow, J., Barrientos, A., Gorbatyuk, M., Taanman, J., Mehaye, B., Rustin, P., Tzagoloff, A., Munnich, A., and Rotig, A. (2000a). A mutation in the human heme A:farnesyltransferase gene (COX10) causes cytochrome c oxidase deficiency. Hum. Mol. Genet. *9*, 1245-1249.

Valnot, I., Osmond, S., Gigarel, N., Mehaye, B., Amiel, J., Cormier-Daire, V., Munnich, A., Bonnefont, J., Rustin, P., and Rotig, A. (2000b). Mutations of the SCO1 gene in mitochondrial cytochrome *c* oxidase deficiency with neonatal-onset hepatic failure and encephalopathy. Am. J. Human Genetics. *67,* 1104-1109.

van der Laan, M., Wiedemann, N., Mick, D.U., Guiard, B., Rehling, P., and Pfanner, N. (2006). A role for Tim21 in membrane-potential-dependent preprotein sorting in mitochondria. Curr. Biol. *16,* 2271-2276.

Vest, K.E., Leary, S.C., Winge, D.R., and Cobine, P.A. (2013). Copper import into the mitochondrial matrix in Saccharomyces cerevisiae is mediated by Pic2, a ,mitochondrial carrier family protein. J. Biol. Chem. *288,* 23884-23892.

Wallace, D.C., Singh, G., Lott, M.T., Hodge, J.A., Schurr, T.G., Lezza, A.M., Elsas 2nd, L.J., and Nikoskelainen, E.K. (1988). Mitochondrial DNA mutation associated with Leber's hereditary optic neuropathy. Science *242,* 1427-1430.

Weraarpachai, W., Antonicka, H., Sasarman, F., Seeger, J., Schrank, B., Kolesar, J.E., Lochmuller, H., Chevrette, M., Kaufman, B.A., Horvath, R., and Shoubridge, E.A. (2009). Mutation in TACO1, encoding a translational activator of COX I, results in cytochrome *c* oxidase deficiency and late-onset Leigh syndrome. Nat. Genet. *41,* 833-837.

Wiedemann, N., van der Laan, M., Hutu, D.P., Rehling, P., and Pfanner, N. (2007). Sorting switch of mitochondrial presequence translocase involves coupling of motor module to respiratory chain. J. Cell. Biol. *179,* 1115-1122.

Williams, S.L., Valnot, I., Rustin, P., and Taanman, J. (2004). Cytochrome c oxidase subassemblies in fibroblast cultures from patients carrying mutations in COX10, SCO1, or SURF1. J. Biol. Chem. *279,* 7462-7469.

Xu, F., Addis, J.B., Cameron, J.M., and Robinson, B.H. (2012). LRPPRC mutation suppresses cytochrome oxidase activity by altering mitochondrial RNA transcript stability in a mouse a model. Biochem. J. *441,* 275-283.

Yamamoto, H., Esaki, M., Kanamori, T., Tamura, Y., Nishikawa, S., and Endo, T. (2002). Tim50 is a subunit of the TIM23 complex that links protein translocation across the outer and inner mitochondrial membranes. Cell *111,* 519-528.

Yang, L., McRae, R., Henary, M.M., Patel, R., Lai, B., Vogt, S., and Fahrni, C.J. (2005). Imaging of the intracellular topography of copper with a fluorescent sensor and by synchotron x-ray fluorescence microscopy. Proc. Natl. Acad. Sci. U. S. A. *102,* 11179-11184.

Yoon, H., Zhang, Y., Pain, J., Lyver, E.R., Lesuisse, E., Pain, D., and Dancis, A. (2011). Rim2, pyrimidine nucleotide exchanger is needed for iron utilization in mitochondria. Biochem. J. *440,* 137-146.

Yoshikawa, S., Muramoto, K., Shinzawa-Itoh, K., and Mochizuki, M. (2012). Structural studies on bovine heart cytochrome *c* oxidase. Biochim. Biophys. Acta. *1817,* 579-589.

Yu, W., Wolfgang, W., and Forte, M. (1995). Subcellular localization of human voltage-dependent anion channel isoforms. J. Biol. Chem. *270,* 13998-14006.

Zalman, L.S., Nikaido, H., and Kagawa, Y. (1980). Mitochondrial outer membrane contains a protein producing nonspecific diffusion channels. J. Biol. Chem. *255,* 1771-1774.

Zee, J.M., and Glerum, D. (2006). Defects in cytochrome oxidase assembly in humans: lessons from yeast. Biochem. Cell Biol. *84,* 859-869.

Zhu, Z., Yao, J., Johns, T., Fu, K., De Bie, I., Macmillan, C., Cuthbert, A.P., Newbold, R.F., Wang, J., Chevrette, M., *et al.* (1998). SURF1, encoding a factor involved in the biogenesis of cytochrome c oxidase is mutated in Leigh syndrome. Nat. Genet. *20,* 337-343.

Zsurka, G., and Kunz, W.S. (2013). Mitochondrial involvement in neurodegenerative diseases. IUBMB Life *65,* 263-272.